UNIVERSIDADE DE LISBOA

FACULDADE DE FARMÁCIA

DEPARTAMENTO DE BIOQUÍMICA

PENTOSE PHOSPHATE PATHWAY IN HEALTH AND DISEASE: FROM METABOLIC DYSFUNCTION TO BIOMARKERS

Rúben José Jesus Faustino Ramos

Orientador: Professora Doutora Maria Isabel Ginestal Tavares de Almeida

Mestrado em Análises Clínicas

2013

Pentose Phosphate Pathway in health and disease:

From metabolic dysfunction to biomarkers

▪

Via das Pentoses Fosfato na saúde e na doença:

Da disfunção metabólica aos biomarcadores

Dissertação apresentada à Faculdade de Farmácia da Universidade de Lisboa para obtenção do grau de Mestre em Análises Clínicas

Rúben José Jesus Faustino Ramos

Lisboa

2013

Orientador: Professora Doutora Maria Isabel Ginestal Tavares de Almeida

The studies presented in this thesis were performed at the Metabolism and Genetics group, iMed.UL (Research Institute for Medicines and Pharmaceutical Sciences), Faculdade de Farmácia da Universidade de Lisboa, Portugal, under the supervision of Prof. Maria Isabel Ginestal Tavares de Almeida, and in collaboration with the Department of Clinical Chemistry, VU University Medical Center, Amsterdam, The Netherlands, Dr. Mirjam Wamelink.

De acordo com o disposto no ponto 1 do artigo nº 41 do Regulamento de Estudos Pós-Graduados da Universidade de Lisboa, deliberação nº 93/2006, publicada em Diário da Republica – II série nº 153 – de 5 julho de 2003, o autor desta dissertação declara que participou na conceção e execução do trabalho experimental, interpretação dos resultados obtidos e redação dos manuscritos.

Para os meus pais e irmão

Table of Contents

Abbreviations

6PGD	6-phosphogluconolactone-dehydrogenase
AFLD	Alcoholic fatty liver disease
ALT	Alanine aminotransferase
AST	Aspartate aminotransferase
A-T	Ataxia telangiectasia
ATM	Ataxia-telangiectasia mutated
ATP	Adenosine triphosphate
bp	Base-pair
BSTFA	Bis(trimethylsilyl)trifluoroacetamide
CAS	Chemical abstract service
cDNA	Complementary DNA
CMV	Cytomegalovirus
CNSHA	Chronic non-spherocytic hemolytic anemia
CO_2	Carbon dioxide
CSF	Cerebrospinal fluid
DHA	Dihydroxyacetone
DNA	Deoxyribonucleic acid
dNTP	Deoxyribonucleotide triphosphates
DSBs	Double-strand breaks
E4P	Erythrose-4-phosphate
F6P	Fructose-6-phosphate
FBP	Fructose-1,6-biphosphate
FBPase-1	Fructose 1,6-biphosphatase 1
G3P	Glyceraldehyde-3-phosphate
G6P	Glucose-6-phosphate
G6PD	Glucose-6-phosphate dehydrogenase
GPX	Glutathione peroxidase
GR	Glutathione reductase
GSH	Glutathione (reduced form)
GSSG	Glutathione (oxidized form)
GXP	Glucoronate-xylulose pathway
H_2O_2	Hydrogen peroxide

HCC	Hepatocellular carcinoma
ICDH	Isocitrate dehydrogenase
IEM	Inborn errors of metabolism
IUGR	Intrauterine growth restriction
Km	Michaelis-Menten constant
LT	Liver transplantation
MDH	Malate dehydrogenase
mRNA	Messenger RNA
MW	Molecular weight
$NADP^+$	Nicotinamide adenine dinucleotide phosphate (oxidized form)
NADPH	Nicotinamide adenine dinucleotide phosphate (reduced form)
NASH	Non-alcoholic steatohepatitis
NMR	Nuclear magnetic resonance
OMIM	Online Mendelian Inheritance in Man
PCR	Polymerase chain reaction
PPP	Pentose Phosphate Pathway
qPCR	Real-time polymerase chain reaction
R5P	Ribose 5-phosphate
RNA	Ribonucleic acid
ROS	Reactive oxygen species
RPI	Ribose-5-phosphate isomerase
Ru5P	Ribulose-5-phosphate
S7P	Sedoheptulose-7-phosphate
SHPK	Sedoheptulokinase
TALDO	Transaldolase
ThDP	Thiamine diphosphate
TKT	Transketolase
TKTL1	Transketolase-like 1 protein
TKTL2	Transketolase-like 2 protein
Tri-Sil-TBT	Trimethylsilyl N-trimethylsilylacetamidate in chlorotrimethylsilane
WHO	World Health Organization
XR	Xylulose reductase
Xu5P	Xylulose-5-phosphate

Summary

The Pentose Phosphate Pathway (PPP) fulfils two unique functions: *(i)* the formation of ribose-5-phosphate (R5P) for the synthesis of nucleotides, RNA and DNA, supporting cell growth and proliferation; and *(ii)* the formation of the reduced form of nicotinamide adenine dinucleotide phosphate (NADPH). NADPH carries chemical energy in the form of reducing power, being essential to the cellular oxidative defense system and is also the universal reducing agent in many anabolic pathways, such as cholesterol and lipid synthesis and fatty acids chain elongation. The PPP comprises two separate branches: *(i)* an oxidative, non-reversible branch, and *(ii)* a non-oxidative, reversible branch. The oxidative branch primarily depends on glucose 6-phosphate dehydrogenase (G6PD), whereas transaldolase (TALDO) is the rate-limiting enzyme for the non-oxidative branch. Although the oxidative branch of the PPP is recognized as the source of NADPH and R5P, the overall contribution of the non-oxidative branch to metabolism and cell survival is poorly understood.

Metabolism of glucose through the PPP influences the development of diverse pathologies. Deficiency of the PPP enzyme G6PD represents the most common genetic defect in humans and leads to NADPH depletion in red blood cells (RBC), predisposing to oxidative stress-induced hemolytic anemia. Recently, two new defects in the PPP were described: ribose-5-phosphate isomerase (RPI) deficiency and transaldolase (TALDO) deficiency. The first defect is associated with progressive leukoencephalopathy and mild peripheral neuropathy. The metabolic profile of the disease is associated with elevated levels of ribitol and arabitol in the brain, as showed by magnetic resonance spectroscopy (MRS), urine, plasma and cerebrospinal fluid (CSF). In contrast, TALDO deficiency is associated with liver symptoms, while other organs are affected to a variable degree. The metabolic phenotype of the disease is characterized by increased urinary concentrations of the polyols: erythritol, arabitol, ribitol, sedoheptitol, perseitol and the sugars: sedoheptulose and mannoheptulose, as well as sedoheptulose-7-phosphate.

The profound influence of TALDO on NADPH levels, mitochondrial dysfunction and oxidative stress is ascribed to the blocked recycling of R5P to glucose 6-phosphate (G6P) and to the proposed linkage to aldose reductase (AR) that converts the accumulated C5-sugar phosphates to C5-polyols at the expense of NADPH. Mitochondrial dysfunction associated to TALDO deficiency leads to liver disease

progressing from non-alcoholic fatty liver disease (NAFLD) to non-alcoholic steatohepatitis (NASH), cirrhosis and hepatocellular carcinoma (HCC). Therefore, TALDO deficiency can account for liver disease of variable severity.

The diagnosis of the PPP deficiencies is possible by biochemical evaluation of polyols' and sugars' profiles in body fluids. Abnormal concentrations of these compounds occur in a number of pathological conditions such as diabetes mellitus, renal and liver disease and several inborn errors of carbohydrate metabolism, such as galactosemia. Therefore, it is necessary to take into account the variability of metabolic profiles and to understand their meaning.

Along the thesis, it is our goal to revise the metabolic pathway of pentose phosphates and its implication in the associated disease states. Furthermore, the development and validation of the analytical methods (GC-FID and GC-MS) will be presented and discussed. We will also present our preliminary results upcoming from two separated studies, focused on the characterization of the PPP intermediate metabolites profile in (*1*) pre-selected cases with unexplained hepatosplenomegaly and/or liver dysfunction in a pediatric population; and (*2*) in adult patients with liver dysfunction (NAFLD or AFLD). We hope to find new biomarkers and metabolic signs which may open new perspectives of research for better understanding liver dysfunction.

Interesting data is described, in the pediatric population, where a patient with an isolated sedoheptulokinase (SHPK) deficiency is reported. All the subsequent studies, some still in course, seem to confirm this new defect in the PPP.

In the adult population our findings point to the putative importance of polyols as possible biomarkers of liver dysfunction progression.

Keywords: Pentose Phosphate Pathway; ribose-5-phosphate isomerase deficiency; transaldolase deficiency; non-alcoholic fatty liver disease; sedoheptulokinase deficiency.

Sumário

A via das pentoses fosfato tem dois objectivos principais: (*i*) a formação de ribose-5-fosfato (R5P) para a síntese de nucleótidos, ARN e ADN, essenciais para o crescimento e proliferação celular; e (*ii*) a redução de nicotinamida adenina dinucleótido fosfato (NADPH). A NADPH transporta energia química sob a forma de poder redutor, sendo essencial para o sistema de defesa oxidativo das células e sendo ainda o agente redutor universal de inúmeras reacções anabólicas, tais como a síntese de colesterol e lípidos e o prolongamento das cadeias dos ácidos gordos.

A via das pentoses fosfato é constituída por dois ramos: (*i*) um ramo oxidativo, não reversível, e (*ii*) um ramo não-oxidativo, completamente reversível. O ramo oxidativo é dependente da actividade da enzima glucose-6-fosfato desidrogenase (G6PD), enquanto a transaldolase (TALDO) é a enzima limitante do ramo não-oxidativo. Apesar do reconhecido papel do ramo oxidativo da via das pentoses fosfato como fonte de NADPH e R5P, a contribuição da via não-oxidativa no metabolismo e sobrevivência celular é pouco conhecida.

O metabolismo da glucose na via das pentoses fosfato influencia o desenvolvimento de diversas patologias. A deficiência em G6PD é o defeito genético mais comum na população humana, levando a níveis reduzidos de NADPH nos eritrócitos e predispondo ao aparecimento de anemia hemolítica induzida por stress oxidativo. Recentemente, foram descritas duas novas deficiências enzimáticas na via das pentoses fosfato: a deficiência em ribose-5-fosfato isomerase (RPI) e a deficiência em transaldolase (TALDO). A primeira deficiência enzimática está associada a leucoencefalopatia progressiva e ligeira neuropatia periférica. O perfil metabólico da doença revela níveis elevados dos polióis: ribitol e arabitol no cérebro, tal como demonstrado por ressonância magnética, na urina, plasma e líquido cefalorraquidiano (LCR). Por outro lado, a deficiência em transaldolase está associada a alterações hepáticas, havendo um grau variado de comprometimento por parte de outros órgãos. O fenótipo metabólico desta deficiência está associado à excreção de níveis elevados dos polióis: eritritol, arabitol, ribitol, sedoheptitol, perseitol e dos açúcares: sedoheptulose e manoheptulose, bem como de sedoheptulose-7-fosfato.

A forte influência da transaldolase nos níveis de NADPH em situações de disfunção mitocondrial e stress oxidativo é atribuída ao bloqueio da reciclagem da glucose-6-fosfato a partir da ribose-5-fosfato e à hipotética ligação à actividade de

aldoses redutases (AR), responsáveis pela conversão dos açúcares-C5-fosfatados a C5-polióis, às custas de NADPH. A disfunção mitocondrial associada à deficiência em transaldolase leva a uma doença hepática progressiva que se inicia com o aparecimento do fígado gordo não alcoólico (NAFLD), passando a esteatohepatite não alcoólica (NASH), cirrose e carcinoma hepatocelular (CHC). Assim, a deficiência em transaldolase está associada a doença hepática de variado grau de severidade.

O diagnóstico dos defeitos da via das pentoses fosfato é possível pela análise dos perfis bioquímico dos açúcares e polióis nos fluidos biológicos. Concentrações elevadas destes compostos aparecem em diversas situações patológicas, tais como a diabetes mellitus, a doença renal e hepática e vários erros hereditários do metabolismo dos hidratos de carbono, tais como a galactosemia. Assim, torna-se imperativo ter em conta a grande variabilidade de perfis metabólicos e o conhecimento dos seus significados.

Ao longo desta tese, é nosso objectivo fazer uma revisão sistematizada da via das pentoses fosfato e a sua implicação em estados de doença. Será ainda apresentado e discutido o desenvolvimento e validação dos métodos cromatográficos (GC-FID e GC-MS) desenvolvidos. Finalmente, apresentaremos os resultados preliminares de dois estudos, iniciados com o objectivo de caracterizar os metabolitos intermediários da via das pentoses fosfato em (*i*) uma população pediátrica de casos pré-seleccionados com hepatoesplenomegália de causa desconhecida e/ou com disfunção hepática; e (*ii*) uma população de adultos com disfunção hepática (fígado gordo não alcoólico ou doença hepática devida ao abuso do consumo de álcool). Esperamos descobrir novos biomarcadores ou alterações metabólicas importantes, que possam abrir a porta a futuros estudos para melhor compreender a disfunção hepática.

No estudo efectuado na população pediátrica são apresentados resultados interessantes de um doente em que se descreve pela primeira vez um défice isolado da enzima sedoheptulose cinase (SHPK). Todos os estudos subsequentes, alguns ainda em curso, apoiam a descoberta desta nova deficiência enzimática na via das pentoses fosfato.

No estudo da população adulta com disfunção hepática, os nossos resultados apontam para uma possível importância do perfil dos polióis como biomarcadores da progressão da disfunção hepática.

Palavras-chave: Via das pentoses fosfato; deficiência em ribose-5-fosfato isomerase; deficiência em transaldolase; fígado gordo não alcoólico; deficiência em sedoheptulose cinase.

CHAPTER 1

Aims and outline of the thesis

1. General aims

The Pentose Phosphate Pathway (PPP) comprises two separate branches: (*i*) an oxidative, non-reversible branch, and (*ii*) a non-oxidative, fully reversible branch, fulfilling two major functions: (*a*) the formation of ribose-5-phosphate (R5P) for the synthesis of nucleotides, supporting cell growth and proliferation; and (*b*) the reduction of nicotinamide adenine dinucleotide phosphate (NADPH). NADPH is used as the reducing agent in many biosynthetic reactions and is also used in the cellular oxidative defense system, protecting against oxidative stress either directly by neutralizing reactive oxygen species (ROS) or indirectly via regenerating reduced glutathione (GSH) from its oxidized form GSSG.

The metabolism of glucose through the PPP influences the development of diverse pathologies. Deficiency of the first enzyme of the oxidative branch of the PPP, glucose-6-phosphate dehydrogenase (G6PD), represents the most common genetic defect in humans and causes the depletion of NADPH in red blood cells (RBC), predisposing to oxidative stress-induced hemolytic anemia.

Recently, two new defects in the PPP, namely in the non-oxidative branch, have been described. The first defect, ribose-5-phosphate isomerase (RPI) deficiency, was described in 1999 by Marjo van der Knaaps' group, in a patient with a slowly progressive leukoencephalopathy with mild peripheral polyneuropathy, who remains until the present date, the only patient described as having this enzymatic defect. The second defect is transaldolase (TALDO) deficiency. The first TALDO deficient patient description was made by Verhoeven and co-workers in 2001. The patient presented clinically with liver cirrhosis and hepatosplenomegaly, thrombocytopenia and dysmorphic features. Since this first TALDO deficient patient description, 22 new cases have been described in the literature.

With the expanding number of newly diagnosed TALDO deficient patients and the description of the only RPI deficient patient, the investigations on these inherited metabolic defects of the PPP have increased, leading to better knowledge of their biochemical significance and clinical phenotypes. However, many questions on the pathophysiology of these defects remains unknown, and research regarding these questions has been initiated leading to this master thesis with the following three major goals.

- ✓ The development and validation of a GC-FID method to allow the qualitative and quantitative analysis of polyols' and sugars' profile in healthy people and patients;

- ✓ The characterization of the PPP's intermediate metabolites pattern in an adult population of patients with either non-alcoholic fatty liver disease (NAFLD) or alcoholic fatty liver disease (AFLD), in order to find new biomarkers and/or metabolic signs that may enlighten the understanding of their liver dysfunction;

- ✓ The characterization of the PPP's intermediate metabolites pattern in pre-selected cases, in a pediatric population with unexplained hepatosplenomegaly and/or liver dysfunction, to discover new putative patients with defects in the PPP.

2. Outline of the thesis

In **chapters 1** and **2**, the aims of the thesis and a comprehensive introduction to the pentose phosphate pathway function and malfunction are presented. In addition to the previously cited deficiencies (RPI and TALDO deficiencies), a brief introduction of two other conditions occurring in (*i*) a parallel pathway linked with the PPP, the glucoronate-xylulose pathway, originating the benign condition essential pentosuria, and (*ii*) a recently described enzymatic defect in the L-arabitol dehydrogenase, originating L-arabinosuria, are presented. These two conditions present, as do the RPI and TALDO deficiencies, abnormal sugars' and polyols' profile, which are easily spotted by the GC-FID method developed and presented (**chapter 3**). Also, in the last part of the general introduction, a link between the PPP and cancer metabolism is presented, in order to allow a better understanding of some of the results obtained in **chapter 4**.

In **chapter 3** the development of the analytical methods where, among other parameters, the conditions of the optimized gas chromatographic systems (GC-FID and GC-MS), the qualitative and quantitative data involved in the validation of the GC-FID

method, plus the preliminary results for the building up of the laboratory's reference values are described.

In **chapter 4** the study of an adult population with liver dysfunction is presented. The pre-selected cases enrolled in this study had a liver disease due to either an unknown cause (Non-alcoholic Fatty Liver Disease) or to alcohol abuse (Alcoholic Liver Disease). The main goal of this chapter was the enlightenment and/or establishment of a link between the biochemical intermediate metabolites of the PPP and liver dysfunction. In order to answer our hypothesis, we searched for new biomarkers and metabolic signs that could lead to a better understanding of the liver dysfunction interplay with cell processes. With this study we can postulate a crucial role of the PPP's intermediate metabolites pattern, in assessing liver disease progression, once the pattern of these compounds appears to be altered in advanced or decompensated forms of liver disease.

In **chapter 5** the study of the urinary sugars' and polyols' profile, in a pediatric population presenting liver dysfunction of unknown cause, is presented. In the last twelve years, several cases of patients with defects in the PPP's enzymatic mechanism (RPI deficiency and TALDO deficiency) have been found. Also, these new disorders have been the thrust for screening of new patients. In this chapter, it will be described the first patient, to our knowledge, with an isolated form of sedoheptulokinase (SHPK) deficiency, proving the importance of this method in newborn screening of inherited errors of metabolism (IEM) and also for the evaluation of liver dysfunction progression and/or severity.

CHAPTER 2

General introduction

1. Introduction

1.1. The Pentose Phosphate Pathway

The pentose phosphate pathway (PPP), also known as phosphogluconate pathway or hexose monophosphate shunt, is a multifunctional pathway that comprises two separated branches, with two specific roles: *i)* an oxidative, non-reversible branch that allows reduction of nicotinamide adenine dinucleotide phosphate ($NADP^+$) while glucose-6-phosphate (G6P) is oxidized to a ketopentose phosphate (ribulose-5-phosphate; Ru5P) and carbon dioxide (CO_2); and *ii)* a non-oxidative, reversible branch that connects pentose phosphates to glycolytic intermediates [1, 2]. The PPP does not require oxygen and does not generate ATP. In the oxidative branch G6P is oxidized to Ru5P by two successive reactions. First, the carbon 1 of G6P is oxidized from an aldol to an internal ester (lactone) by glucose-6-phosphate dehydrogenase (G6PD) and 6-phosphoglucono-δ-lactone is formed. The lactone is hydrolyzed to 6-phosphogluconate (the free acid) by a specific lactonase (6-phosphogluconolactonase) and then 6-phosphogluconolactone dehydrogenase (6PGD) further oxidizes carbon 1 to CO_2 leaving the 5-carbon sugar, Ru5P [2]. Two molecules of NADPH (both formed in the two dehydrogenases reactions) and one molecule of Ru5P are the end products of the oxidative phase in the PPP, as shown in Fig. 1.

Ru5P is necessary for the biosynthesis of nucleic acids (RNA and DNA). Higher rates of nucleic acids biosynthesis occurs in growing and regenerating tissues, like the bone marrow, skin and intestinal mucosa, as well as in tumors. The PPP ends, in many tissues, with the formation of ribose 5-phosphate (R5P), CO_2 and two molecules of NADPH and two H^+.

NADPH carries chemical energy in the form of reducing power. NADPH is used almost universally as a major cellular reducing agent in many biosynthetic pathways, being also vital to the cellular oxidative defense system, counteracting the damaging effects of reactive oxygen species (ROS) either directly or indirectly via the regeneration of reduced glutathione (GSH) from its oxidized form (GSSG) [3], as shown in Fig. 2.

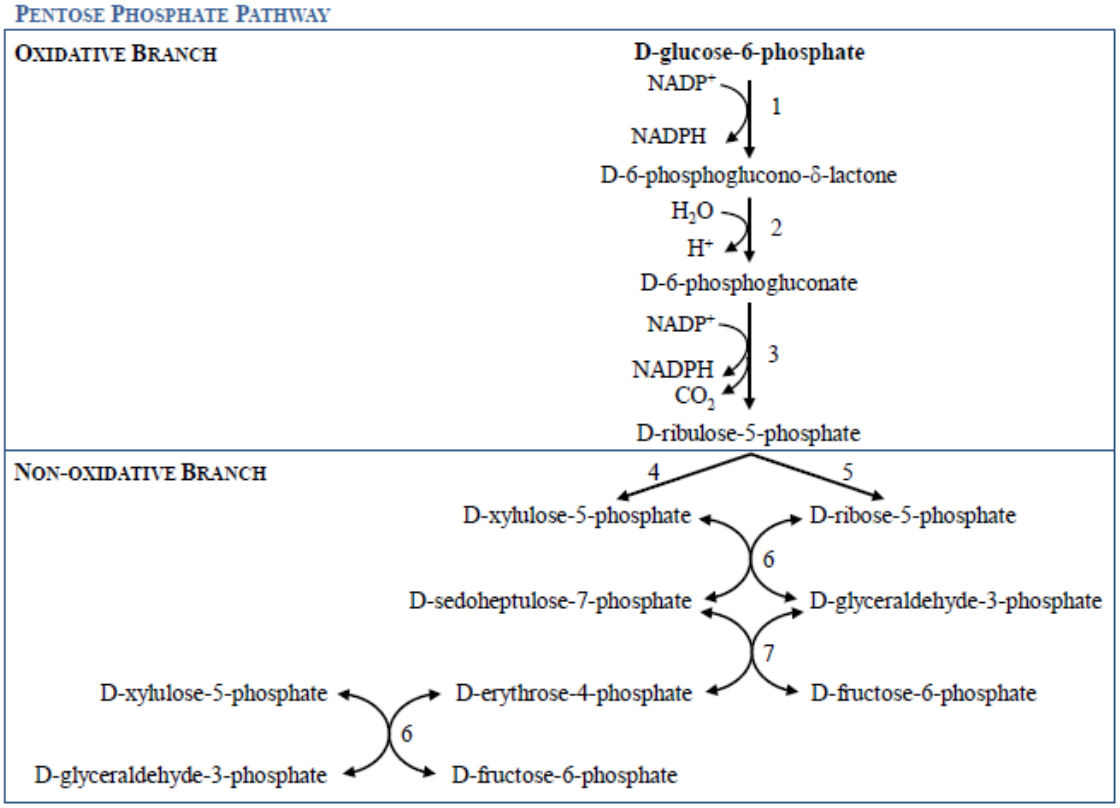

Fig. 1. The oxidative and non-oxidative phases of the pentose phosphate pathway. $NADP^+$, nicotinamide adenine dinucleotide phosphate; NADPH, reduced form; **1)** glucose-6-phosphate dehydrogenase; **2)** 6-phosphogluconolactonase; **3)** 6-phosphogluconolactone dehydrogenase; **4)** ribulose-5-phosphate epimerase; **5)** ribose-5-phosphate isomerase; **6)** transketolase; **7)** transaldolase.

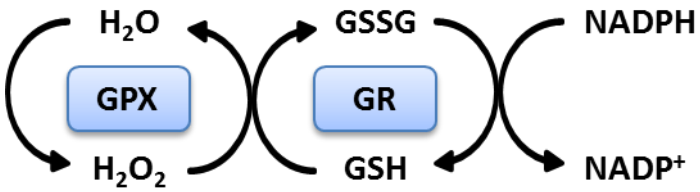

Fig. 2. The glutathione redox cycle. The reduced and active form of glutathione (GSH) converts hydrogen peroxide into water with the help of glutathione peroxidase (GPX). The oxidized form of glutathione (GSSG) is reduced by glutathione reductase (GR) back to GSH in the presence of its cofactor, the reduced form of nicotinamide adenine dinucleotide phosphate (NADPH).

In mammalian tissues actively synthesizing fatty acids and steroids (e.g. mammary gland, adrenal cortex, liver and adipose tissue), NADPH is the major reducing power in these anabolic pathways. NADPH is used in the reduction of the double bonds and carbonyl groups of intermediates in the synthetic process. In tissues

less active in synthesizing fatty acids (e.g. skeletal muscle), the PPP is virtually absent [2].

G6PD is the principal source of NADPH for the antioxidant system, but not the only one. Three other enzymatic sources for NADPH reductions are known: *i*) 6-phosphogluconolactone-dehydrogenase (6PGD); *ii*) malate dehydrogenase (MDH; also known as malic enzyme); and *iii*) cytoplasmic isocitrate dehydrogenase (ICDH) [4].

In tissues that require primarily NADPH rather than R5P, the non-oxidative branch is of major importance and is responsible for the recycling of pentose phosphates to G6P. The first reaction of the non-oxidative phase begins with Ru5P being either epimerized to xylulose-5-phosphate (Xu5P) or isomerized to ribose-5-phosphate (R5P). Then, in a series of rearrangements of the carbon skeletons, six five-carbon sugar phosphates are converted to five six-carbon sugar phosphates, completing the cycle and allowing continued oxidation of G6P with production of NADPH, as shown in Fig. 3 [2].

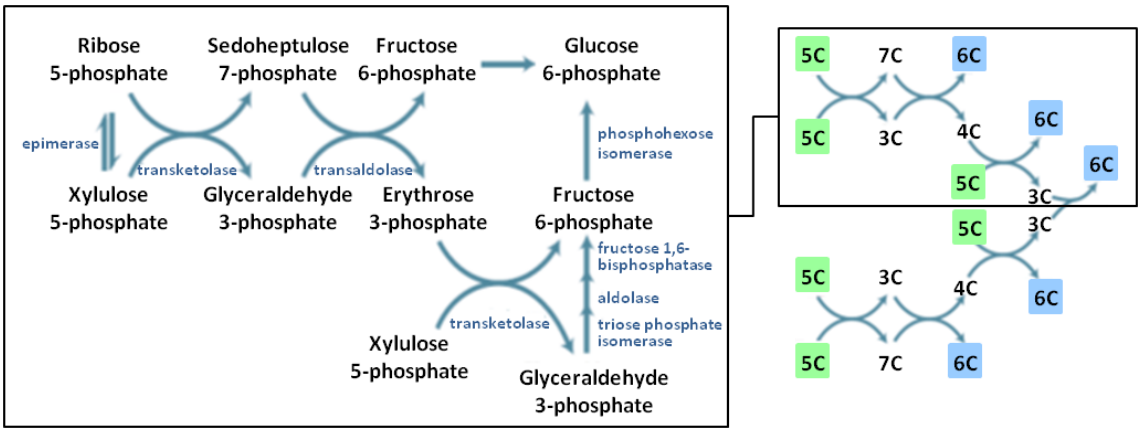

Fig. 3. Reversible (non-oxidative) reactions of the pentose phosphate pathway. Six pentoses (5C) originate five hexoses (6C). Adapted from [2].

There are two enzymes unique to the PPP: transketolase (TKT) and transaldolase (TALDO). TKT is the enzyme responsible for the transfer of C-1 and C-2 of Xu5P to R5P, forming the seven-carbon product (sedoheptulose-7-phosphate; S7P) and a three-carbon fragment (glyceraldehyde-3-phosphate; G3P). After this first step, TALDO catalyzes the removal of a three-carbon fragment from S7P and condenses it with G3P, forming fructose-6-phosphate (F6P) and the tetrose erythrose-4-phosphate (E4P). After this step TKT acts again, this time forming F6P and G3P from E4P and a new molecule of Xu5P. Two molecules of G3P, formed by two cycles of these reactions, can be

converted to a molecule of fructose-1,6-bisphosphate (FBP) as in gluconeogenesis, and finally fructose-1,6-biphosphatase 1 (FBPase-1) and phosphohexose isomerase can convert FBP back to G6P.

The deficient metabolism of glucose through the PPP is associated with development of diverse pathologies. Deficiency of the PPP enzyme G6PD represents the most common genetic defect in humans, accounting for more than 400 million people, and causes the depletion of NADPH in red blood cells (RBC), predisposing to oxidative stress-induced hemolytic anemia [5]. Recently, two new defects in the non-oxidative branch of the PPP were discovered: ribose-5-phosphate isomerase (RPI) deficiency [6] and transaldolase (TALDO1) deficiency [7]. Other defects in metabolic pathways linked to the PPP are known for some time. L-Xylulose reductase, an enzyme responsible for the conversion of L-xylulose to L-xylitol, is an important enzyme in the glucoronate-xylulose pathway (GXP). D-Xylulose can, through the action of xylulokinase, produce Xu5P, and therefore do the connection with the PPP. Also, Diabetes Mellitus and Galactosemic patients have fingerprint profiles of sugars and polyols, and although the deficits in these diseases are not in the PPP, accumulation of characteristic sugars and polyols are the underlying cause of some of the clinical symptoms and health related problems observed in those disorders.

1.2. Glucose-6-phosphate dehydrogenase (G6PD; EC 1.1.1.49)

G6PD is the first and rate-limiting enzyme of the oxidative phase of the PPP. The main role of this enzyme is the provision of reducing power to all cells in the form of reduced nicotinamide adenine dinucleotide phosphate (NADPH) [3] rather than glucose utilization (G6PD accounts for less than 10% of glucose metabolism) [8]. G6PD is a housekeeping enzyme encoded by a housekeeping gene. The gene is expressed in all cells of the body, and although G6PD is a typical cytoplasmic enzyme, some activity is associated with peroxisomes in liver and kidney cells [8]. The G6PD deficiency (**OMIM #305900**) is an X-linked, hereditary genetic defect caused by mutations in the *G6PD* gene. The *G6PD* gene (**ID 2539**) is located on the telomeric region of the long arm of the X chromosome (Xq28 region), and consists of 13 exons. The gene was firstly cloned in 1986 by Persico and co-workers, who isolated cDNA

clones from HeLa cells, SV40-transformed human fibroblasts, human placenta and human teratocarcinoma cell lines, although without mapping the exact localization of the functional sites for G6P and $NADP^+$ binding sites [9].

The G6PD protein, in its active state, consists of homodimers and homotetramers, the proportion of both being pH dependent. The primary structure of the single subunit has been determined from cDNA sequence and consists of 515 amino acids [10].

G6PD deficiency was discovered as the result of a series of investigations performed to understand the reasons behind the development of hemolytic anemia in some individuals treated for malaria with 6-methoxy-8-aminoquinoline drug (primaquine) [7, 8]. Primaquine is just one of many drugs that shorten the RBC lifespan in G6PD deficient patients [10].

More than 400 biochemical variants of G6PD have been described according to measurements of residual enzyme activity, electrophoretic mobility, physicochemical properties (thermostability and chromatographic behavior) and kinetic variables (concentration of substrate needed for an enzymatic reaction at half the maximum speed (*Km*) for G6P; *Km* for $NADP^+$ and pH dependence).

About 140 mutations in the *G6PD* gene have been reported, most of which are single-base substitutions leading to amino acid replacements [3]. In 1967, the World Health Organization (WHO) made the first recommendations to classify the G6PD deficient variants, using only the measurements of residual enzyme activity and electrophoretic mobility for biochemical characterization of the enzyme. In 1989 the same organism expanded the biochemical characteristics of the enzyme [13]. The variants were classified in five classes: *i)* class I variants are severely deficient and patients are associated with a chronic non-spherocytic haemolytic anaemia (CNSHA); *ii)* class II variants have less than 10% of residual enzyme activity but without CNSHA (include the common Mediterranean and common severe oriental variants); *iii)* Class III variants are moderately deficient with 10-60% residual enzyme activity (include the common African form); *iv)* Class IV variants have normal enzyme activity; *v)* and in Class V the enzyme activity is increased [13].

G6PD deficient individuals may be asymptomatic throughout life. The illness generally manifests as: (*1*) chronic non-spherocytic hemolytic disease; (*2*) acute haemolytic anaemia or (*3*) neonatal jaundice triggered by infection, administration of oxidative drugs or ingestion of fava beans [3].

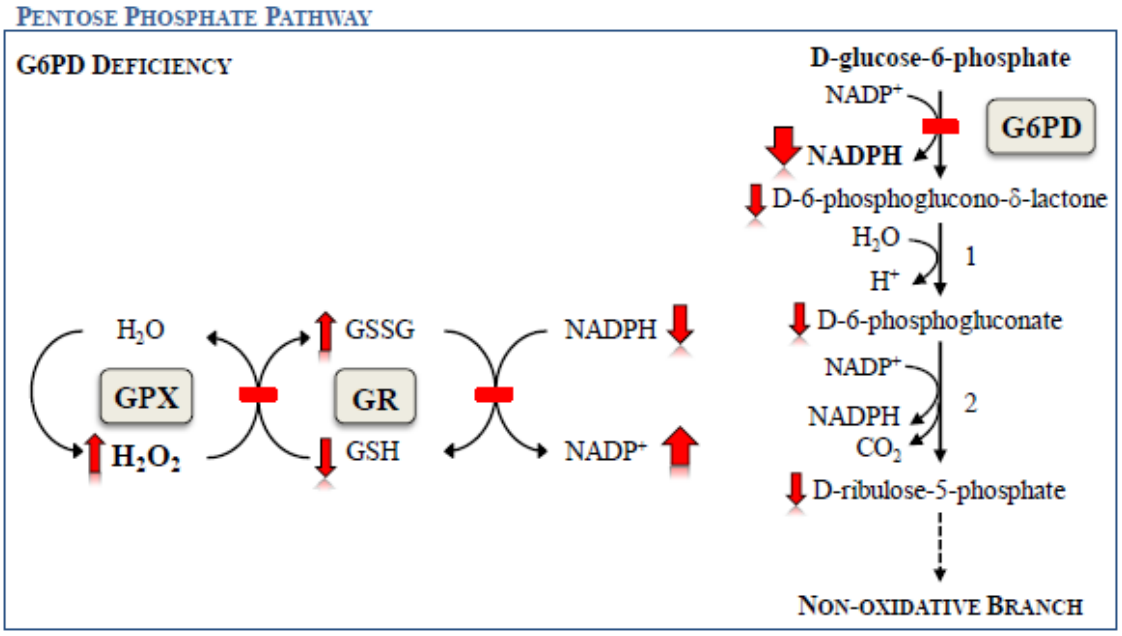

Fig. 4. Schematic presentation of the oxidative phase of the pentose phosphate pathway in glucose-6-phosphate dehydrogenase (G6PD) deficiency. **1)** 6-phosphogluconolactonase; **2)** 6-phosphogluconolactone dehydrogenase. G6PD deficiency leads to reduced levels of NADPH. NADPH is crucial for the detoxification of hydrogen peroxide (H_2O_2) in all cells, but particularly in RBC. NADPH is the substrate of glutathione reductase (GR), the enzyme responsible for catalyzing the regeneration of GSSG to GSH, when it has been oxidized by glutathione peroxidase (GPX).

1.3. Ribose-5-phosphate isomerase (RPI; EC 5.3.1.6)

RPI catalyzes the reversible conversion between the ketose R5P and its isomer, the aldose Ru5P. The enzyme exists as two distinct proteins, RpiA and RpiB. RpiA is present in nearly all organisms, while RpiB is present in bacteria and trypanosomatids. Although the same reaction is catalyzed by both proteins, they show no sequence or structural homology [14].

The human *RPIA* gene (**ID 22934**) is located in the short arm of chromosome 2 (2p11.2 region) and is highly conserved in most organisms. Mutations in this gene cause ribose-5-phosphate isomerase deficiency (RPI deficiency, **OMIM #608611**). In 1999, van der Knaap and co-workers [15] described a patient with slowly progressive brain white matter disease (leukoencephalopathy) of unknown origin, and mild peripheral polyneuropathy. The patient had no organomegaly or dysfunction of internal organs. The usual metabolic screening done to this patient revealed no abnormal results in the amino acids', organic acids', purines', pyrimidines', oligosaccharides' and mucopolysaccharides' patterns [15]. The only altered results were marked elevations of

arabitol and ribitol in urine, plasma and cerebrospinal fluid (CSF). A defect in the PPP was hypothesized and in 2004 Huck and co-workers characterized the defect as RPI deficiency (see Fig. 5) [6]. Until now, only one single diagnosed case of RPI deficiency has been described, making it one of the rarest diseases [16]. Because of these biochemical findings, the full-length *RPIA* cDNA was sequenced, and the authors found two different mutations, a single base-pair deletion (c.540delG) and a nucleotide substitution (c.182C>T), inherited from the mother and the father, respectively. The deletion causes a frameshift change with asparagine 181, leading to a premature termination of RPI protein translation, with a stop codon 17 amino acids downstream (p.N181fsX17). The missense mutation, c.182C>T, leads to the substitution of an alanine by a valine at codon 61 (p.A61V) [6].

These mutations were not found in 220 control chromosomes of individuals of Northern Europe descent, indicating that those mutations are not likely to represent polymorphisms, but instead are pathogenic mutations. The truncated RPI protein encoded by the frameshift allele was not detected by Western blot, indicating that this protein is not expressed or is rapidly degraded. RPI concentrations in both lymphoblasts and fibroblasts of the patient showed a marked decline. These results were confirmed by quantitative mass spectrometry and a decline of around 30% in RPI levels was measured in the lymphoblasts of the patient, when compared to controls. Reinforcing these data, qPCR demonstrated that *RPIA* mRNA levels were strongly reduced in patient's cells, around 40% in lymphoblasts and about 1% in fibroblasts, when compared to controls. A cell type-dependency was demonstrated, having been reported an enzyme activity of 30% in lymphoblasts and an activity bellow the assay's detection limit in fibroblasts [16].

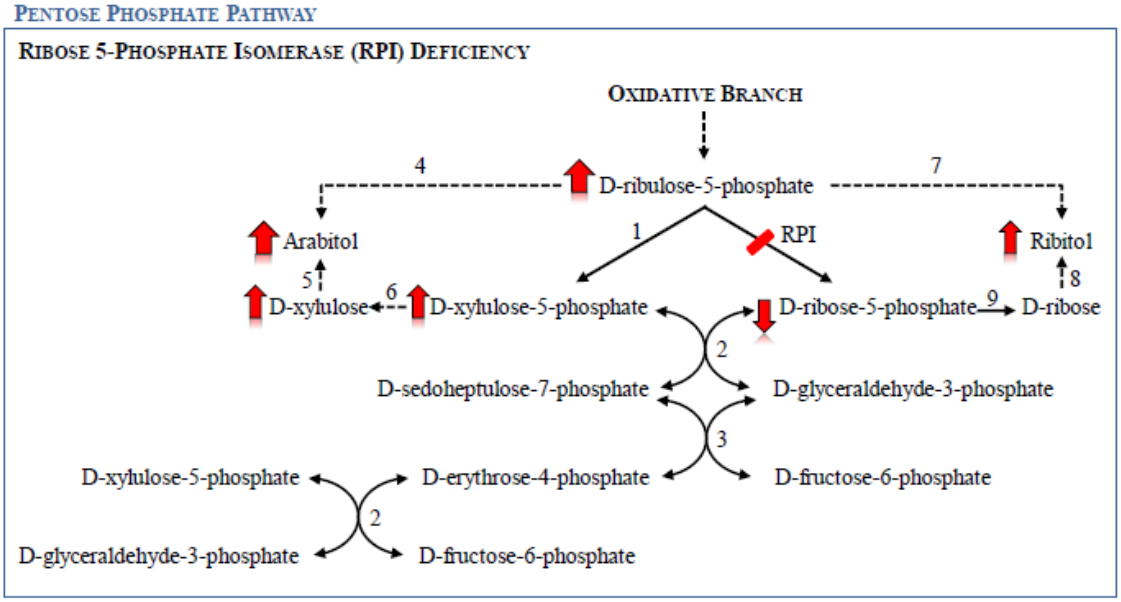

Fig. 5. Schematic presentation of the pentose phosphate pathway in a ribose-5-phosphate isomerase (RPI) deficiency situation. **1)** ribulose-5-phosphate epimerase, **2)** transketolase, **3)** transaldolase, **4)** D-ribulose reductase, **5)** D-arabitol dehydrogenase; **6)** xylulokinase; **7)** NAD(P)-independent ribitol dehydrogenase, **8)** D-ribose reductase, **9)** ribokinase. Little is known about mammalian pentitols formation. The dotted arrows represent presumed reactions, based in reactions occurring in microorganisms. Adapted from [6].

1.4. Transaldolase (TALDO; E.C.2.2.1.2)

TALDO is the second and rate limiting-enzyme of the non-oxidative branch of the PPP, catalyzing the reversible transfer of a three-carbon keto unit, corresponding to dihydroxyacetone (DHA), from sedoheptulose-7-phosphate (S7P) to glyceraldehyde-3-phosphate (G3P) generating erythrose-4-phosphate (E4P) and fructose-6-phosphate (F6P) [2]. The *TALDO1* gene (**ID 6888**) is located in the short arm of chromosome 11 (11p15.4-p15.5 region) [17], and is highly conserved in most organisms. Humans possess a single gene for transaldolase [18], and until now no isoforms of TALDO are known. Mutations in this gene cause TALDO deficiency (**OMIM #606003**).

The first description of a TALDO deficient patient was made by Verhoeven and co-workers in 2001 [7]. The patient was the first child of healthy, consanguineous Turkish parents. The patient presented low birth weight, mild bleeding problems and underwent, soon after birth, a surgical correction of aortic coarctation. Within several months, this patient developed liver cirrhosis and hepatosplenomegaly. She was diagnosed at the age of 10 years. At this age she presented thrombocytopenia,

hepatosplenomegaly, enlarged clitoris, and mildly increased coagulation times. Her neurological examinations showed normal results [7].

In 2005, Verhoeven and co-workers [19] described the second patient with TALDO deficiency. The patient was the first of dizygotic female twins delivered by emergency at 36 weeks' gestation. The parents were of Turkish origin (as the first case reported), and also consanguineous. Clinical symptoms in the neonatal period were related to severe liver failure (severe coagulopathy, low serum protein, elevated blood ammonia and hypoglycemia), generalized oedema, and this patient also featured moderate muscular hypotonia and dysmorphic signs (down-slanting palpebral fissures, low-set ears and increased intermamillary distance). Karyotype analysis demonstrated XX/XO mosaicism. The patient died at day 18 due to bradycardic heart failure. Remarkably, both patients showed transaminases and γ-glutmayltransferase levels within the reference range [19].

In 2006, Valayannopoulos and co-workers [20] described four patients from the same family. The parents were first cousins from Turkish origin. The couple had no healthy children. The four patients shared the same biochemical and molecular defect. They had hydrops fetalis and congenital multiorgan involvement. The major clinical signs described were: dysmorphic features, liver dysfunction with elevated aminotransferase levels and low albumin, hepatosplenomegaly, thrombocytopenia, hemolytic anemia (with schistocytes), renal involvement and heart problems [20]. Neurological examination showed normal results for all surviving patients [7, 19, 20].

In 2007, Fung and co-workers [21] described a boy of a consanguineous Pakistan couple, with intrauterine growth retardation (IUGR) in the antenatal period; and hypoglycemia, thrombocytopenia, hepatosplenomegaly and deranged liver function and coagulation in the post-natal period. The patient developed failure to thrive, transient hypoglycemia and persistently mild thrombocytopenia [21].

In 2008, Wamelink and co-workers [22] described a new TALDO deficient patient. The patient was the fourth child of consanguineous parents of Arabic ethnicity. The patient was born with hepatosplenomegaly and developed jaundice and thrombocytopenia. He had to be ventilated at day 9 because of poor respiratory effort. The patient developed cirrhosis but had no inflammatory infiltrate. Until now, this is the only TALDO deficient patient that has been described with rickets and deafness [22].

In 2009, Tylki-Szymanska and co-workers [23] described two cases of TALDO deficient patients of Polish origin. The patients were siblings of a healthy

consanguineous couple. Both patients presented hemolytic anemia and hypoproteinemia, hepatosplenomegaly (with mildly elevated serum transaminases in the first child and normal levels in the younger brother), thrombocytopenia and haemorrhagic diathesis with skin bleeding [23].

In 2011, Balasubramaniam and co-workers [24] described the first TALDO deficient patient born from a nonconsanguineous couple of Chinese ethnicity. He presented at birth with hydrops fetalis and hypoalbuminemia. At the age of 2.5 months a splenomegaly (with normal liver and kidney function and blood parameters) with febrile illness was noted. Shortly after this febrile episode he was readmitted with seizures, jaundice, discrete dysmorphic features (cutis laxa), hepatosplenomegaly (with mildly elevated transaminases, bilirrubinemia and raised alkaline phosphatase), thrombocytopenia and Coombs negative hemolytic anemia. The patient died at the age of 4.5 months with flavobacterium sepsis and multiorgan failure [24].

In 2013, Eyaid and co-workers [25] described twelve new cases of TALDO deficient patients from six Saudi consanguineous families. All patients shared clinical signs, being the principal findings IUGR, dysmorphic features, cardiac defects, hepatosplenomegaly, anemia and thrombocytopenia. As the authors followed part of the patients along childhood, it permitted to track the natural history of the disease over a larger number of years. The authors described that dysmorphic features (e.g. anti-mongoloid slant, low set ears, cutis laxa) tend to disappear after the infancy, being more recognizable in the neonatal period. The bleeding tendency and liver involvement follows a more irregular course. The liver involvement was not always progressive and its severity was variable even within different members of the same family. None of these twelve patients presented hemolytic anemia, in contrast to the previously described patients, and all presented cardiac problems [25].

All twenty-three patients described so far [7, 19–25] have the same sugars' and polyols' profile: elevated urinary concentrations of arabitol, ribitol, erythritol and sedoheptulose (see Fig. 6), and normal CSF profile. All patients, but the patients described by Tylki-Szymanska and co-workers and Fung and co-workers, presented elevated levels of D-arabitol, ribitol and erythritol in plasma. One can deduce that these patients would show the same plasmatic pattern of these compounds (i.e. elevated levels of D-arabitol, ribitol and erythritol) if plasma samples would have been analyzed.

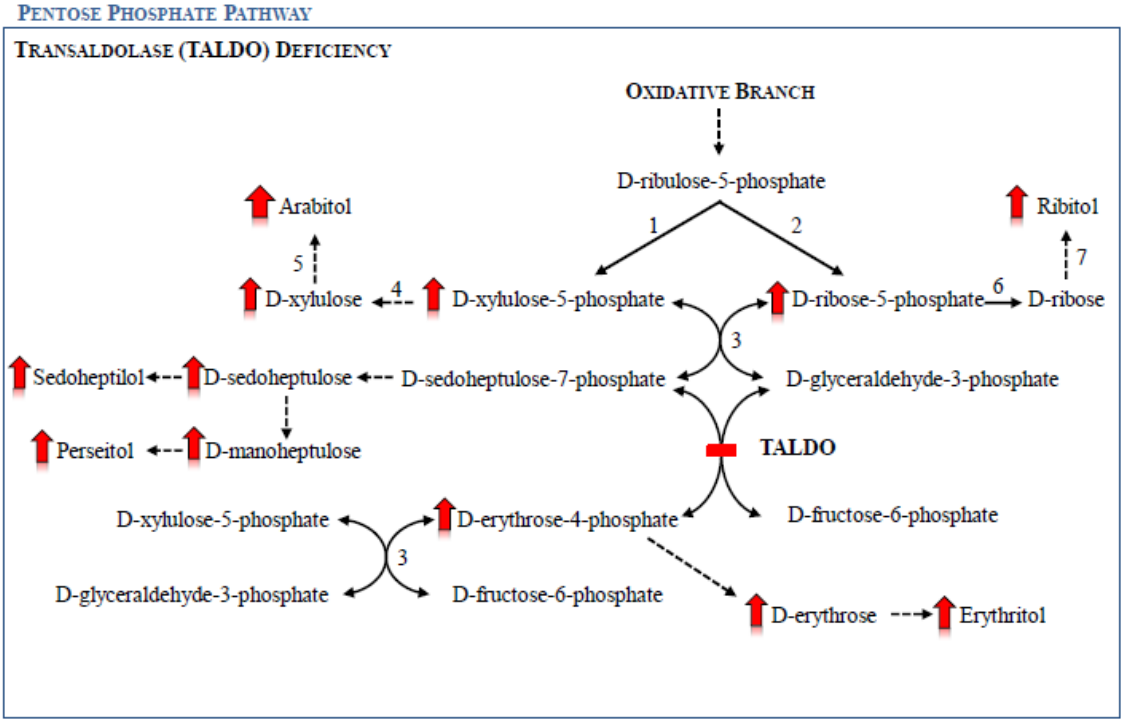

Fig. 6. Schematic presentation of the pentose phosphate pathway in a transaldolase (TALDO) deficiency situation. **1)** ribulose-5-phosphate epimerase, **2)** ribose-5-phosphate isomerase, **3)** transketolase, **4)** xylulokinase, **5)** D-arabitol dehydrogenase; **6)** ribokinase, **7)** D-ribose reductase. The dotted arrows represent presumed reactions, based in reactions occurring in microorganisms. Adapted from [26]

Until now, the mutations found in TALDO deficient patients were: *i)* the homozygous deletion of three residues (corresponding to nucleotides 511-513) of the human *TALDO1* cDNA, leading to the deletion of the amino acid serine at position 171 (p.Ser171del) [15, 17]; *ii)* the homozygous missense mutation c.575G>A leading to the substitution of the amino acid arginine by a histidine at position 192 (p.Arg192His) [19]; *iii)* the homozygous missense mutation c.574C>T leading to the substitution of the amino acid arginine by a cysteine at position 192 (p.Arg192Cys) [9]; *iv)* the homozygous single base pair deletion (c.793delC) leading to a frameshift with premature truncation (p.Gln265ArgfsX56) [25]; and *v)* two heterozygous missense mutations: *a)* a deletion of 3 nucleotides in exon 7 (c.895_897delAAC), leading to the deletion of an asparagine at position 299 (p.Asn299del), inherited from the father; and *b)* a missense mutation c.931G>A in exon 7, leading to the substitution of the amino acid glycine by arginine at position 311 (p.Gly311Arg), inherited from the mother of the patient [24].

The deletion of three base pairs (c.511_513delTCC) is responsible for the production of a TALDO enzyme with no activity. Northern-blot analysis showed

normal *TALDO*Δ511-513 mRNA levels but Western-blot analysis showed no TALDOΔS171 protein in fibroblasts and lymphoblasts of the patient. The gene is transcribed and translated *in vitro*, but TALDOΔS171 has no detectable activity. The deletion of Ser171 resulted in conformational changes affecting the correct protein folding, leading to: *1)* aggregation of misfolded protein, *2)* dominance of the mutant protein leading to loss of wild-type activity, and *3)* loss of function due to degradation of the mutant protein [27].

Arginine 192 has been proposed to be part of the catalytic site of the enzyme. This region is highly conserved, as are the amino acids asparagine at position 299 and glycine at position 311 [28]. This, and the fact that in 210 control alleles none had a mutation in this region, indicates that those missense mutations p.Arg192His, p.Arg192Cys, and the p.Asn299del mutation, are pathogenic [22]. Table 1 summarizes the clinical and molecular features of all patients described until now.

Table 1. Clinical and molecular features of the 23 TALDO deficient patients diagnosed to date.

Clinical Features	**Cases reported**[b]
Consanguinity	22/23
Hepatosplenomegaly	22/23
Anemia	21/23
Thrombocytopenia	21/23
Cardiac problems	20/23
Liver dysfunction	18/23
Dysmorphia	17/23
Wrinkly skin	16/23
Neonatal edema	7/23
Renal abnormalities	7/23
Premature death	6/23
Respiratory dysfunction	3/23
Developmental delay	2/23[a]
Molecular Features	
c.793delC (p.Gln265ArgfsX56) homozygous	12/23
c.511_513delTCC (p.Ser171del) homozygous	5/23
c.575G>A (p.Arg192His) homozygous	4/23
c.574C>T (p.Arg192Cys) homozygous	1/23
c.931G>A (p.Gly311Arg)/c.895_897delAAC (p.Asn299del) compound heterozygous	1/23

[a] Sensor neural deafness in one patient and initial mild delay with later catch-up in the other
[b] Verhoeven 2001, Verhoeven 2005, Valayannopoulos 2006, Fung 2007, Wamelink 2008, Tylki-Szymanska 2009, Balasubramaniam 2011 and Eyaid W, 2013

1.5. Xylulose reductase (XR; E.C.1.1.1.10)

L-xylulosuria or Essential Pentosuria (**OMIM #608347**) was firstly appointed as an inborn error of metabolism, with no apparent clinical consequences, in 1908 by Sir Archibald Garrod in his fourth Croonian Lecture [29]. The disease is characterized by high excretion of L-xylulose in the urine (1 to 4 g of the pentose *per* day) [30]. The disorder had been first described in 1892 by Salkowski and Jastrowitz [31], but it was only with the work of Levene and La Forge [32], in 1914, that the sugar excreted in such high concentrations was established as being xylulose [32]. In 1930, Greenwald characterized it as the enantiomorph D-xylulose [33]. However, in the same year, he wrote a correction letter to the same review stating that the sugar was indeed L(+)-xylulose and not the previous D-xylulose [34]. The metabolic defect in essential pentosuria is at the level of xylulose reductase, an important enzyme of the glucoronic acid oxidation pathway, responsible for the conversion of L-xylulose to L-xylitol [30]. The condition was described in 1936, by Lasker and co-workers, as an inherited autosomal recessive characteristic [35] almost limited to persons of the Ashkenazi Jewish ancestry. The first reported case of a non-Hebrew patient with pentosuria was done by Barnes and Bloomberg in 1953, where they described the condition in two Lebanese sisters with no known Jewish ancestry [36]. After this case report, Politzer and Fleishmann in 1962 studied 127 members of a Lebanese family and found 10 cases of pentosuria. Nevertheless, due to the fact that not all samples of the ten affected members gave positive results at all times (the study lasted for four years), the authors postulated that the inheritance could be considered as dominant with poor penetrance [37]. It was also in 1962 that Khachadurian described twelve cases of pentosuria in three highly inbred Lebanese families, establishing, once and for all, the inheritance of pentosuria as having a Mendelian recessive pattern [38].

By ion-exchange chromatography of red cells' L-xylulose reductase, Lane and co-workers [39] showed in 1984 that the enzyme existed in two isoforms, a minor and a major. The authors also showed that the pentosuric patients lacked the major isozyme, the isoform responsible for the conversion of the bulk of L-xylulose to xylitol in the glucoronic acid pathway, thus leading to the accumulation and excretion of high amounts of L-xylulose in urine (Fig. 7). The major and minor isoforms were postulated to be encoded by two separate genes, since normal individuals and pentosuric patients had similar amounts of the minor isozyme [39].

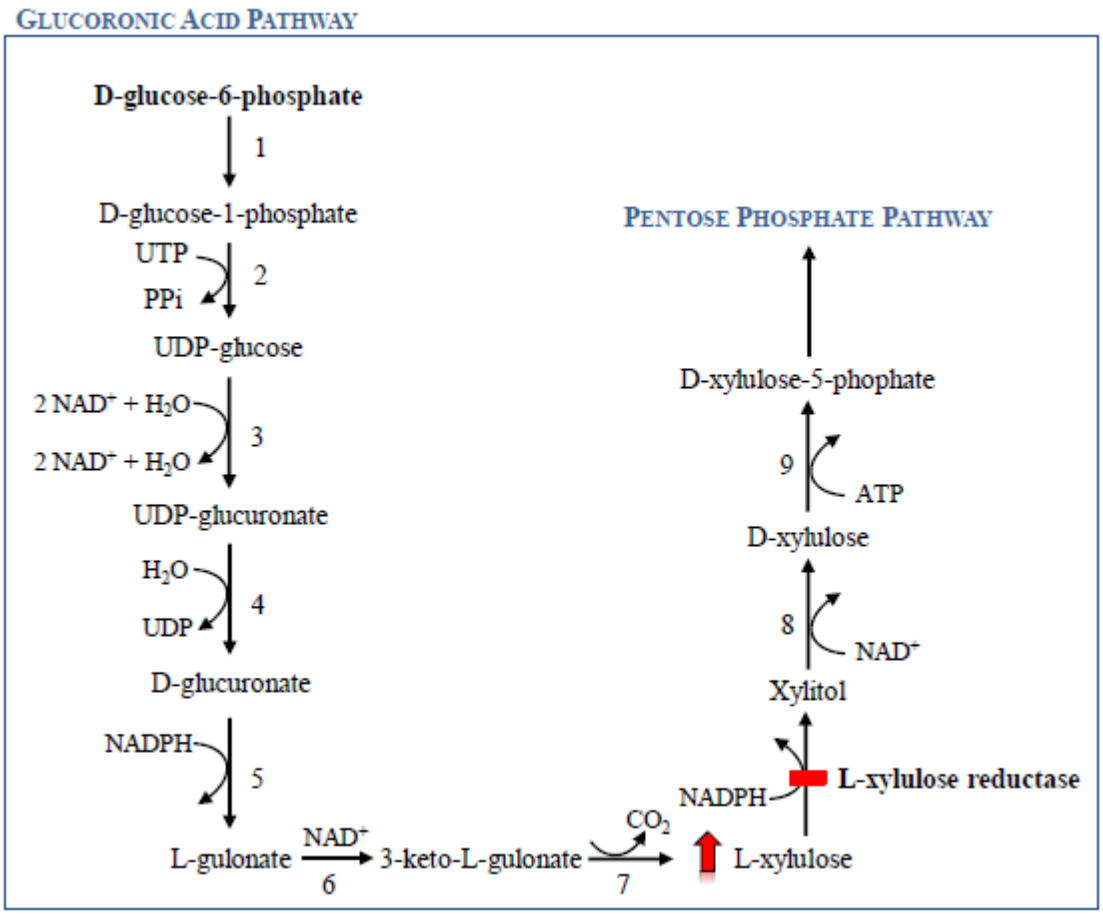

Fig. 7. Schematic presentation of the glucoronic acid pathway and its link to the PPP. **1)** Phosphoglucomutase, **2)** UDP-Glucose pyrophosphorylase, **3)** UDP-Glucose dehydrogenase, **4)** UDP-Glucuronidase; **5)** Glucuronate reductase, **6)** L-Gulonate 3-dehydrogenase, **7)** Decarboxylase, **8)** Xylitol dehydrogenase, **9)** D-Xylulokinase. Adapted from [40].

In 2002, Nakagawa and co-workers [41] characterized a ubiquitous enzyme that was highly expressed in liver and kidney, with a NADPH-linked reductase activity for α-dicarbonyl compounds and responsible for the conversion between L-xylulose and xylitol. Due to its activity, the enzyme was designated as dicarbonyl/L-xylulose reductase (DCXR), belonging to the short-chain dehydrogenase/reductase (SDH) superfamily [41].

The *DCXR* gene (**ID 51181**) is located in the long arm of chromosome 17 (17q25.3 region). The active protein is a homotetramer, with each subunit consisting of 244 amino acid residues. Xylulose reductases (XRs) are highly conserved in organisms. The amino acid sequences of human, mouse, rat, guinea pig, and hamster share very high identities (83–99%) [42]. Pierce and co-workers [43] studied the *DCXR* gene in members of fifteen previously described pentosuric families, and found that the most

prevalent mutation was a single base-pair deletion, *DCXR* c.583ΔC, inducing a frameshift that led to a premature stop codon six residues downstream (p.His195fs6X). This mutation was found in homozygosity in six probands. Furthermore, six children of deceased probands were also carriers for this mutation. Another mutation altering the splice donor site of intron 1, *DCXR* c.52+1G>A, was also found in homozygosity in one proband and in heterozygosity in combination with the previous mutation (c.52+1G>A and c.583ΔC) in two other patients [43].

The c.583ΔC mutation leads to a protein lacking more than 50 C-terminal amino acids, translating in a non-functional protein, once the C-terminal domain is responsible for the interactions between the monomers [42]. The *DCXR* c.52+1G>A mutation leads to mutant *DCXR* alternative transcripts. No DCXR protein was detectable in pentosuric patients with both genotypes, and heterozygous individuals had DCXR protein levels substantially lower than controls [43].

Essential pentosuria did not seem to have deleterious health or lifespan effects in patients and it was considered a benign condition. Furthermore, because the first biochemical tests used were not specific and gave raise to misleading diagnosis of diabetes, the screening for this condition was abandoned. The last update of the number of cases with established essential pentosuria (*ca.* 200) was reported, in 1958, by Eugen Knox [44].

1.6. L-Arabinosuria

L-Arabinosuria is a benign condition, marked by the excretion of high amounts of L-arabinose and L-arabitol in urine, plasma and CSF, after ingestion of fruit. The proposed enzyme defect is thought to be in L-arabitol dehydrogenase (**E.C.1.1.1.12**), although this has not yet been proven [45]. In 2002, Onkenhout and co-workers [45] described the only known case of L-arabinosuria, a sixteen-months-old girl of Egyptian/Dutch origin (non-consanguineous parents). The patient presented delayed motor development and facial dysmorphism (macrocephaly, palatoschizis and skeletal abnormalities). The mental development seemed to be normal at that time (although difficult to assess), and she was on a regular diet. No liver or kidney malfunctions were present. At the age of four years, her mental development was evaluated and considered normal (she was sociable and spoke Dutch and Arabic). All tests (plasma amino acids,

lactate, pyruvate, very-long-chain fatty acids and sialotransferrine isoelectric focusing, as well as urinary oligosaccharides, mucopolysaccharides and (free) sialic acid) showed normal results, except for reducing sugars in urine, although normal glucose levels were found. Galactose was high, but clinical background excluded galactosemia. Urinary sugars' and polyols' profiling by GC-MS was performed, and showed high excretion of arabitol (see Fig. 8), and a slightly increased excretion of fructose and xylose in urine (xylitol was in the normal range). Increased levels of arabitol and arabinose were also found in patient's plasma and CSF. Urinary organic acids showed a large unknown peak, later identified as arabinoic acid (-lactone). When the patient had fruit removed from her diet, the excretion of arabinose normalized in one week, and in a six-week interval, urine, plasma and CSF presented normal levels of arabitol and arabinose. Although the treatment is based on a fruit-free diet, prolonged intake of L-arabinose food sources does not seem to have deleterious effects in human health [45].

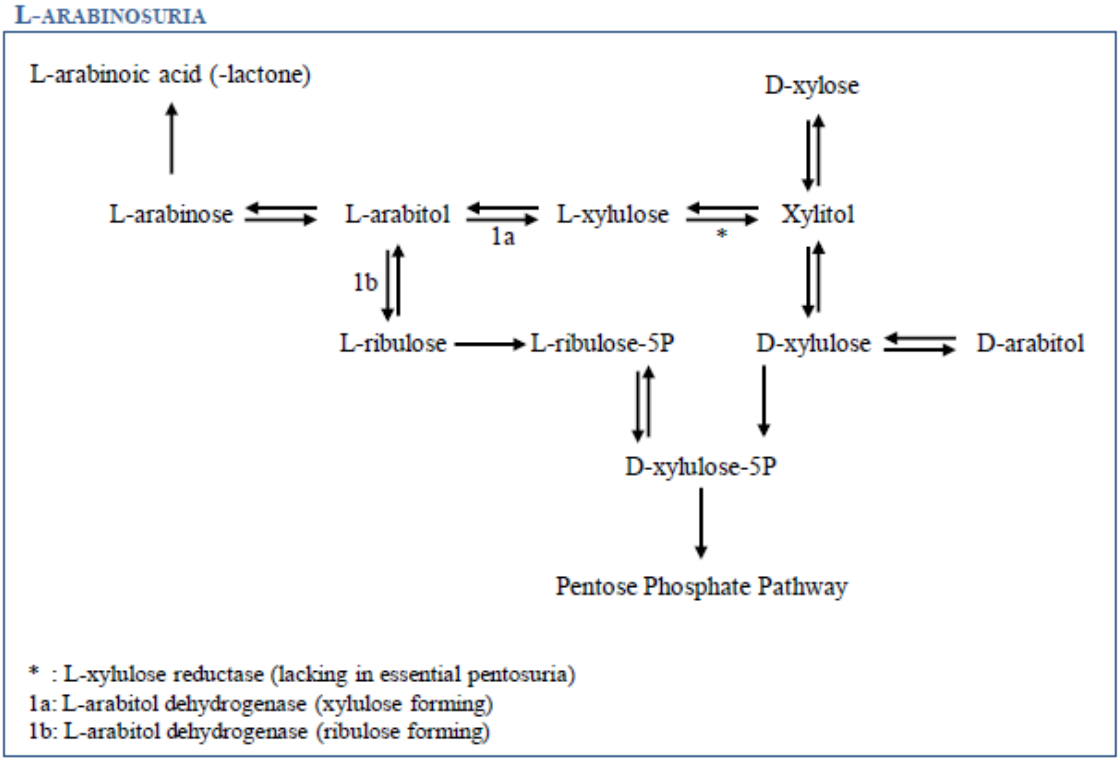

Fig. 8. Human pentose inter-conversion suggested by Onkenhout *et al.*, explaining the formation of L-arabinoic acid (-lactone), D-arabitol and L-arabitol. L-arabitol metabolism seems more likely to occur *via* L-xylulose than through L-ribulose. Adapted from [45].

1.7. The PPP and tumor cells' metabolism

Since the 1920s it is known that tumor cells display increased rates of glucose metabolism compared with normal tissues. Normal cells mainly produce energy from mitochondrial oxidative phosphorylation, whereas tumor cells mainly rely on fermentation to produce the energy needed, even in the presence of oxygen [46]. This phenomenon is denominated as the Warburg effect or aerobic glycolysis. In 1926, Warburg and co-workers demonstrated that about 66% of the glucose consumption, in tumor slices, was through fermentation, and the remainder through respiration despite the availability of oxygen [46]. The same authors also showed that in the time needed for a cancer tissue to metabolize 1 molecule of glucose by oxidative phosphorylation (yielding 36 ATP molecules), 12 more glucose molecules were converted to 24 lactic acid molecules, in normoxic conditions, by the so called aerobic glycolysis (yielding a total of 60 ATP molecules) [47]. The oxidative phosphorylation persists at the same time as aerobic glycolysis in the vast majority of tumors, if not all, continuing to supply energy necessary for housekeeping functions and biosynthetic reactions [41, 42]. For most mammalian cells metabolism, the major catabolic molecules are glucose and glutamine, being responsible for supplying carbon, nitrogen, free energy, and reducing equivalents required to cell growth and division [50]. So, if all glucose molecules were to be catabolized to CO_2 by the oxidative phosphorylation to produce ATP, all the other needs of a growing cell (e.g. acetyl-CoA to produce fatty acids, glycolytic intermediates for nonessential amino acids to produce proteins, and ribose for nucleotides) would not be supplied. In 2007, using ^{13}C Nuclear Magnetic Resonance (NMR) spectroscopy, DeBerardinis and co-workers [51] showed that more than 90% of total glucose metabolism was spent in the production of lactate and alanine, and 60% of total glutamine utilization was also used in the production of these compounds. Very importantly, a by-product of glutaminolysis, *i.e.* glutamine conversion to lactate by the action of malate dehydrogenase (malic enzyme; ME), is NADPH [51]. Also lactate production involving the enzyme lactate dehydrogenase (LDH) produces NADPH [50]. These NADPH molecules can supply other anabolic processes such as fatty acid synthesis and, together with ribose-5-phosphate (derived from the PPP), nucleotide synthesis [52]. The majority of acetyl-CoA is derived from glucose, and the majority of oxaloacetate (OOA) is derived from glutamine (accounting for a very important anaplerotic role in the TCA cycle) [51]. So, an inefficient usage of cellular resources, as

it appeared to be the Warburg effect, in which glucose produces lactate, ergo not exploiting the full capacity of oxidative metabolism to produce the so needed ATP, proved in fact to be an important pathway for faster incorporation of carbon into biomass, facilitating the huge requirements of rapid cell divisions [48, 49].

Many metabolic routes regarding (de)regulation of cell metabolism in cancer cells, like fatty acids synthesis and mitochondrial respiration, are known and have been strongly studied, but in the purpose of this thesis, only aspects linked with the PPP have been highlighted and will be further discussed. Increased understanding of these complex networking pathways is needed to better characterize tumor cells metabolism, allowing the future development of new therapeutic targets in inhibition of cancer cells growth and proliferation.

1.7.1. The PPP and tumor cells' metabolism: p53 and G6PD

The PPP is an important pathway for glucose catabolism and biosynthesis, playing a major role in providing key biosynthetic intermediates as NADPH and R5P. These intermediate metabolites are pivotal to cell proliferation, turning the PPP in an attractive metabolic route of target in tumor cells [53]. Recent studies have demonstrated that G6PD is overexpressed in certain tumor types (gastric, colorectal [54] and kidney tumors [55]). Furthermore, G6PD has been shown to be negatively regulated by wild-type but not mutant p53 [56]. p53 is a known tumor suppressor responsible for cell cycle arrest, DNA repair and apoptosis [57], and now an important role in modulating cancer cell metabolism is being "awarded" to p53.

p53 is the most frequently mutated tumor suppressor gene in human cancers, and since its product binds to G6PD (inhibiting its activity), a mutated p53 will lead to a strong enhancement of PPP flux (~ 50%) by lack of G6PD activity regulation [56]. Studies performed by Jiang and co-workers [56] in $p53^{-/-}$ human colon cancer HCT116 cell line showed a strong increase in NADPH levels (~ 2 folds). The authors also studied the NADPH levels in heart, liver, kidney and lung tissues from $p53^{-/-}$ mice, finding elevated levels compared to the corresponding tissues from $p53^{+/+}$ mice. Furthermore, p53 does not change the levels of *G6PD* transcript. It acts by disrupting the formation of the dimeric G6PD holoenzyme. G6PD needs $NADP^+$ for the formation of the holoenzyme, and the diminished interaction between G6PD and $NADP^+$ when

p53 binds, leads to disruption of the active dimeric G6PD formation (Fig. 9). These results are highlighted by the impaired interaction of G6PD and p53 in the presence of NADPH, in a dose-dependent manner [56].

1.7.2. The PPP and tumor cells' metabolism: p53 and TIGAR

TIGAR (*TP53-induced glycolysis and apoptosis regulator*) gene is located in the short arm of chromosome 12 (12p13-3 region) and contains six potential coding exons and two possible p53 binding sites (BS1, upstream of the first exon, and BS2 within the first intron). By microarray analysis, *TIGAR* gene was identified as inducible by p53 [58]. Bensaad and co-workers [58] demonstrated that TIGAR protein shares similarities with proteins from the phosphoglycerate family (PGM), mainly with the biphosphatase domain of the different isoform products of the four genes (*pfkfb* 1-4) encoding the enzyme 6-phosphofructokinase 2/fructose-2,6-biphosphatase (PFK-2/FBPase-2). This is a bifunctional enzyme, with both kinase (NH_2-terminal region of the enzyme) and phosphatase (COOH-terminal region) activities. TIGAR only shows similarities with the biphosphatase domain of PFK-2/FBPase-2, therefore only having the capability to dephosphorilate substrates [58].

PFK-2/FBPase-2 regulates the synthesis (PFK-2; **E.C.2.7.1.105**) and degradation (FBPase-2; **E.C.3.1.3.46**) of intracellular fructose-2,6-biphosphate (Fru-2,6-P_2). This compound is a potent allosteric effector of 6-phosphofructokinase 1 (PFK-1), stimulating glycolysis and inhibiting gluconeogenesis. TIGAR, through the dephosphorylation of Fru-2,6-P_2, inhibits PFK-1 leading to accumulation of fructose-6-phosphate (F6P). F6P is isomerized to glucose-6-phosphate (G6P) by phosphoglucose isomerase and G6P is diverted to the PPP (Fig. 9). The shift of G6P to the PPP leads to increased production of NADPH and R5P, important precursors of DNA biosynthesis and repair, also lowering apoptosis due to increased generation of reduced glutathione (GSH) and removal of reactive oxygen species (ROS) [58].

1.7.3. The PPP and tumor cells' metabolism: The transketolase family

Transketolase (**TKT; E.C.2.2.1.1**) is the first enzyme of the non-oxidative branch of the PPP and, together with transaldolase, links the oxidative branch of the PPP with glycolysis. TKT is an ubiquitous homodimeric enzyme [59], responsible for the reversible transfer of two-carbon units (1,2-dihydroxyethyl) in two major reactions: *(i)* conversion of Xu5P and R5P to S7P and G3P, and *(ii)* conversion of Xu5P and E4P to F6P and G3P [2]. The *TKT* gene (**ID 7086**) is located in the short arm of chromosome 3 (3p14.3 region) [60].

TKT is a thiamine diphosphate (ThDP, the active derivative of vitamin B1) and Ca^{2+} ion dependent enzyme [33, 34], presenting high degree of sequence similarities in different species [59].

The human genome encodes two related TKT proteins, TKTL1 and TKTL2 (transketolase-like 1 and 2 protein) [63]. TKTL1 and TKTL2 share a sequence identity at the amino acid level of 61% and 66% compared to TKT, respectively. Not much is known about the biochemical properties of TKTL1 and TKTL2, and until now there are no reports on enzymatic or cellular functions of TKTL2 enzyme, and little is known about TKTL1 [59]. TKTL1 mRNA and protein levels, but not TKTL2 and TKT, are overexpressed in a wide variety of solid cancers and have been associated with transformation to a more malignant phenotype in different carcinoma entities [55]. This overexpression is connected to poor patient survival [64]. The enhancement of both oxidative and non-oxidative branch of the PPP in proliferating cells, due to huge needs in energy, amino acids, fatty acids, nucleotides and NADPH, explains the overexpression of TKTL1 (Fig. 9). Zhang and co-workers [65] showed that TKTL1 accounts for approximately 50% of total transketolase content (TKT, TKTL1 and TKTL2), and that the use of TKTL1 RNA interference (RNAi-mediated suppression) leads to inhibition of more than 50% of total transketolase activity [65]. TKT plays an important role in recruiting glucose and synthesizing ribose, accounting for more than 85% of newly synthesized ribose in cancer cells [66]. Boros and co-workers [66] also described that the usage of oxythiamine, an inhibitor of TKT, leads to decrease in the synthesis of nucleic acids and a huge reduction in cell volume and proliferation [66].

Taking all these data together, inhibiting TKTL1 or TKT activity can become a promising therapeutic target in future cancer therapy.

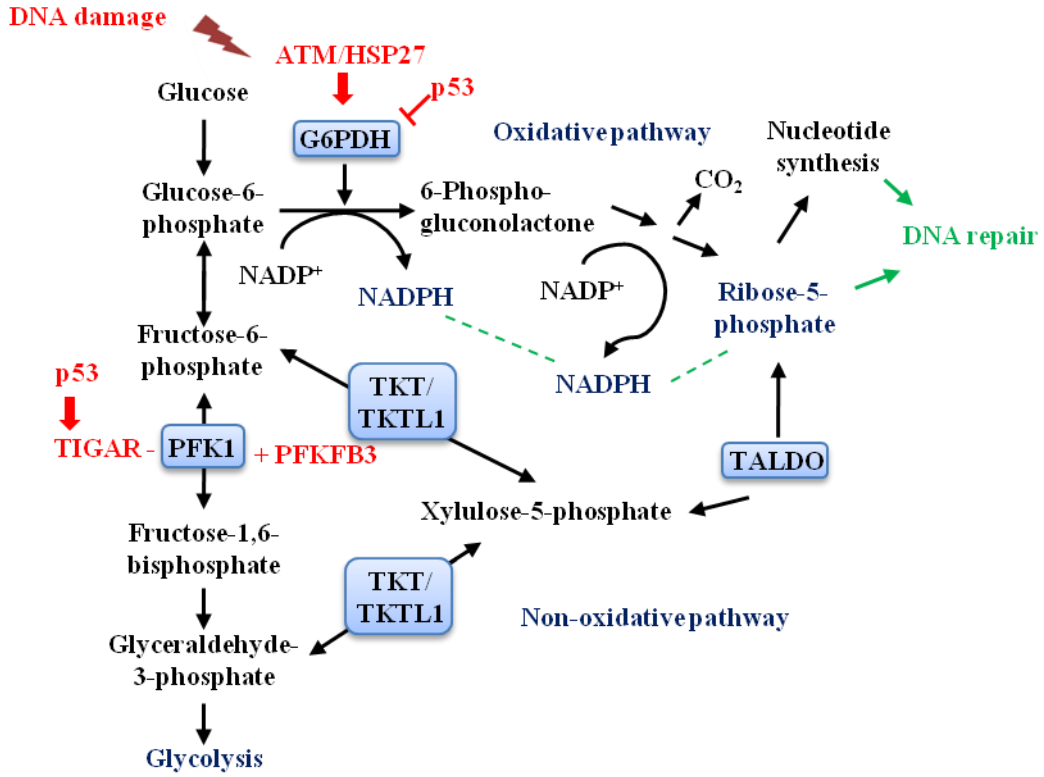

Fig. 9. Key components and intermediates of the pentose phosphate pathway (PPP). DNA damage can activate ATM, leading to Hsp27 phosphorylation that in turn will lead to the activation of G6PD. p53, an important tumor suppressor, regulates the PPP activity, by either disrupting the formation of the active dimeric G6PD; or by activating the TIGAR protein, which will inhibit glycolysis, leading to accumulation of fructose-6-phosphate (F6P), shifting the metabolism of G6P to the PPP. TKTL1 protein overexpression leads to enhancement of the PPP, being responsible for the production of newly synthesized ribose in cancer cells. Scheme adapted from [53].

1.7.4. The PPP and tumor cells' metabolism: ATM

Ataxia telangiectasia (A-T) is a rare autosomal recessive disorder, characterized by progressive neuronal degeneration, oculomotor apraxia, telangiectasias of the conjunctivae, immunodeficiency, frequent infections, radiosensitivity and an increased risk for malignancy, particularly leukemia and lymphoma [38, 39].

The human A-T disease results from null mutations in the *ATM* gene, which encodes the protein kinase ATM (ataxia-telangiectasia mutated). ATM is rapidly activated when cells are exposed to DNA double-strand breaks (DSBs), a highly cytotoxic DNA lesion [38, 40]. The absence of ATM leads to impairment of DSBs repair [68]. ATM is responsible for the phosphorylation of numerous proteins involved

in cell cycle checkpoint control, apoptotic responses and DNA repair [69]. Moreover, an important role in the PPP metabolism has been ascribed to ATM. It has been described that ATM activates the p38-MK2 pathway, which is responsible for phosphorylation of the small heat shock protein Hsp27 upon DNA damage [70]. In 2011, Consentino and co-workers [68] described the relation between ATM, Hsp27 and G6PD. Although the mechanisms explaining the affinity of Hsp27 for G6PD through ATM induction are not well established, Hsp27 was described as regulator of G6PD activity in a non-transcriptional manner. ATM induces G6PD activity by increasing the affinity of Hsp27 for G6PD (Fig. 9). This regulation leads to an activation of the PPP, being of utmost importance in the increasing need of the dNTPs pool which allows DNA repair and NADPH production, pivotal for control of the redox metabolism [68].

2. Bibliography

[1] M.M. Wamelink, E.A. Struys, C. Jakobs, The biochemistry, metabolism and inherited defects of the pentose phosphate pathway: a review, J. Inherit. Metab. Dis. 31 (2008) 703–17.

[2] D.L. Nelson, M.M. Cox, Lenhinger Principles of Biochemistry, Worth Publishers, 3rd edition (2000) chapter 15.

[3] M.D. Cappellini, G. Fiorelli, Glucose-6-phosphate dehydrogenase deficiency, Lancet 371 (2008) 64–74.

[4] Y. Xu, Z. Zhang, J. Hu, I.E. Stillman, J.A. Leopold, D.E. Handy, J. Loscalzo, R.C. Stanton, Glucose-6-phosphate dehydrogenase-deficient mice have increased renal oxidative stress and increased albuminuria, FASEB J. 24 (2010) 609–16.

[5] M.R. Noori-Daloii, M. Daneshpajooh, Molecular basis of G6P deficiency: current status and its perspective, Acta Medica Iranica, 46 (2008) 167–182.

[6] J.H. Huck, N.M. Verhoeven, E.A. Struys, G.S. Salomons, C. Jakobs, M.S. van der Knaap, Ribose-5-phosphate isomerase deficiency: new inborn error in the pentose phosphate pathway associated with a slowly progressive leukoencephalopathy, Am. J. Hum. Genet. 74(2004) 745-51.

[7] N.M. Verhoeven, J.H. Huck, B. Roos, E.A. Struys, G.S. Salomons, A.C. Douwes, M.S. van der Knaap, C. Jakobs, Transaldolase deficiency: liver cirrhosis associated with a new inborn error in the pentose phosphate pathway, Am. J. Hum. Genet. 68 (2001) 1086–92.

[8] L. Luzzatto, A. Mehta, T. Vulliamy, Glucose-6-Phosphate dehydrogenase deficiency, In C. Scriver, A. Beaudet, W. Sly, D. Valle, The Metabolic & Molcecular Bases of Inherited Diseases, 8th ed. New York, McGraw-Hill (2001) 4517–4553.

[9] M.G. Persico, G. Viglietto, G. Martini, D. Toniolo, G. Paonessa, C. Moscatelli, R. Dono, T. Vulliamy, L. Luzzatto, M. D'Urso, Isolation of human glucose-6-phosphate dehydrogenase (G6PD) cDNA clones: primary structure of the protein and unusual 5' non-coding region, Nucleic Acids Res. 14 (1986) 2511–2522.

[10] E. Beutler, G6PD deficiency, Blood 84 (1994) 3613–36.

[11] E. Beutler, Glucose-6-phosphate dehydrogenase deficiency: a historical perspective, Blood 111 (2008) 16–24.

[12] E. Beutler, The hemolytic effect of primaquine and related compounds: a review, Blood 14 (1959) 103–139.

[13] W.W. Group, Glucose-6-phosphate dehydrogenase deficiency, Bull. World Health Organ. 67 (1989) 601–611.

[14] M.A. Holmes, F.S. Buckner, W.C. Van Voorhis, C.L. Verlinde, C. Mehlin, E. Boni, G. DeTitta, J. Luft, A. Lauricella, L. Anderson, O. Kalyuzhniy, F. Zucker, L.W. Schoenfeld, T.N. Earnest, W.G. Hol, E.A. Merritt, Structure of ribose 5-phosphate isomerase from Plasmodium falciparum, Acta Crystallogr. Sect. F Struct. Biol. Cryst. Commun. 62 (2006) 427–31.

[15] M.S. van der Knaap, R.A. Wevers, E.A. Struys, N.M. Verhoeven, P.J. Pouwels, U.F. Engelke, W. Feikema, J. Valk, and C. Jakobs. Leukoencephalopathy Associated with a Disturbance in the Metabolism of Polyols, Ann. Neurol. 46 (1999) 925–928.

[16] M.M. Wamelink, N.M. Grüning, E.E. Jansen, K. Bluemlein, H. Lehrach, C. Jakobs, M. Ralser, The difference between rare and exceptionally rare: molecular characterization of ribose 5-phosphate isomerase deficiency, J. Mol. Med. (Berl) 88 (2010) 931–9.

[17] K. Banki, R.L. Eddy, T.B. Shows, D.L. Halladay, F. Bullrich, C.M. Croce, V. Jurecic, A. Baldini, A. Perl, The human transaldolase gene (TALDO1) is located on chromosome 11 at p15.4-p15.5, Genomics 45 (1997) 233–8.

[18] A.K. Samland, G.A. Sprenger, Transaldolase: from biochemistry to human disease, Int. J. Biochem. Cell. Biol. 41 (2009) 1482–94.

[19] N.M. Verhoeven, M. Wallot, J.H. Huck, O. Dirsch, A. Ballauf, U. Neudorf, G.S. Salomons, M.S. van der Knaap, T. Voit, C. Jakobs, A newborn with severe liver failure, cardiomyopathy and transaldolase deficiency, J. Inherit. Metab. Dis. 28 (2005) 169–79.

[20] V. Valayannopoulos, N.M. Verhoeven, M. Karine, G.S. Salomons, S. Daniéle, M. Gonzales, G. Touati, P. Lonlay, C. Jakobs, J.M. Saudubray, Transaldolase deficiency: a new case of hydrops fetalis and neonatal multi-organ disease, J. Pediatr. 149 (2006) 713–717.

[21] C.W. Fung, S. Siu, C. Mak, G. Poon, K.Y. Wong, P.T. Cheung, L. Low, S. Tam, V. Wong, A rare cause of hepatosplenomegaly - Transaldolase deficiency, J. Inherit. Metab. Dis. 30 (Suppl 1) (2007) 62.

[22] M.M. Wamelink, E.A. Struys, G.S. Salomons, D. Fowler, C. Jakobs, P.T. Clayton, Transaldolase deficiency in a two-year-old boy with cirrhosis, Mol. Genet. Metab. 94 (2008) 255–8.

[23] A. Tylki-Szymańska, T.J. Stradomska, M.M. Wamelink, G.S. Salomons, J. Taybert, J. Pawłowska, C. Jakobs, Transaldolase deficiency in two new patients with a relative mild phenotype, Mol. Genet. Metab. 97 (2009) 15–7.

[24] S. Balasubramaniam, M.M. Wamelink, L.H. Ngu, A. Talib, G.S. Salomons, C. Jakobs, W.T. Keng, "Novel heterozygous mutations in TALDO1 gene causing transaldolase deficiency and early infantile liver failure, J. Pediatr. Gastroenterol. Nutr. 52 (2011) 113–6.

[25] W. Eyaid, T. Al Harbi, S. Anazi, M.M. Wamelink, C. Jakobs, M. Al Salammah, M. Al Balwi, M. Alfadhel, F.S. Alkuraya, Transaldolase deficiency: report of 12 new cases and further delineation of the phenotype, J. Inherit. Metab. Dis. [Epub ahead of print] (2013).

[26] M.M. Wamelink, D.E. Smith, E.E. Jansen, N.M. Verhoeven, E.A. Struys, C. Jakobs, Detection of transaldolase deficiency by quantification of novel seven-carbon chain carbohydrate biomarkers in urine, J. Inherit. Metab. Dis. 30 (2007) 735–42

[27] C.E. Grossman, B. Niland, C. Stancato, N.M. Verhoeven, M.S. van Der Knaap, C. Jakobs, L.M. Brown, S. Vajda, K. Banki, A. Perl, Deletion of Ser-171 causes inactivation, proteasome-mediated degradation and complete deficiency of human transaldolase, Biochem. J. 382 (2004) 725–31.

[28] S. Thorell, P. Gergely, K. Banki, A. Perl, G. Schneider, The three-dimensional structure of human transaldolase, FEBS let. 475 (2000) 205–8.

[29] A.E. Garrod, The Croonian Lectures on Inborn Errors of Metabolism, The Lancet II (1908) 1-7.

[30] Y.M. Wang, J. van Eys, The enzymatic defect in essential pentosuria, N. Engl. J. Med. 282 (1970) 892–896.

[31] E. Salkowski, M. Jastrowitz, Uber eine bisher nicht Beobachtete Zuckerart im Harn, Zbl. Med. Wissensch. 30 (1892) 22–24.

[32] P.A. Levene, F.B. La Forge, Note on a case of pentosuria, J. Biol. Chem. 18 (1914) 319–327.

[33] I. Greenwald, The nature of the sugar in four cases of pentosuria, J. Biol. Chem. 88 (1930) 1–7.

[34] I. Greenwald, The nature of the sugar in four cases of pentosuria, a Correction, J. Biol. Chem. 88 (1930) 501.

[35] M. Lasker, M. Enklewitz, G.W. Lasker, The inheritance of L-xyloketosuria (essential pentosuria), Hum. Biol. 8 (1936) 243–255.

[36] Barnes, Bloomberg, Essential Pentosuria, Br. Med. J. 1 (1963) 1628–1629.

[37] W.M. Politzer, H. Fleischmann, L-xylulosuria in a Lebanese family, Am. J. Hum. Genet. 14 (1962) 256–60.

[38] A.K. Khachadurian, Essential pentosuria, Am. J. Hum. Genet. 14 (1962) 249–55.

[39] A.B. Lane, On the nature of L-xylulose reductase deficiency in essential pentosuria, Biochem. Genet. 23 (1985) 61–72.

[40] C.L. Linster, E. Van Schaftingen, Vitamin C. Biosynthesis, recycling and degradation in mammals, FEBS J. 274 (2007) 1–22.

[41] J. Nakagawa, S. Ishikura, J. Asami, T. Isaji, N. Usami, A. Hara, T. Sakurai, K. Tsuritani, K. Oda, M. Takahashi, M. Yoshimoto, N. Otsuka, K. Kitamura, Molecular characterization of mammalian dicarbonyl/L-xylulose reductase and its localization in kidney, J. Biol. Chem. 277 (2002) 17883–91.

[42] O. El-Kabbani, S. Ishikura, C. Darmanin, V. Carbone, R.P. Chung, N. Usami, A. Hara, Crystal structure of human L-xylulose reductase holoenzyme: probing the role of Asn107 with site-directed mutagenesis, Proteins 55 (2004) 724–32.

[43] S.B. Pierce, C.H. Spurrell, J.B. Mandell, M.K. Lee, S. Zeligson, M.S. Bereman, S.M. Stray, S. Fokstuen, M.J. MacCoss, E. Levy-Lahad, M.C. King, A.G. Motulsky, Garrod's fourth inborn error of metabolism solved by the identification of mutations causing pentosuria, Proc. Natl. Acad. Sci. U. S. A. 108 (2011) 18313–7.

[44] W.E. Knox, Sir Archibald Garrod's Inborn Errors of Metabolism. IV. Pentosuria, The Am. J. Hum. Genet. 10 (1958) 385–397.

[45] W. Onkenhout, J.E. Groener, N.M. Verhoeven, C. Yin, L.A. Laan, L-Arabinosuria: a new defect in human pentose metabolism, Mol. Genet. Metab. 77 (2002) 80–85.

[46] O. Warburg, F. Wind, E. Negelein, The Metabolism of Tumors in the Body, J. Gen. Physiol. 8 (1926) 519–530.

[47] O. Warburg, K. Posener, E. Negelein, Uber den Stoffwechsel der Carcinomzelle, Biochem. Zeitschr. 152 (1924) 309–344.

[48] W.H. Koppenol, P.L. Bounds, The Warburg effect and metabolic efficiency: re-crunching the number, Science. [Online]. Available: http://www.sciencemag.org/content/324/5930/1029/reply#sci=398be983-ebcd-4502-817d-e3f931b9bc37.

[49] M.G. Vander Heiden, L.C. Cantley, C.B. Thompson, Response to W.H. Koppenol and P. L. Bounds, Science. [Online]. Available: http://www.sciencemag.org/content/324/5930/1029/reply#sci=398be983-ebcd-4502-817d-e3f931b9bc37.

[50] M.G. Vander Heiden, L.C. Cantley, C.B. Thompson, Understanding the Warburg Effect: The Metabolic Requirements of Cell Proliferation, Science, 324 (2010) 1029–1033.

[51] R.J. DeBerardinis, A. Mancuso, E. Daikhin, I. Nissim, M. Yudkoff, S. Wehrli, and C.B. Thompson, Beyond aerobic glycolysis: transformed cells can engage in glutamine metabolism that exceeds the requirement for protein and nucleotide synthesis, Proc. Natl. Acad. Sci. U. S. A. 104 (2007) 19345–50.

[52] O. Feron, Pyruvate into lactate and back: from the Warburg effect to symbiotic energy fuel exchange in cancer cells, Radiother. Oncol. 92 (2009) 329–33.

[53] N.P. Jones, A. Schulze, Targeting cancer metabolism--aiming at a tumour's sweet-spot, Drug Discov. Today 17 (2012) 232–41.

[54] Y. Kekec, S. Paydas, A. Tuli, S. Zorludemir, G. Sakman, G. Seydaoglu, Antioxidant enzyme levels in cases with gastrointesinal cancer, Eur. J. Intern. Med. 20 (2009) 403–6.

[55] S. Langbein, W.M. Frederiks, A. zur Hausen, J. Popa, J. Lehmann, C. Weiss, P. Alken, J.F. Coy, Metastasis is promoted by a bioenergetic switch: new targets for progressive renal cell cancer, Int. J. Cancer 122 (2008) 2422–8.

[56] P. Jiang, W. Du, X. Wang, A. Mancuso, X. Gao, M. Wu, and X. Yang, p53 regulates biosynthesis through direct inactivation of glucose-6-phosphate dehydrogenase, Nat. Cell. Biol. 13 (2011) 310–316.

[57] L. Shen, X. Sun, Z. Fu, G. Yang, J. Li, L. Yao, The fundamental role of the p53 pathway in tumor metabolism and its implication in tumor therapy, Clin. Cancer Res. 18 (2012) 1561–7.

[58] K. Bensaad, A. Tsuruta, M.A. Selak, M.N. C. Vidal, K. Nakano, R. Bartrons, E. Gottlieb, K.H. Vousden, TIGAR, a p53-inducible regulator of glycolysis and apoptosis, Cell, 126 (2006) 107–20.

[59] L. Mitschke, C. Parthier, K. Schröder-Tittmann, J. Coy, S. Lüdtke, K. Tittmann, The crystal structure of human transketolase and new insights into its mode of action, J. Biol. Chem. 285 (2010) 31559–70.

[60] N.M. Lapsys, E. Baker, D.F. Callen, G.R. Sutherland, M. Abedinia, P.F. Nixon, J.S. Mattick, Chromosomal location of the human transketolase gene, Cytogenet. Cell. Genet. 61 (1992) 274–275.

[61] G. Schneider, Y. Lindqvist, Crystallography and mutagenesis of transketolase: mechanistic implications for enzymatic thiamin catalysis, Biochim. Biophys. Acta 1385 (1998) 387–98.

[62] L. Pácal, J. Tomandl, J. Svojanovsky, D. Krusová, S. Stepánková, J. Rehorová, J. Olsovsky, J. Belobrádková, V. Tanhäuserová, M. Tomandlová, J. Muzík, K. Kanková, Role of thiamine status and genetic variability in transketolase and other pentose phosphate cycle enzymes in the progression of diabetic nephropathy, Nephrol. Dial. Transplant. 26 (2011) 1229–36.

[63] J.F. Coy, S. Dübel, P. Kioschis, K. Thomas, G. Micklem, H. Delius, A. Poustka, Molecular cloning of tissue-specific transcripts of a transketolase-related gene: implications for the evolution of new vertebrate genes, Genomics 32 (1996) 309–16.

[64] A. Ramos-Montoya, W.N. Lee, S. Bassilian, S. Lim, R.V. Trebukhina, M.V Kazhyna, C.J. Ciudad, V. Noé, J.J. Centelles, and M. Cascante, Pentose phosphate cycle oxidative and nonoxidative balance: A new vulnerable target for overcoming drug resistance in cancer, Int. J. Cancer 119 (2006) 2733–41.

[65] S. Zhang, J.H. Yang, C.K. Guo, P.C. Cai, Gene silencing of TKTL1 by RNAi inhibits cell proliferation in human hepatoma cells, Cancer Lett. 253 (2007) 108–14.

[66] L.G. Boros, J. Puigjaner, M. Cascante, W.N. Lee, J.L. Brandes, S. Bassilian, F. I. Yusuf, R.D. Williams, P. Muscarella, W.S. Melvin, W.J. Schirmer, Oxythiamine and Dehydroepiandrosterone Inhibit the Nonoxidative Synthesis of Ribose and Tumor Cell Proliferation, Cancer Res. 57 (1997) 4242–4248.

[67] S. Biton, I. Dar, L. Mittelman, Y. Pereg, A. Barzilai, Y. Shiloh, Nuclear ataxia-telangiectasia mutated (ATM) mediates the cellular response to DNA double strand breaks in human neuron-like cells, J. Biol. Chem. 281 (2006) 17482–91.

[68] C. Cosentino, D. Grieco, V. Costanzo, ATM activates the pentose phosphate pathway promoting anti-oxidant defence and DNA repair, EMBO J. 30 (2011) 546–55.

[69] J.H. Lee, T.T. Paull, Activation and regulation of ATM kinase activity in response to DNA double-strand breaks, Oncogene 26 (2007) 7741–8.

[70] M. Raman, S. Earnest, K. Zhang, Y. Zhao, M.H. Cobb, TAO kinases mediate activation of p38 in response to DNA damage, EMBO J. 26 (2007) 2005–14.

CHAPTER 3

Gas-Chromatography (GC) analysis of sugars and polyols: optimization of a GC-FID and a GC-MS method

1. Introduction

Sugars' and polyols' profiling in biological samples, such as urine, plasma and CSF, has become an invaluable tool in the assessment of the recently described diseases, RPI and TALDO deficiency, which affect the PPP. Intermediate sugars' and polyols' pattern found in patients carrying these diseases seem to be pathognomonic or, at least, highly predictive of the type of blockage in the PPP. Furthermore, the role of the PPP in several pathologies, such as liver and cancer diseases, has become very recently, subject of intensive study and the intermediate sugars and polyols of the PPP started to be regarded as possible predictive biomarkers of the referred pathologies or, even, of their progress. Assessment to those metabolites is not part of the general metabolic screening.

The analysis of those metabolites has been addressed by specific analytical chromatographic methods such as: HPLC, GC-FID, GC-MS and more recently by LC/MS or LC-MS/MS. The qualitative and quantitative analysis of those metabolites can be quite complicated due the similarity of compounds structure, weight and charge and also due to the huge difference, often seen, among metabolites' concentration in the same sample [1]. The optimization of the pre-analytical and analytical conditions is crucial for the precision of the qualitative and quantitative analysis.

We were interested in setting-up a method able to analyze simultaneously sugars and polyols allowing, in a single run, an informative profile of the PPP intermediate metabolites. Therefore, a GC-FID method was developed based on the previous method published by Jansen and co-workers [1]. Minor modifications were introduced and all the analytical process was validated after the optimization of the analytical conditions. Moreover, the analysis by GC-MS was also accomplished having in mind the possibility of its input on the qualitative analysis. Furthermore, laboratory reference values for adult urinary sugars and polyols were established.

2. Material

2.1. Standards

The monosaccharides – Arabinose, Ribose, Xylose, Glucose, Galactose, Fructose and Fucose –, the disaccharides – Lactose, Maltose, Sucrose, Cellobiose and Melibiose –, the polyols – Threitol, Erythritol, Xylitol, Ribitol, *Myo*-inositol and Mannitol – as well as the internal standards (IS) – Mannoheptulose (IS-1) and Trehalose (IS-3) – were obtained from Sigma-Aldrich Co (St. Louis, MO USA). Perseitol (IS-2) was kindly supplied by Dr. Mirjam Wamelink from VU University Medical Center, Amsterdam, The Netherlands. Sugars' and polyols' main features are summarized in Table 1.

2.2. Reagents

The derivatization reagent Trimethylsilyl N-trimethylsilylacetamidate in chlorotrimethylsilane (BSA + TMCS + TMSI, 3:2:3), also known as Tri-Sil-TBT, and n-hexane CHROMASOLV® for HPLC were purchased from Sigma-Aldrich Co (St. Louis, MO USA). Hydrochloric acid fuming 37%, methanol p.a. and butanol p.a. were obtained from Merck Darmstadt, FRG.

2.3 - Biological Samples

2.3.1. *Controls*

2.3.1.1. *Urine samples*

For the assessment of control sugars' and polyols' chromatographic profiles and reference values, a random urine sample from 16 volunteers (9 female, 7 male; ages 23-50 yrs), healthy adults, all members of laboratory`s staff, was collected in the same day. All the samples were well homogenized and a pool was built by the mixture of equal volume of each urine sample. The created pool was divided in 1.5 mL aliquots, immediately frozen and kept at -20 °C until analysis.

Table 1. Sugars' and polyols' properties: name and purity degree, chemical formula, molecular weight, chemical abstracts service (CAS) number, original reference from manufacturer and chemical structure.

Sugar / Polyol, purity	Chemical Formula	MW (g/mol)	CAS-Number	Ref.	Chemical Structure
D-(-)-Arabinose, ≥ 98%	$C_5H_{10}O_5$	150.10	10323-20-3	A6085	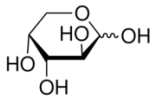
D-(+)-Arabitol, ≥ 99%	$C_5H_{12}O_5$	152.15	488-82-4	A3381	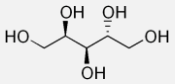
D-(+)-Cellobiose, ≥ 98%	$C_{12}H_{22}O_{11}$	342.30	528-50-7	C7252	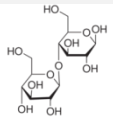
Meso-erythritol, ≥ 99%	$C_4H_{10}O_4$	122.12	149-32-6	E7500	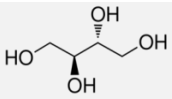
D-(-)-Fructose, ≥ 99%	$C_6H_{12}O_6$	180.16	57-48-7	F0127	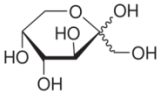
D-(+)-Fucose, ≥ 98%	$C_6H_{12}O_5$	164.16	3615-37-0	F8150	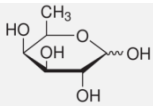
Galactitol, ≥ 99%	$C_6H_{14}O_6$	182.17	608-66-2	D0256	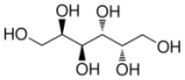
D-(+)-Galactose, ≥ 99%	$C_6H_{12}O_6$	180.16	59-23-4	G0750	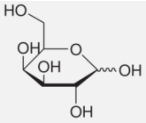
D-(+)-Glucose, ≥ 99.5%	$C_6H_{12}O_6$	180.16	50-99-7	G8270	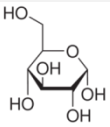
Myo-inositol, ≥ 99%	$C_6H_{12}O_6$	180.16	87-89-8	I5125	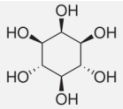
Lactose, Ph Eur, anhydrous	$C_{12}H_{22}O_{11}$	342.30	63-42-3	17814	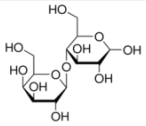
D-(+)-Maltose monohydrate, ≥ 99%	$C_{12}H_{22}O_{11}$. H_2O	360.31	6363-53-7	M9171	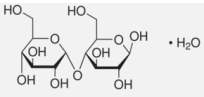

Table 1 (cont.). Sugars' and polyols' properties: name and purity degree, chemical formula, molecular weight, chemical abstracts service (CAS) number, original reference from manufacturer and chemical structure.

Sugar / Polyol, purity	Chemical Formula	MW (g/mol)	CAS-Number	Ref.	Chemical Structure
D-Mannitol, ≥ 98%	$C_6H_{14}O_6$	182.17	69-65-8	M4125	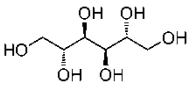
D-Mannoheptulose, ≥ 99%	$C_7H_{14}O_7$	210.18	3615-44-9	97318	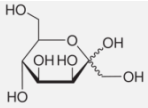
D-(+)-Melibiose, ≥ 99%	$C_{12}H_{22}O_{11}$	342.30	585-99-9	63630	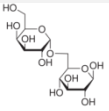
Perseitol, ≥ 97%	$C_7H_{16}O_7$	212.20	527-06-0	P8295	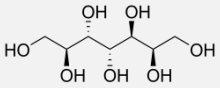
Ribitol, ≥ 99%	$C_5H_{12}O_5$	152.15	488-81-3	A5502	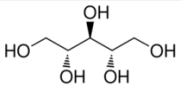
D-(-)-Ribose, ≥ 99%	$C_5H_{10}O_5$	150.13	50-69-1	R7500	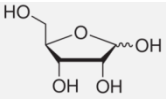
D-Sorbitol, ≥ 99%	$C_6H_{14}O_6$	182.17	50-70-4	240850	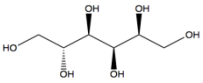
Sucrose, ≥ 99.5%	$C_{12}H_{22}O_{11}$	342.30	57-50-1	S9378	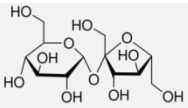
D-(+)-Trehalose dihydrate, ≥ 99%	$C_{12}H_{22}O_{11} . 2H_2O$	378.33	6138-23-4	T9531	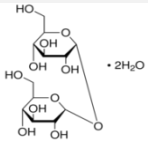
D-Threitol, ≥ 99%	$C_4H_{10}O_4$	122.12	2418-52-2	377619	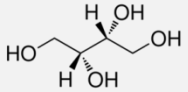
Xylitol, ≥ 99%	$C_5H_{12}O_5$	152.15	87-99-0	X3375	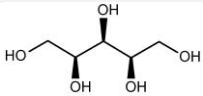
D-(+)-Xylose, ≥ 99%	$C_5H_{10}O_5$	150.13	58-86-6	X1500	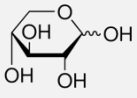

2.3.1.2. *Plasma samples*

To test the efficacy of the chromatographic method for the analysis of plasma samples, the laboratory pool of plasmas was built and used as the method's internal control. Moreover, plasma samples from patients with the established diagnosis of galactosemia, under dietetic control, were as well analyzed to test the chromatographic method's ability to evaluate galactitol.

3. Methods

3.1. Standard Solutions

Individual stock solutions for all the monosaccharides, disaccharides and polyols tested, as well as the compounds used as internal standards, were prepared in distilled water (Milli-Q, Millipore Corporation, Bedford, Ma EUA). These stock solutions (see Table 2 for details) were aliquoted in 1.5 mL microtubes and kept at – 20 ºC until further need. These individual stock solutions were used in the preparation of all the working solutions used in this study.

Table 2. Individual stock solutions of sugars and polyols.

Sugar / Polyol	Stock Solution (mM)	Sugar / Polyol	Stock Solution (mM)
Threitol	100	Mannitol	100
Erythritol	100	Sorbitol	100
Arabinose	100	Galactitol	100
Ribose	100	**Mannoheptulose (IS-1)**	**100**
Fucose	100	*Myo*-inositol	100
Xylose	10	**Perseitol (IS-2)**	**20**
Xylitol	100	Sucrose	100
Arabitol	30	Lactose	100
Ribitol	100	Maltose	100
Fructose	100	Cellobiose	10
Galactose	100	**Trehalose (IS-3)**	**100**
Glucose	100	Melibiose	100

IS: Internal Standard

3.2. Sample preparation

Due to the fact that sugars and polyols do not contain functional groups allowing their direct selective isolation from biological materials, as already mentioned by Jansen *et al.*, the sample`s pre-purification procedure is based on the removal of the other polar compounds (such as organic acids, amino acids and urea), after trimethylsilylation of the dry residue, by acidic hydrolysis and organic solvent extraction (see below) [1].

3.2.1. *Urine samples*

Urine aliquots were defrosted, at room temperature, homogenized by vortex spin (VXR basic Vibrax model, from IKA®, Staufen, Germany) and pH was verified using pH paper strips and adjusted, if necessary, to pH 5-7 with hydrochloric acid (0.1 mol/L). After pH adjustment, the urines were centrifuged (Eppendorf centrifuge 5810R, from Eppendorf AG, Hamburg, Germany) at 4000 rpm for 2 min at 24 ºC. The supernatant was collected and used for further extraction and derivatization. An aliquot was used for the measurement of creatinine (Creat) by the Jaffe method on a routine clinical chemistry analyzer (Pentra C200, from HORIBA ABX SAS, Montpellier, France).

The amount of urine to be used was determined by the creatinine value. Two different approaches were used along this study: *a*) the urine volume was fixed for established ranges of creatinine (GC-MS analysis), as referred in Table 3 or *b*) it was calculated using formula A (GC-FID analysis), displayed below.

Table 3. Volume of urine to be processed according to creatinine range.

Creatinine (mM)	Urine Volume (µL)
< 1.0	200
1.0 – 5.0	100
> 5.0	50

Formula A:

$$V = 1 / (X*Creat)$$

V = volume of urine; **X = 2**, when Creat is lower than 1 mmol/L; the age of the individual is between 0-3 months and/or the individual displays a severe presence of oligosaccharides through the strip test; **X = 1**, in the absence of all the previous conditions. The maximum volume of urine that can be used is 500 µL.

The urine sample, which volume was calculated as described, was then supplemented with 100 µL of a mixture of the internal standards (IS-1, IS-2 and IS-3, at 200 µM, 200 µM and 100 µM, respectively). The sample was then evaporated, at 60 ºC, under a gentle stream of nitrogen, to dryness. For further information see protocol in Annex 1.

3.2.2. *Blood samples*

Blood samples, were collected in the presence of an anticoagulant agent (EDTA or Heparin). The plasma was separated by centrifugation for 10 min at 2000 rpm at room temperature. Plasma (500 µL) was supplemented with 100 µL of the IS mixture solution and it was deproteinized through the addition of 2 mL of methanol, left for 30 min at -20 ºC. After centrifugation (3000 rpm for 10 min, at 24 ºC) the supernatant was transferred to a glass vial and extracted with 4 mL of hexane. After centrifugation (3000 rpm for 2 min, at 24 ºC) the methanol layer was evaporated to dryness as previously described. See Annex 2 for protocol.

3.2.3. *Calibrators*

The calibrators were included in each batch of samples. They were prepared at a final concentration of 125 µM and 250 µM, from the individual stock solutions previously prepared (see Table 2 for details), aliquoted and kept at -20 ºC. For analysis, the aliquots were defrosted and to 100 µL of each working solution 100 µL of the IS mixture solution was added. The dry residue was obtained as described above.

3.2.4. *Derivatization: sugars and polyols trimethylsilylether derivatives*

The selective isolation of sugars and polyols from a biological matrix is quite difficult and time consuming. The biological samples pre-purification was achieved taking into consideration the stability of the sugars and polyols trimethylsilylether derivatives towards hydrolysis. The trimethylsilylation of the dried residues followed by reaction with aqueous hydrochloric acid solution leads to the hydrolysis of the formed trimethylesters and trimethylsilylated amines which are no further extractable by the organic solvent. Therefore, we follow the derivatization method described by Jansen *et al.*. To the obtained dry residue (urine, plasma or aqueous working solutions) the derivatization reagent, Tri-sil-TBT (300 µL), was added, vigorously shaken and incubated at 100 ºC for 30 min. After cooling to room temperature, 1 mL of water (milli-Q) was added, vigorously shaken, followed by 1 mL of hexane, shaken for 2 min in the vortex, and then centrifuged for 2 min at 4000 rpm. The hexane layer was collected and washed with 1 mL of 0.1 mol/L hydrochloric acid aqueous solution. After centrifugation, at 4000 rpm for 2 min, the hexane layer was collected, transferred to a glass vial and a drop of bis(trimethylsilyl)trifluoroacetamide (BSTFA) was added to assure that the anomeric hydroxyl group of our compounds is trimethylsilylated. The hexane layer was then dried, at room temperature, under a gentle stream of nitrogen. The dry residue was re-dissolved with 100 µL of hexane. The vials were capped and stored at 4 ºC, until further analysis. See Annex 3 for protocol.

3.3. High Performance Gas Chromatography (GC)

3.3.1. Gas chromatography-flame ionization detector (GC-FID) system

Gas chromatography was performed using an Agilent Technologies' 7890A model, equipped with an autosampler G4513A model (also from Agilent Technologies) and interfaced with an Agilent ChemStation data system.

The column used was a CP SIL 5 CB, 25 m x 0.25 mm (I.D.) x 0.39 mm (UD), d_f = 0.12 µm, (Agilent Technologies), which is a fused-silica capillary column, containing 100 % dimethylpolysiloxane phase. Gas flow rate (helium) was 0.5 mL/min and detector and injector temperatures were 300 ºC and 275 ºC, respectively. The oven program was as follow: start point temperature 110 ºC, increased by 1.5 ºC/min to

156 ºC and then 4 ºC/min from 156 ºC to 265 ºC followed by 10 ºC/min from 265 ºC to 295 ºC, and hold at 295 ºC for 20 min. The total run time was approximately 80 min *per* sample. In order to optimize the chromatographic resolution, several approaches to establish the best oven program conditions were tested (for further information see Annex 4). Fig. 1 represents the selected temperature program adopted.

Samples (2 µL) were injected in the split mode (1/15) using the automatic injector. The syringe was washed before each sample injection with 3 rinses of hexane and immediately after with 3 rinses of butanol.

Summary of chromatographic conditions:

Injector: split / splitless
Injector Temperature: 275 ºC
Split flow: 17 mL / min
Carrier gas: Helium (Air Liquide, LDA); flow rate of 0.5 mL / min
Make-up and detector gas: Air, Hydrogen and Nitrogen (Air liquide, LDA)
Capillary column: WCOT fused silica
Stationary phase: CP Sil 5 CB
Length: 25 m
Internal diameter: 0.25 mm
Film thickness: 0.12 µm
Detector: Flame ionization detector (FID); temperature: 300 ºC

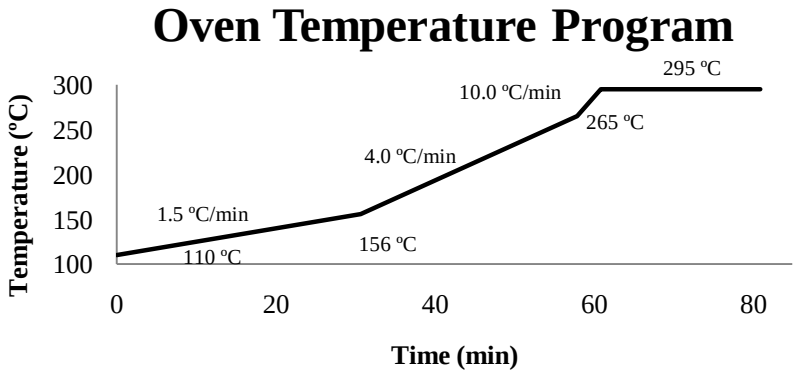

Step	Temperature (ºC)	Rate (ºC/min)	Time (min)
i	110	1.5	0
ii	156	4.0	0
iii	265	10.0	0
iv	295	-	20

Fig. 1. Oven temperature program: starting at 110 ºC rising to 295 ºC in four steps, with a total run time of approximately 80 min/sample.

3.3.2. Gas chromatography-mass spectrometry (GC-MS) system

Gas chromatography with mass spectrometry detection was performed using a GC-2010 model, equipped with an autosampler AOC-20i model (both from Shimadzu Co, Japan) and interfaced with a GC-MS solution 2.53 data system, from Lab. Solutions, Shimadzu Co, Japan.

The column used was a CP SIL 19 CB, 25 m x 0.25 mm (I.D.), df = 0.2 µm (Agilent Technologies), which is a fused-silica capillary column bonded with 14% cyanopropyl-phenyl / 86% dimethylpolysiloxane. Gas flow rate (helium) was kept at 0.6 mL/min and the split ratio was 1:15. The mass spectrometer parameters were as follows: source temperature, 250 ºC; collision energy, 70 eV and injector temperature, 275 ºC. The oven program used was the one previously established for the GC-FID system (see Fig. 1).

The sample volume injected was 0.5 µL and the syringe cleaning program was the same as described above for the GC-FID system (see 3.3.1).

Summary of chromatographic conditions:

Injector: split / splitless
Injector Temperature: 275ºC
Purge flow: 3.0 mL / min
Split ratio: 1:15
Carrier gas: Helium (flow rate: 0.6 mL / min) (Air liquide, LDA)

Capillary column: WCOT fused silica
Stationary phase: CP Sil 19 CB
Length: 25 m
Internal diameter: 0.25 mm
Film thickness: 0.2 µm

Mass spectrometer parameters:
Ion Source Temperature: 250 ºC
Interface Temperature: 230 ºC
Ionization energy: 70 eV
Acquisition mode: Scan
Event time: 0.5 sec
Start *m/z*: 40.00
End *m/z*: 700.00

4. Results

4.1. Qualitative analysis

4.1.1. *GC-FID Profiles*

A representative GC-FID profile of the 21 sugars and polyols, as trimethylsilylether derivatives, of an aqueous standard solution, obtained under the adopted chromatographic conditions is shown in Fig. 2. All tested compounds are well separated, displaying a base line resolution, except xylose (peak 1) and fucose (peak 2) which co-elute. Different oven temperature programs as well as mobile phase flow rates were tested (see Annex 4). In spite of all the modifications, the resolution between xylose (peak 1) and fucose (peak 2) was not improved. Therefore the previous chromatographic conditions based on the work of Jansen *et al.*, with some modifications (see Fig. 1), were the ones adopted along this work.

4.1.2. *Retention Time (RT) and Relative Retention Time (RRT)*

Taking into consideration that the majority of the trimethylsilyl-sugars give rise to a second derivative peak (peak 2), it is of the upmost importance that each laboratory, under the adopted working conditions, establish their proper list of retention time (*RT*) for the tested compounds. *RT* and relative retention time (*RRT*) of pure compounds are crucial chromatographic parameters for the subsequent qualitative analysis of unknown samples. *RT* is a characteristic of each compound, under given chromatographic conditions, therefore being the fingerprint of the compound.

Due to the complexity of the chromatographic profile, a total of 33 peaks (peak 1 plus peak 2 in most sugars) corresponding to 24 distinct sugars and polyols were analyzed. Different standard working solutions were prepared containing all selected sugars and/or polyols, at a final concentration of 125 µM. The carbohydrates in each working solution were selected in order to avoid chromatographic co-elution. This precaution allowed the correct identification of the analytes and their corresponding *RT*. The composition of each standard solution is displayed in Table 4.

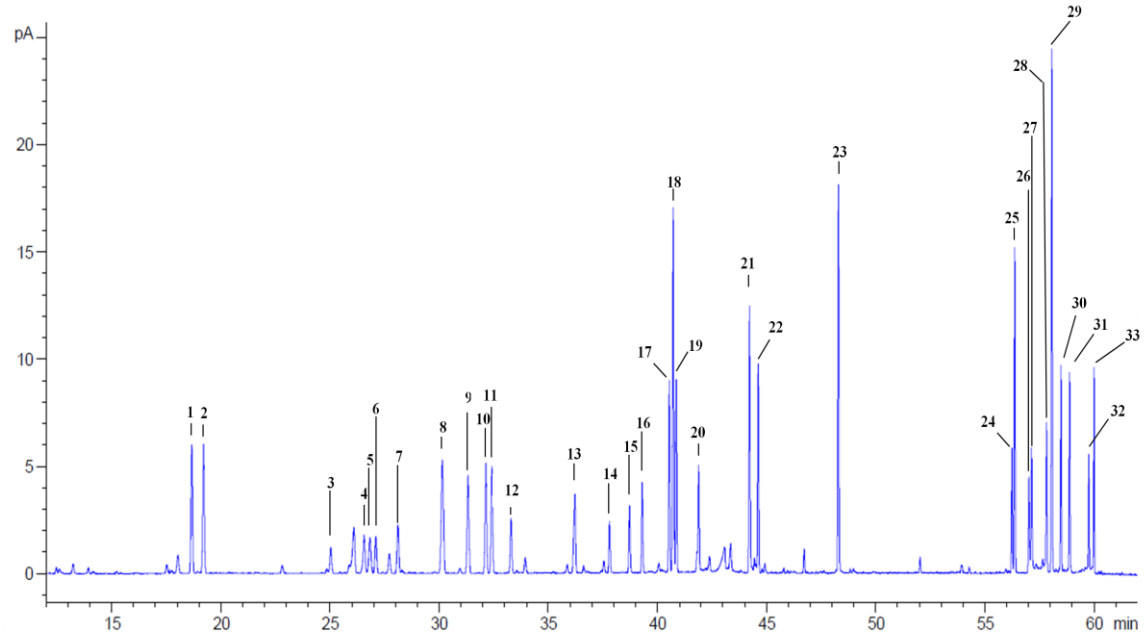

Fig. 2. A GC-FID chromatographic profile of all 21 tested sugars and polyols plus the three IS, as trimethylsilylether derivatives. All analytes are present in a concentration of 125 µM, except IS-1, IS-2 and IS-3, in a concentration of 200 µM, 200 µM and 100 µM respectively.

Peak		Peak		Peak	
	C4		**C6**		**C7**
1	Threitol	**7**	Fucose peak 1*	**21**	**Mannoheptulose (IS-1)**
2	Erythritol	**8**	Fucose peak 2	**23**	**Perseitol (IS-2)**
		13	Fructose		
	C5	**14**	Galactose peak 1		**Disaccharides**
3	Arabinose peak 1	**15**	Glucose peak 1*	**24**	Lactose peak 1
4	Arabinose peak 2*	**16**	Galactose peak 2*	**25**	Sacarose
5	Ribose peak 1	**17**	Mannitol	**26**	Maltose peak 1*
6	Ribose peak 2*	**18**	Sorbitol	**27**	Cellobiose peak 1
8	Xylose peak 1	**19**	Galactitol	**28**	Maltose peak 2
9	Xylitol	**20**	Glucose peak 2	**29**	**Trehalose (IS-3)**
10	Arabitol	**22**	*Myo*-inositol	**30**	Lactose peak 2*
11	Ribitol			**31**	Cellobiose peak 2*
12	Xylose peak 2*			**32**	Melibiose peak 1
				33	Melibiose peak 2*

*Peak used to calculate sugars concentration.

Table 4. Composition of standard solutions used for the determination of the retention time. All carbohydrates were in a concentration of 125 µM.

Standard Solutions	Sugar / Polyol
1	Threitol; Arabinose; Mannitol and Galactitol
2	Erythritol; Ribose; Xylose and Sorbitol
3	Fucose; Xylitol; Arabitol; Ribitol and Fructose
4	Galactose; Maltose; Sacarose and Melibiose
5	Glucose; *Myo*-inositol; Lactose and Cellobiose

To calculate the *RRT* of each sugar and polyol, a mixture of the 21 tested compounds (125 µM each) plus the three IS was used. The *RRT* of each compound was determined using one of the three IS, as indicated in Table 5. The choice was based in structure similarity and/or chromatographic proximity.

Table 5. List of tested compounds and indication of the IS to be used in calculation of the *RRT*

Sugar / Polyol	IS	Sugar / Polyol	IS
Threitol	2	Sorbitol	2
Erythritol	2	Galactitol	2
Arabinose peak 1	1	Glucose peak 2	1
Arabinose peak 2	1	**Mannoheptulose (IS-1)**	-
Ribose peak 1	1	*Myo*-inositol	2
Ribose peak 2	1	**Perseitol (IS-2)**	-
Fucose peak 1	1 (2)[a]	Lactose peak 1	3
Xylose peak 1/ Fucose peak 2	1/2[b]	Sacarose	3
Xylitol	2	Maltose peak 1	3
Arabitol	2	Cellobiose peak 1	3
Ribitol	2	Maltose peak 2	3
Xylose peak 2	1	**Trehalose (IS-3)**	-
Fructose	1	Lactose peak 2	3
Galactose peak 1	1	Cellobiose peak 2	3
Glucose peak 1	1 (2)[a]	Melibiose peak 1	3
Galactose peak 2	1 (2)[a]	Melibiose peak 2	3
Mannitol	2		

[a] Internal standards used for quantitative analysis.
[b] Xylose peak 1 and Fucose peak 2 co-elute.
IS: Internal standard used for *RRT* calculation (1- mannoheptulose, 2- perseitol and 3-trehalose).

Nevertheless, the compound *RRT* relative to each of the three ISs were calculated. The *RRT* of all the tested sugars and polyols in aqueous standard solutions, analyzed as trimethylsilylether derivatives under the adopted chromatographic conditions, are shown in Table 6. Excellent reproducibility for all the *RRT* was observed regardless of the IS used.

Table 6. Reproducibility of the *RRT* of the sugars and polyols trimethylsilylethers derivatives in the aqueous standard solutions.

		***RRT* (IS-1)**		***RRT* (IS-2)**		***RRT* (IS-3)**	
Sugar / Polyol	**Peak #**	**Mean [a] (n = 10)**	**%RSD**	**Mean [a] (n = 10)**	**%RSD**	**Mean [a] (n = 10)**	**%RSD**
Threitol	1	0.423	0.03	0.388	0.08	0.323	0.08
Erythritol	2	0.435	0.03	0.398	0.08	0.331	0.09
Arabinose peak 1	3	0.567	0.02	0.519	0.07	0.432	0.08
Arabinose peak 2	4	0.602	0.02	0.551	0.06	0.458	0.06
Ribose peak 1	5	0.614	0.02	0.562	0.07	0.468	0.07
Ribose peak 2	6	0.628	0.02	0.575	0.07	0.478	0.07
Fucose peak 1	7	0.637	0.02	0.583	0.06	0.485	0.07
Xylose peak 1/Fucose peak 2 [b]	8	0.683	0.02	0.625	0.06	0.520	0.06
Xylitol	9	0.709	0.02	0.650	0.05	0.542	0.91
Arabitol	10	0.727	0.01	0.666	0.01	0.554	0.01
Ribitol	11	0.734	0.01	0.672	0.04	0.559	0.04
Xylose peak 2	12	0.753	0.01	0.690	0.04	0.574	0.04
Fructose	13	0.819	0.01	0.750	0.02	0.624	0.03
Galactose peak 1	14	0.855	0.00	0.783	0.02	0.651	0.02
Glucose peak 1	15	0.876	0.00	0.802	0.02	0.667	0.02
Galactose peak 2	16	0.889	0.01	0.814	0.02	0.677	0.02
Mannitol	17	0.917	0.01	0.840	0.02	0.698	0.02
Sorbitol	18	0.921	0.01	0.843	0.02	0.702	0.02
Galactitol	19	0.924	0.01	0.846	0.02	0.704	0.02
Glucose peak 2	20	0.947	0.01	0.867	0.04	0.721	0.04
Mannoheptulose (IS-1)	21	1.000	0.00	0.916	0.00	0.762	0.01
Myo-inositol	22	1.009	0.01	0.924	0.01	0.769	0.01
Perseitol (IS-2)	23	1.092	0.00	1.000	0.00	0.832	0.01
Lactose peak 1	24	1.272	0.00	1.165	0.01	0.969	0.01
Sacarose	25	1.275	0.01	1.167	0.01	0.971	0.01
Maltose peak 1	26	1.289	0.00	1.181	0.01	0.982	0.01
Cellobiose peak 1	27	1.292	0.01	1.183	0.01	0.984	0.00
Maltose peak 2	28	1.308	0.01	1.197	0.01	0.996	0.01
Trehalose (IS-3)	29	1.313	0.01	1.202	0.01	1.000	0.00
Lactose peak 2	30	1.322	0.00	1.211	0.01	1.007	0.00
Cellobiose peak 2	31	1.331	0.00	1.219	0.01	1.014	0.00
Melibiose peak 1	32	1.351	0.01	1.237	0.01	1.029	0.00
Melibiose peak 2	33	1.357	0.01	1.242	0.01	1.033	0.00

[a] *RRT* represents the mean of 10 independent analyses of the standard solution.
[b] Xylose peak 1 and Fucose peak 2 co-elute

4.1.3. *Area of Peak 1/Peak 2 Ratio: another parameter in qualitative analysis*

As already referred, the majority of the sugar trimethylsilylether derivatives give rise, at least, to two peaks (peak 1 and 2) with distinct chromatographic characteristics. From a quantitative point of view, it is a disadvantage either due to loss of sensitivity and/or quality of the results. On the other hand, from a qualitative point of view, it may help the identification, since the ratio of peak 1 area relative to the one of peak 2 is a characteristic of the compound. In Table 7, the peak 1 *versus* peak 2 area ratio of the tested sugars, in aqueous standard solutions, is presented. According to Mirjam Wamelink (personal communication) the range to be used for further identification of peaks in unknown samples should be defined as the mean ± 3 STD, due to the variability of peak 1/peak 2 area ratio, which in part is determined by the efficiency of the derivatization procedure in each moment. Nevertheless, the calculated % RSD (8.0 – 14.6) is still acceptable for these type of compounds, the formed trimethylsilylether derivatives and the analytical method.

Table 7. Sugars peak 1 / peak 2 area ratio after analysis of aqueous standard solutions under the adopted chromatographic conditions.

	Peak 1 Area / Peak 2 Area			
Sugar	**Mean[a] (n=26)**	**STD**	**% RSD**	**Mean ± 3STD**
Arabinose	0.555	0.044	8.0	0.422 - 0.687
Ribose	2.071	0.193	9.3	1.491 - 2.652
Galactose	0.549	0.062	11.2	0.364 - 0.734
Glucose	0.745	0.109	14.6	0.419 - 1.071
Lactose	0.683	0.096	14.0	0.396 - 0.970
Maltose	0.675	0.092	13.6	0.399 - 0.952
Cellobiose	0.782	0.081	10.3	0.539 - 1.024
Melibiose	0.608	0.063	10.4	0.418 - 0.797

[a]Mean of 26 independent experiments analysed along 1 month

4.1.4. *Precision of the Qualitative Analysis*

In Fig. 3 the chromatograms of an aqueous standard solution (A), a pooled control sample respectively of urine (B) and plasma (C), of healthy adults, as well as that of a galactosemic patient plasma sample (D), under dietetic treatment, are displayed. As it can be observed, in all displayed profiles, the chromatographic resolution was not apparently affected by the biological matrix. The identification of the peaks was made through the peak *RRT* calculated *versus* the internal standards, as shown in Table 8. One additional tool, the peak 1/peak 2 area ratio, was used in the identification of the sugars. The calculated range, mean ± 3 STD, for peak 1/peak 2 area ratio, is displayed in Table 9.

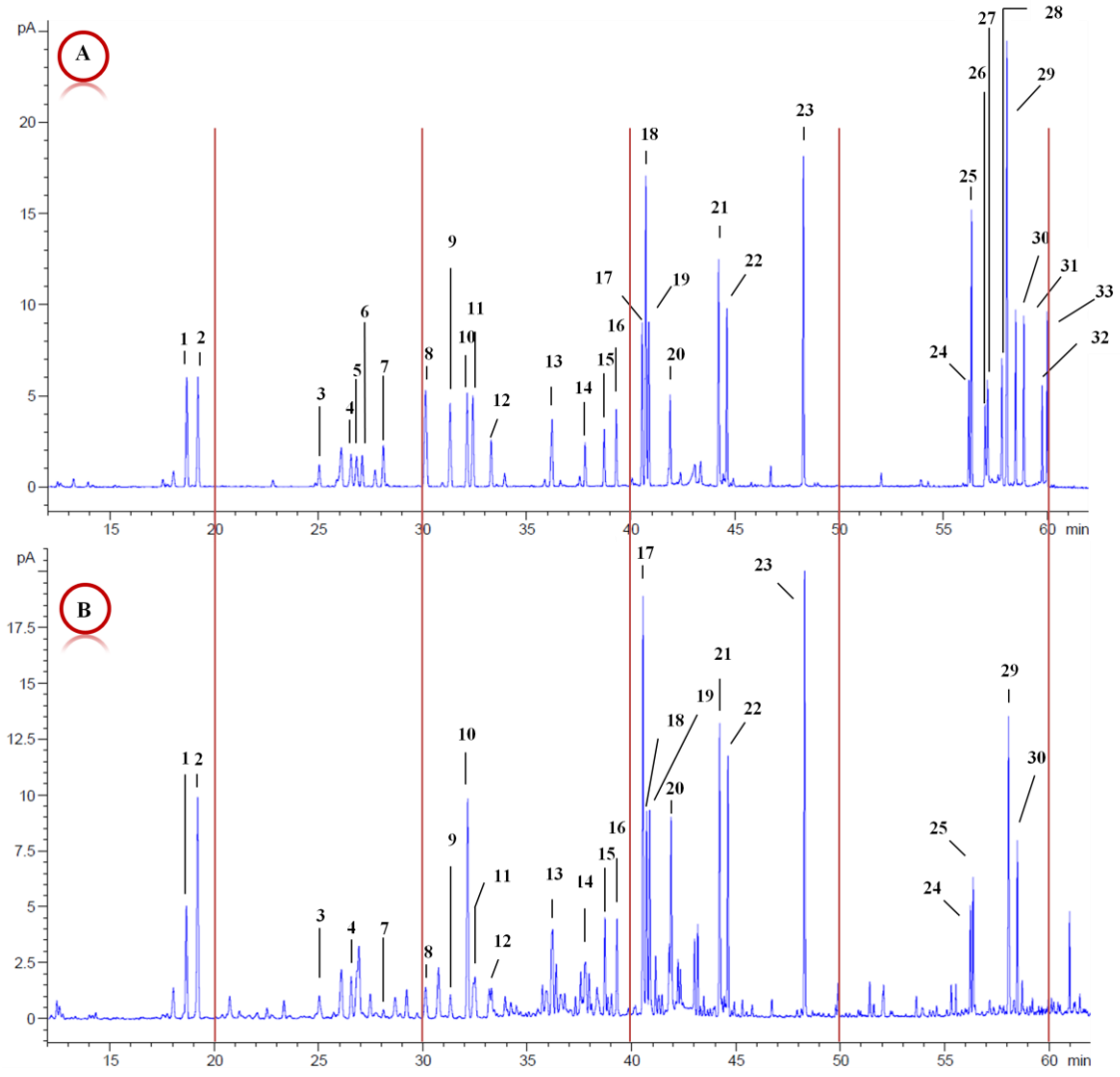

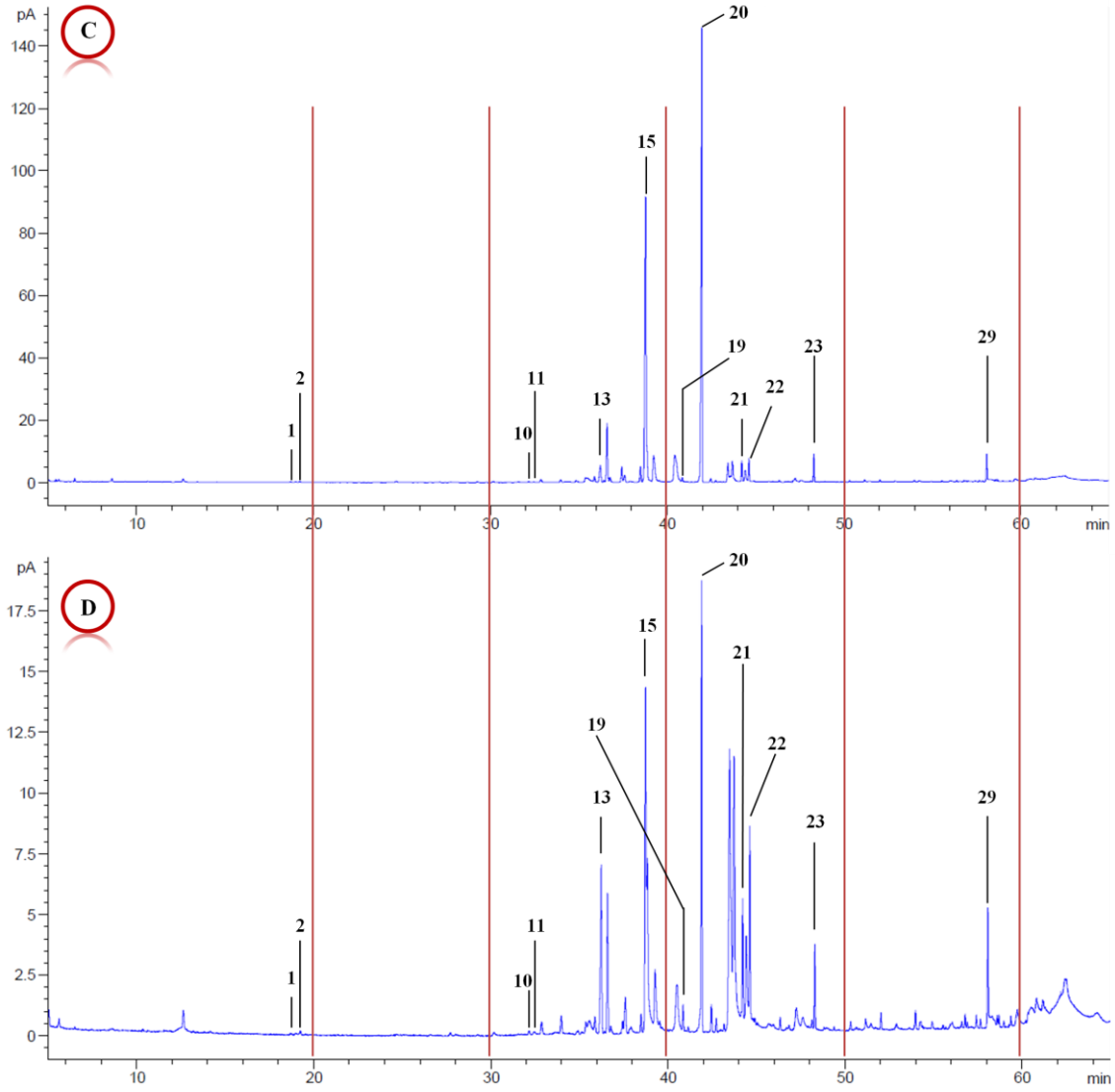

Fig. 3. Chromatograms of: (A) aqueous standard solution; (B) pooled urine sample of healthy adults under free diet; (C) pooled plasma sample, used in the lab for the preparation of internal controls and (D) plasma sample of a Galactosemic patient, under diet restriction. The analysis conditions are the same as shown in Fig. 1. The peak numbers correspond to the ones displayed in Fig. 2.

Table 8. Reproducibility of the Relative Retention Time (*RRT*) of the sugars and polyols trimethylsilylether derivatives in the pooled urine sample used as control (see 2.3).

		RRT [a]					
		Mannoheptulose (IS-1)		**Perseitol (IS-2)**		**Trehalose (IS-3)**	
Sugar / Polyol	**Peak #** [b]	**Mean (n= 23)**	**% RSD**	**Mean (n = 23)**	**% RSD**	**Mean (n = 23)**	**% RSD**
Threitol	1	0.423	0.04	0.387	0.09	0.322	0.09
Erythritol	2	0.435	0.04	0.398	0.07	0.331	0.08
Arabinose peak 1	3	0.567	0.04	0.519	0.08	0.432	0.09
Arabinose peak 2	4	0.602	0.04	0.551	0.07	0.458	0.07
Ribose peak 1	5	0.614	0.06	0.562	0.06	0.467	0.07
Ribose peak 2	6	0.628	0.04	0.575	0.05	0.478	0.06
Fucose peak 1	7	0.636	0.03	0.583	0.07	0.485	0.08
Xylose peak 1/ Fucose peak 2 [c]	8	0.683	0.04	0.625	0.06	0.520	0.06
Xylitol	9	0.709	0.03	0.649	0.05	0.540	0.06
Arabitol	10	0.727	0.02	0.666	0.04	0.554	0.05
Ribitol	11	0.734	0.03	0.672	0.04	0.559	0.05
Xylose peak 2	12	0.753	0.03	0.690	0.04	0.574	0.05
Fructose	13	0.819	0.03	0.750	0.03	0.624	0.04
Galactose peak 1	14	0.855	0.01	0.783	0.02	0.651	0.02
Glucose peak 1	15	0.876	0.01	0.802	0.02	0.667	0.02
Galactose peak 2	16	0.889	0.01	0.814	0.02	0.677	0.02
Mannitol	17	0.917	0.01	0.840	0.01	0.698	0.01
Sorbitol	18	0.921	0.01	0.843	0.01	0.701	0.02
Galactitol	19	0.924	0.01	0.846	0.01	0.704	0.02
Glucose peak 2	20	0.947	0.01	0.868	0.01	0.722	0.01
Mannoheptulose (IS-1)	**21**	**1.000**	**0.00**	**0.916**	**0.00**	**0.762**	**0.01**
*Myo-*inositol	*22*	1.009	0.00	0.924	0.01	0.768	0.01
Perseitol (IS-2)	**23**	**1.092**	**0.00**	**1.000**	**0.00**	**0.832**	**0.01**
Lactose peak 1	24	1.272	0.00	1.164	0.01	0.969	0.01
Sacarose	25	1.275	0.01	1.167	0.01	0.971	0.01
Maltose peak 1	26	1.289	0.01	1.181	0.01	0.982	0.01
Cellobiose peak 1	27	1.292	0.02	1.183	0.02	0.984	0.03
Maltose peak 2	28	1.308	0.01	1.197	0.01	0.996	0.01
Trehalose (IS-3)	**29**	**1.313**	**0.01**	**1.202**	**0.01**	**1.000**	**0.00**
Lactose peak 2	30	1.323	0.01	1.211	0.01	1.007	0.01
Cellobiose peak 2	31	1.331	0.01	1.219	0.01	1.014	0.01
Melibiose peak 1	32	1.351	0.01	1.237	0.01	1.029	0.00
Melibiose peak 2	33	1.357	0.01	1.242	0.01	1.033	0.00

[a] *RRT* represents the mean of 23 independent analyses of the pooled urine control sample.
[b] Peak number corresponding with those in Fig.2.
[c] Xylose peak 1 and Fucose peak 2 co-elute.
IS: Internal standard.

The reproducibility of the compounds *RRT* was excellent, despite the complexity of the urine matrix. The similarity of the *RRT*s of unknown compounds with the ones corresponding to the pure compounds clearly showed that the biological matrix did not interfere in the chromatographic characteristics of the compounds, therefore allowing their unequivocal identification.

Table 9. Sugars' peak 1 *versus* peak 2 area ratio after analysis of control pooled urine samples under the adopted chromatographic conditions.

	Peak 1 Area / Peak 2 Area			
Sugar	**Mean [a] (n=26)**	**STD**	**% RSD**	**Mean ± 3 STD**
Arabinose	0.434	0.033	7.6	0.335 - 0.532
Galactose	0.484	0.061	12.5	0.302 - 0.666
Glucose	0.623	0.057	9.2	0.451 - 0.794
Lactose	0.694	0.029	4.1	0.608 - 0.781
Maltose	0.596	0.024	4.0	0.524 - 0.669
Cellobiose	0.919	0.044	4.8	0.787 - 1.051
Melibiose	0.511	0.016	3.1	0.463 - 0.558

[a] Mean of 26 independent determinations of the pooled urine control sample.
Ribose - not detected.

The information given by the area of peak 1/peak 2 ratio shows that the range of reference is in accordance with that calculated for the pure compounds. Nevertheless, as it is established as a mean ± 3 STD, it turns to be less straightforward in its usefulness as an isolated parameter and, accordingly, must be used as a second tool of information, exclusively. However, when there is no match with the pure compound peak 1/peak 2 area ratio, this parameter clearly rules out the identity of the compound in the unknown sample compared to the pure compound. The precision of the qualitative analysis was also tested through the analysis of urine samples from patients with established diagnosis of transaldolase (TALDO) deficiency, galactosemia, as well as from a diabetic patient with liver dysfunction. Samples were kindly supplied by Dr. Mirjam Wamelink from the VU University Medical Center, Amsterdam, The Netherlands. The chromatograms are shown in Fig. 4. These examples confirm the applicability of the present method to the biochemical diagnosis of carbohydrates metabolism defects.

Furthermore, the analysis of TALDO patient`s sample allowed the evaluation of the *RT* and *RRT* of sedoheptulose, a sugar which is not available in the market as a standard.

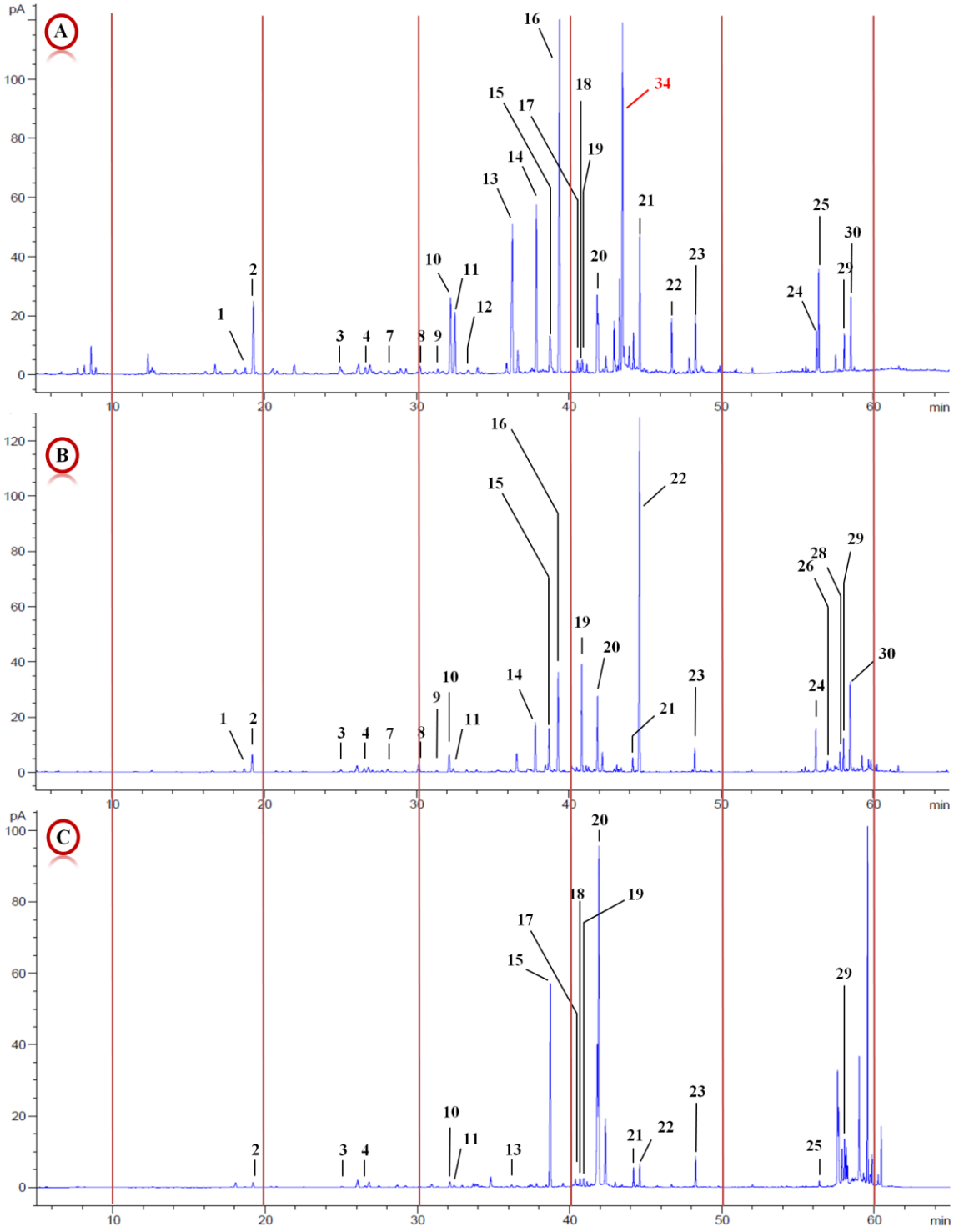

Fig. 4. Chromatograms of urine samples of: (A) TALDO deficient patient; (B) Galactosemic patient (C) Diabetic patient (10 times diluted). The analysis conditions are the same as shown in Fig. 1. The peak numbers correspond to the ones displayed in Table 8 and Fig. 2. Peak 34 corresponds to sedoheptulose.

4.1.5. *GC-MS Profiles*

The analysis of the sugars and polyols, as trimethylsilyl derivatives, was also performed by GS-MS with the objective to evaluate if the mass spectra could be an additional tool for peak identification in unknown samples.

A representative total ion chromatogram (TIC) of 21 sugars and polyols trimethylsilylether derivatives, plus the three internal standards, obtained using the previous established chromatographic conditions (see **3.3.2**.), is shown in Fig. 5. The chromatographic resolution was not complete for all the tested compounds. Although, no co-elution between xylose peak 1 and fucose peak 2 is observed, maltose peak 1 and cellobiose peak 1, arabitol and ribitol, and sorbitol and galactose peak 2 show total co-elution. A partial co-elution is also observed between the peak of sorbitol plus galactose peak 2 and galactitol, turning this chromatographic system unsuitable for the quantification of galactitol. Furthermore, and finally, in this chromatographic system, fructose displays two derivatives (peak 1 and peak 2).

Two working solutions, as displayed in Table 10, were prepared taking into consideration the relative chromatographic position of the tested compounds, to avoid erroneous identification between flanking peaks. These working solutions were used to obtain the *RT* of the analytes and subsequently to calculate their *RRT*.

Table 10. Composition of working standard solutions

Sugar / Polyol	**A [µM]**	**B [µM]**	**Sugar / Polyol**	**A [µM]**	**B [µM]**
Threitol	-	125	Glucose	250	-
Erythritol	-	125	Mannitol	250	-
Arabinose	250	-	Sorbitol	-	125
Ribose	250	-	Galactitol	250	-
Fucose	-	125	*Myo*-inositol	250	-
Xylitol	250	-	Sucrose	250	-
Ribitol	250	-	Lactose	250	-
Xylose	-	125	Maltose	250	-
Fructose	250	-	Melibiose	-	125
Galactose	250	-	Cellobiose	-	125

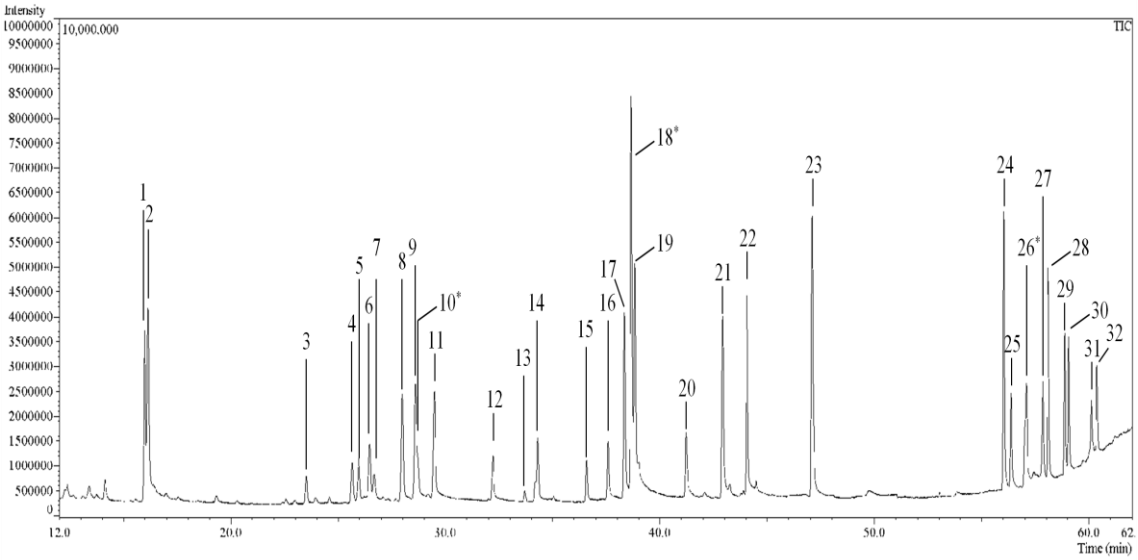

Fig. 5. GC-MS total ion chromatogram profile of 21 tested sugars and polyols plus the three IS, as trimethylsilylether derivatives. All analytes were in a concentration of 125 µM, except IS-1, IS-2 and IS-3, in a concentration of 200 µM, 200 µM and 100 µM, respectively.

Peak #		Peak #		Peak #	
	C4		**C6**		**C7**
1	Threitol	**6**	Fucose peak 1	**21**	Mannoheptulose (IS-1)
2	Erythritol	**11**	Fucose peak 2	**23**	Perseitol (IS-2)
		13	Fructose peak 1		
	C5	**14**	Fructose peak 2		**Disaccharides**
3	Arabinose peak 1	**15**	Galactose peak 1	**24**	Sacarose
4	Ribose peak 1	**16**	Glucose peak 1	**25**	Lactose peak 1
5	Arabinose peak 2	**17**	Mannitol	**26**	Maltose peak 1
7	Ribose peak 2	**18**	Sorbitol	**26**	Cellobiose peak 1
8	Xylitol	**18**	Galactose peak 2	**27**	Maltose peak 2
9	Xylose peak 1	**19**	Galactitol	**28**	Trehalose (IS-3)
10	Arabitol	**20**	Glucose peak 2	**29**	Lactose peak 2
10	Ribitol	**22**	*Myo*-inositol	**30**	Cellobiose peak 2
12	Xylose peak 2			**31**	Melibiose peak 1
				32	Melibiose peak 2

IS: Internal standard

The *RRT* of all tested compounds was calculated, for details see Table 11. The *RRT* of all 21 sugars and polyols trimethylsilyl derivatives analyzed by GC-MS, presented a % RSD < 0.6 %. The results confirm the excellent reproducibility of the gas-chromatographic system.

Table 11. Reproducibility of the *RRT* of the sugars and polyols trimethylsilylether derivatives in the aqueous standard solutions analyzed by GC-MS.

		RRT [a]					
		Mannoheptulose (IS-1)		**Perseitol (IS-2)**		**Trehalose (IS-3)**	
Sugar / Polyol	**Peak #** [b]	**Mean (n = 8)**	**% RSD**	**Mean (n = 8)**	**% RSD**	**Mean (n = 8)**	**% RSD**
Threitol	1	0.372	0.010	0.339	0.040	0.274	0.050
Erythritol	2	0.375	0.020	0.342	0.050	0.277	0.060
Arabinose peak 1	3	0.547	0.030	0.499	0.020	0.404	0.030
Ribose peak 1	4	0.597	0.030	0.544	0.030	0.441	0.020
Arabinose peak 2	5	0.604	0.010	0.551	0.020	0.446	0.020
Fucose peak 1	6	0.616	0.020	0.562	0.040	0.455	0.040
Ribose peak 2	7	0.621	0.020	0.566	0.020	0.458	0.020
Xylitol	8	0.651	0.030	0.594	0.020	0.481	0.020
Xylose peak 1	9	0.665	0.030	0.607	0.030	0.491	0.030
Arabitol	10*	0.667	0.020	0.609	0.030	0.493	0.030
Ribitol	10*	0.668	0.020	0.609	0.030	0.493	0.030
Fucose peak 2	11	0.686	0.030	0.626	0.030	0.507	0.040
Xylose peak 2	12	0.750	0.020	0.684	0.020	0.554	0.030
Fructose peak 1	13	0.785	0.020	0.716	0.020	0.580	0.020
Fructose peak 2	14	0.799	0.020	0.729	0.020	0.590	0.020
Galactose peak 1	15	0.852	0.010	0.777	0.010	0.629	0.010
Glucose peak 1	16	0.876	0.010	0.798	0.010	0.646	0.010
Mannitol	17	0.894	0.010	0.815	0.020	0.660	0.010
Sorbitol	18*	0.901	0.030	0.821	0.030	0.665	0.020
Galactose peak 2	18*	0.902	0.010	0.822	0.000	0.666	0.000
Galactitol	19	0.905	0.010	0.825	0.030	0.668	0.030
Glucose peak 2	20	0.960	0.010	0.875	0.000	0.709	0.010
Mannoheptulose (IS-1)	21	1.000	0.000	0.912	0.000	0.738	0.010
Myo-inositol	22	1.027	0.010	0.936	0.010	0.758	0.010
Perseitol (IS-2)	23	1.097	0.000	1.000	0.000	0.810	0.010
Sucrose	24	1.306	0.010	1.191	0.010	0.964	0.010
Lactose peak 1	25	1.314	0.010	1.198	0.010	0.970	0.010
Maltose peak 1	26*	1.329	0.000	1.212	0.010	0.981	0.000
Cellobiose peak 1	26*	1.331	0.030	1.213	0.020	0.982	0.020
Maltose peak 2	27	1.349	0.010	1.229	0.010	0.995	0.000
Trehalose (IS-3)	28	1.355	0.010	1.235	0.010	1.000	0.000
Lactose peak 2	29	1.373	0.010	1.251	0.010	1.013	0.010
Cellobiose peak 2	30	1.377	0.030	1.256	0.020	1.017	0.020
Melibiose peak 1	31	1.402	0.010	1.278	0.010	1.035	0.010
Melibiose peak 2	32	1.408	0.030	1.283	0.020	1.039	0.020

[a] Mean of 8 independent determinations
[b] Peak number corresponding with those in Fig. 5.
* Co-elution between Sorbitol and Galactose peak 2, and maltose peak 1 and cellobiose peak 1.

Following the same rationale, as for the analysis by GC-FID, the sugars peak 1 *versus* peak 2 area ratio was also calculated. Results are shown in Table 12. As expected there is no match with the results previously calculated for GC-FID analysis, since this parameter is defined by the type of chromatographic system. Therefore, for each chromatographic system it is necessary to calculate peak 1/peak 2 area ratios to use this parameter in the qualitative analysis.

Table 12. Sugars' peak 1/peak 2 area ratio after analysis of the aqueous standard solutions under the adopted chromatographic conditions for GC-MS.

	Peak 1 Area / Peak 2 Area			
Sugars	**Mean (n=4)**	**STD**	**% RSD**	**Mean ± 3STD**
Arabinose	0.732	0.020	2.8	0.670 - 0.793
Ribose	3.940	0.147	3.7	3.498 - 4.382
Fucose	0.521	0.016	3.2	0.472 - 0.570
Xylose	0.710	0.097	13.7	0.419 - 1.002
Fructose	0.153	0.010	6.7	0.122 - 0.184
Glucose	0.849	0.052	6.1	0.693 - 1.006
Lactose	0.701	0.041	5.9	0.577 - 0.824
Maltose	0.551	0.049	9.0	0.403 - 0.700
Cellobiose	0.869	0.080	9.2	0.630 - 1.108
Melibiose	0.545	0.050	9.2	0.394 - 0.695

[a] Mean of 4 independent analysis of the trimethylsilyl-sugars in the aqueous standard solutions

Moreover, the mass spectrum of each of the tested compounds was established. In order to be ensured, for each tested compound, the unequivocal identification of the mass-to-charge ratio (*m/z*) of the most abundant ions, the pure tested compounds were analyzed one by one, in a scan detection mode. The characteristic *m/z* values of each carbohydrate are summarized in Table 13. The similarities of the *m/z* among the tested compounds ruled out the usefulness of the mass spectrum of the trimethylsilyl-sugars' and –polyols' derivatives as one unique tool in the identification of unknown compounds.

Table 13. Summary of the most abundant ions *m/z* for the tested carbohydrates

Sugar / Polyol	***m/z* (mass-to-charge ratio)**
D-Arabinose peak 1	73, 217, 204, 191, 147, 45, 133
D-Arabinose peak 2	73, 217, 204, 191, 147, 45, 133
D-Arabitol	73, 217, 147, 103, 129, 205, 307, 189
D-Cellobiose peak 1	73, 204, 191, 217, 147, 103, 129, 243, 361
D-Cellobiose peak 2	73, 204, 191, 217, 147, 103, 129, 243, 361
meso-Erythritol	73, 147, 217, 103, 117, 205, 189, 133, 204, 129
D-Fructose peak 1	73, 204, 147, 217, 437, 45, 129, 103, 189, 292
D-Fructose peak 2	73, 204, 147, 217, 437, 45, 129, 103, 189, 292
D-Fucose peak 1	73, 204, 147, 191, 189, 205
D-Fucose peak 2	73, 204, 191, 147, 189, 217
Galactitol	73, 217, 147, 103, 205, 319, 129, 307, 117
D-Galactose peak 1	73, 204, 191, 217, 147, 129, 45, 103
D-Galactose peak 2	73, 204, 191, 217, 147, 129, 45, 103
D-Glucose peak 1	73, 204, 191, 147, 217, 45, 129, 103
D-Glucose peak 2	73, 204, 191, 147, 217, 45, 129, 103
Myo-inositol	73, 217, 147, 305, 191, 318, 265, 204, 129, 103
Lactose peak 1	73, 204, 191, 217, 147, 129, 103
Lactose peak 2	73, 204, 191, 217, 147, 129, 103
D-Maltose peak 1	73, 204, 191, 147, 217, 361, 103, 129
D-Maltose peak 2	73, 204, 191, 147, 217, 361, 103, 129
D-Mannitol	73, 147, 205, 319, 103, 217, 117, 129, 157, 307
D-Mannoheptulose (IS-1)	204, 73, 147, 129, 217, 45, 103, 191, 117, 359
D-Melibiose peak 1	73, 204, 44, 191, 147, 129, 217, 103
D-Melibiose peak 2	73, 204, 44, 191, 147, 129, 217, 103
Perseitol (IS-2)	73, 147, 217, 103, 205, 319, 129, 117, 191, 157
Ribitol	73, 103, 217, 147, 129, 205, 319, 117, 189, 307
D-Ribose peak 1	73, 217, 191, 204, 147
D-Ribose peak 2	73, 217, 191, 204, 147
D-Sorbitol	73, 147, 319, 217, 103, 205, 117, 129, 157
Sucrose	73, 361, 217, 147, 103, 169, 129, 271, 437
D-Trehalose (IS-3)	73, 361, 191, 147, 217, 103, 129, 204, 169, 271
D-Threitol	73, 147, 217, 103, 117, 57, 189, 133
Xylitol	73, 43, 217, 57, 103, 147, 129, 319, 307
D-Xylose peak 1	73, 204, 147, 217, 191, 189, 205, 133
D-Xylose peak 2	73, 204, 147, 217, 191, 189, 205, 133

IS: Internal Standard

4.2.Quantitative analysis

4.2.1. Linearity

The linearity was studied for all the tested compounds, along this study, through the analysis of standards aqueous solutions at the following concentrations: 25, 50, 125 and 250 µM for each analyte. All calibration curves displayed a coefficient of correlation (R^2) > 0.99, except for threitol and erythritol (≥ 0.98) and for ribose (= 0.97). Table 14 summarizes the full results. Calibrations curves are shown in Annex 5.

Table 14. Coefficient of linear correlation for the 21 sugars and polyols studied in aqueous solutions. Concentration range: 25-250 µM.

Sugar / Polyol	Linear Regression	R^2
Threitol	y = 0.0048 x	0.9801
Erythritol	y = 0.0049 x	0.9821
Arabinose	y = 0.0022 x	0.9975
Ribose	y = 0.0010 x	0.9700
Fucose	y = 0.0018 x	0.9994
Xylitol	y = 0.0033 x	0.9999
Arabitol	y = 0.0031 x	0.9962
Ribitol	y = 0.0034 x	0.9999
Xylose	y = 0.0026 x	0.9998
Fructose	y = 0.0041 x	0.9999
Galactose	y = 0.0022 x	0.9987
Glucose	y = 0.0017 x	0.9993
Mannitol	y = 0.0043 x	0.9997
Sorbitol	y = 0.0079 x	0.9995
Galactitol	y = 0.0041 x	0.9994
Myo-inositol	y = 0.0044 x	0.9992
Lactose	y = 0.0053 x	0.9999
Sacarose	y = 0.0098 x	0.9998
Maltose	y = 0.0031 x	0.9949
Cellobiose	y = 0.0049 x	0.9999
Melibiose	y = 0.0045 x	0.9998

4.2.2. Intra-assay and inter-assay precision and recovery

The results were obtained by making use of the internal standards indicated in Table 5. The quantification of the sugars was performed using the peak1 area or peak 2 area as indicated in Figure 2.

For the inter-assay precision analysis, the pooled urine was analyzed along one month without and with supplementation, 125 µM or 250 µM, with different sugars and polyols. The results are summarized in Table 15.

Table 15. Imprecision and recoveries of the sugars and polyols trimethylsilylether derivatives in the pooled urine control sample by GC-FID.

Sugar	**Peak # [a]**	**Intra-assay [b] (n= 6)**	**Inter-assay [c] (n= 11)**	**Recovery (%)[d] (n= 4)**
Threitol	1	7.7 (14.6 %)	6.6 (27.1 %)	72.8 (11.2 %)
Erythritol	2	26.4 (12.9 %)	23.0 (26.2 %)	81.0 (11.1 %)
Arabinose	4	15.9 (5.8 %)	14.2 (13.7 %)	105.6 (3.3 %)
Ribose	6	n.d.	n.d.	n.p.
Fucose	7	3.3 (7.5 %)	2.8 (14.8 %)	79.7 (4.1 %)
Xylitol	9	4.9 (5.3 %)	4.6 (10.0 %)	81.5 (3.6 %)
Arabitol	10	22.9 (4.0 %)	21.9 (8.0 %)	n.p.
Ribitol	11	6.5 (5.1 %)	5.9 (15.1 %)	100.5 (3.5 %)
Xylose	12	2.4 (17.2 %)	2.3 (22.7 %)	n.p.
Fructose	13	11.9 (1.0 %)	11.8 (4.8 %)	n.p.
Glucose	15	28.3 (0.2 %)	24.8 (11.3 %)	n.p.
Galactose	16	17.5 (2.2 %)	16.8 (6.8 %)	103.0 (5.2 %)
Mannitol	17	26.7 (3.2 %)	26.2 (4.0 %)	98.8 (2.3 %)
Sorbitol	18	1.9 (8.2 %)	2.0 (5.3 %)	96.5 (1.8 %)
Galactitol	19	3.8 (3.2 %)	3.6 (5.8 %)	95.2 (1.7 %)
Myo-inositol	22	7.3 (1.8 %)	7.3 (3.8 %)	98.3 (1.6 %)
Sacarose	25	7.0 (6.2 %)	6.6 (7.3 %)	n.p.
Maltose	28	n.d.	n.d.	87.2 (6.5 %)
Cellobiose	31	n.d.	n.d.	95.1 (6.0 %)
Lactose	30	15.0 (3.9 %)	14.3 (5.5 %)	n.p.
Melibiose	33	n.d.	n.d.	94.1 (8.5 %)

[a] Peak numbers corresponding with those in Fig. 2 and Table 5
[b] Concentration (mmol/mol creatinine), mean (% RSD).
[c] Concentration (mmol/mol creatinine), mean (% RSD).
[d] Mean (% RSD).
n.d. not detected; n.p. not performed.

The intra-assay and the inter-assay variations range were 0.2 – 17.2% and 4.8 - 27.1%, respectively. The highest variation was observed for the two first polyols – threitol and erythritol – mainly in the inter-assay. This variation may reflect the efficiency of the observed recovery, respectively 72.8% and 81.0%, which are among the lowest of the tested compounds. Clearly, when these two polyols are present at low

concentrations, the imprecision of their quantification must be considered. For all the other tested compounds, the recovery was in the range of 79.7 - 105.6%.

4.2.3. Reference Values

In Table 16, the reference values obtained with the optimized method and determined through the analysis of random urines collected from 16 adult healthy volunteers, under free diet and out of any medication, are compared with the ones reported by Jansen *et al.* and Wamelink *et al*. [1,2]. High similarity in the results was observed.

Table 16. Urinary concentrations (mmol/mol creatinine) of major sugars and polyols in a group of healthy adults. Comparison with published results by Jansen *et al.*.

Sugar / Polyol	Peak # [a]	Mean (n = 16)	Ref. Range [b] (20 – 30 yrs)	Ref. Range [c] (18-77 yrs)	Ref. Range [d] (5-80 yrs)
Threitol	1	9.3	2 - 32	4.8 - 34.3	0 - 35
Erythritol	2	28.2	17 - 48	19.2 - 75.5	14 - 88
Arabinose	4	18.3	9 - 30	8.2 - 36.7	-
Ribose	6	2.8	n.d. - 4	-	-
Fucose	7	3.3	n.d. - 8	n.d. - 12.3	-
Xylitol	9	5.8	3 - 12	1.3 - 20.0	0 - 12
Arabitol	10	26.1	18 - 45	10.2 - 43.9	6 - 60
Ribitol	11	6.8	3 - 16	1.8 - 5.4	0 - 7
Xylose	12	3.9	-	3.7 - 53.6	-
Fructose	13	38.5	5 - 97	4.6 - 57.0	-
Glucose	15	28.4	15 - 65	3.7 - 27.7	-
Galactose	16	17.8	2 - 40	n.d. - 21.7	-
Mannitol	17	13.5	8 - 114	3.1 - 60.5	2 - 28
Sorbitol	18	4.4	1 - 34	2.3 - 26.3	0 - 15
Galactitol	19	4.4	1 - 7	1.5 - 5.6	-
Myo-inositol	22	8.4	2 - 21	2.3 - 22.7	-
Sacarose	25	8.5	n.d. - 41	0.8 - 30.6	-
Maltose	26	1.2	n.d. - 2	-	-
Lactose	30	15.7	2 - 26	1.3 - 7.4	-
Cellobiose	31	-	-	-	-
Melibiose	33	-	-	-	-

[a] Peak numbers corresponding with those in Fig. 2 and Table 5.
[b] Reference values determined by the GC-FID method developed in the laboratory.
[c] Reference values from Jansen *et al.* [1].
[d] Reference values from Wamelink *et al.* [2].
n.d., not detectable.

5. Discussion

The profiling of sugars and polyols in body fluids regained an increased relevance with the recently discovery of new enzymatic defects in the non-oxidative branch of the PPP. Specific profiles of PPP intermediate metabolites were associated with distinct blockages and therefore started to be a useful tool in the screening of this group of pathologies.

The analysis of sugars and polyols has been accomplished essentially by chromatographic methodologies, namely Liquid (LC) or Gas Chromatography (GC). HPLC analysis has been useful for the analysis of phosphate forms of intermediate sugars but it is quite time consuming for routine laboratory work. Recently, LC-MS/MS methods for the analysis of different sugar-phosphates [3, 4] and polyols in urine were developed [2]. GC with flame ionization detection or coupled to mass detection offers high chromatographic resolution as well as good sensitivity. A simple pre-purification sample procedure was proposed by Jansen and co-workers [1], therefore being suitable for screening purposes.

Based on the work of Jansen and co-workers, a GC- FID and GC-MS methods were optimized for the simultaneous analysis of sugars and polyols in body fluids. The selected chromatographic conditions allowed a resolution to the base line for the majority of the peaks of interest. Two parameters were used in the qualitative analysis, namely relative retention time (*RRT*) and the ratio of the areas of the two peaks (peak 1 and 2) assigned to the corresponding sugar trimethylsilylether derivatives. The combination of these two parameters allowed a correct qualitative analysis of unknown samples in comparison with pure standards. As already highlighted the mass spectrum analysis did not add additional data in terms of unequivocal qualitative analysis but it allows to distinguish matrix interference from a true sugar or polyol.

The reproducibility of the used parameters in the qualitative as well as the quantitative analysis was excellent as the agreement of our reference values for urinary`s sugars and polyols proves. In conclusion, the optimized method seems to be an useful tool for the study of the PPP, allowing not only to expand the screening program capability of the laboratory but to contribute to the exploration of the biochemistry determinants of the PPP which is far from being fully understood as well.

6. Bibliography

[1] G. Jansen, F.A. Muskiet, H. Schierbeek, R. Berger, W. van der Slik, Capillary gas chromatographic profiling of urinary, plasma and erythrocyte sugars and polyols as theirtrimethylsilyl derivatives, preceded by a simple and rapid prepurification method, Clin. Chim. Acta. 157 (1986) 277-93.

[2] M.M. Wamelink, D.E. Smith, C. Jakobs, N.M. Verhoeven, Analysis of polyols in urine by liquid chromatography-tandem mass spectrometry: a useful tool for recognition of inborn errors affecting polyol metabolism, J. Inherit. Metab. Dis. 28(2005) 951-63.

[3] M.M. Wamelink, E.A. Struys, J.H. Huck, B. Roos, M.S. van der Knaap, C. Jakobs, N.M. Verhoeven, Quantification of sugar phosphate intermediates of the pentose phosphate pathway by LC-MS/MS: application to two new inherited defects of metabolism, J. Chromatogr. B. Analyt. Technol. Biomed. Life Sci. 823 (2005) 18-25.

[4] J.H. Huck, E.A. Struys, N.M. Verhoeven, C. Jakobs, M.S. van der Knaap, Profiling of pentose phosphate pathway intermediates in blood spots by tandem mass spectrometry: application to transaldolase deficiency, Clin. Chem. 49 (2003) 1375-80.

CHAPTER 4

Pentose phosphate pathway intermediates:
a study in adult patients with liver dysfunction

1. Introduction

Non-alcoholic fatty liver disease (NAFLD) is the most common liver disease recognized in Europe and North America. The prevalence of NAFLD is estimated in 20 – 30% in general population of Western countries [1, 2]. However, these estimations need to be confirmed by testing the significance of the risk factors identified by clinical series in the general population [3]. NAFLD was thought to be a benign condition, but is nowadays recognized as a major cause of liver-related morbidity and mortality [4]. In many cases, NAFLD is associated with obesity, hyper- or dyslipidemia, hyperglycemia, type II diabetes and insulin resistance [5-7]. NAFLD is currently defined as fat accumulation in the liver exceeding 5% to 10% of the weight of the liver [2]. NAFLD is an asymptomatic condition and the diagnosis is mostly made when liver alanine aminotransferase (ALT) and/or aspartate aminotransferase (AST) enzymes are elevated [5], or alternatively when hepatomegaly is detected in ultrasonography performed for another purpose, and without abnormal liver tests [6]. Non-alcoholic steatohepatitis (NASH) is the progressive form of NAFLD that carries a risk for development of fibrosis, cirrhosis, and hepatocellular carcinoma (HCC) [3]. NAFLD is differentiated from alcoholic fatty liver disease (AFLD) by the alcohol intake. The distinction is based on the intake of ethanol under two standard drinks a day (140 g ethanol/week) for men, and one standard drink a day (70 g ethanol/week) for women. Liver biopsy is the only way to confirm the presence or absence of NASH in a NAFLD patient [6].

Transketolase (TKT; **E.C.2.2.1.1**) and transaldolase (TALDO; **E.C.2.2.1.2**) are the key enzymes of the non-oxidative branch of the pentose phosphate pathway (PPP). TKT is the first enzyme, a thiamine diphosphate (ThDP, active vitamin B1) and Ca^{2+} ion dependent enzyme [7], and TALDO is the second enzyme, a cofactor-less enzyme [8]. Together, these two enzymes create a reversible link between the oxidative branch of the PPP and glycolytic intermediates. The PPP activity is regulated according to the needs of the organism and the metabolic situation. If the PPP products are not needed, they are readily transformed into glycolytic intermediates and oxidized [7].

Since the description in 2001, by Verhoeven and co-workers [9], of the first patient with transaldolase deficiency, associated with liver cirrhosis and hepatosplenomegaly, in the first child of healthy, consanguineous Turkish parents [9], the non-oxidative branch of the PPP has regained notoriety, although the contribution to metabolism and cell survival remains poorly understood [8]. Since this first case,

twenty-two other patients have been described in the literature [10-16] and almost all patients presented with hepatosplenomegaly (22/23) and liver dysfunction of similar magnitude (18/23).

In 2009 Hanczko and co-workers demonstrated that homozygote (*Taldo1*$^{-/-}$) and heterozygote (*Taldo1*$^{+/-}$) *Taldo1* deficient mice presented increased rates of cirrhosis and that HCC was the leading cause of death, 17% and 46% respectively, when compared to *Taldo1*$^{+/+}$ littermates. The authors also observed the formation of microvesicular and macrovesicular lipid droplets indicative of steatosis or non-alcoholic fatty liver disease, hepatocyte ballooning and inflammatory changes like non-alcoholic steatohepatitis [17].

Taken together, the liver dysfunction, the recent cases of enzymatic defects in the PPP, namely transaldolase deficiency, and the findings described by Hanczko *et al.*, this study was started with the main goal of understanding a putative link between the biochemical intermediate metabolites of the PPP and the hepatic dysfunction in patients with liver disease of unknown cause (NAFLD) or patients with hepatic dysfunction due to alcohol abuse (AFLD), in the presence or absence of inflammation, cirrhosis and HCC.

In patients with liver dysfunction due to alcohol abuse, the evaluation of these PPP intermediate metabolites may allow the definition of new predictive biomarkers either of disease progression or of the effectiveness of the established treatment.

2. Material

To characterize the pattern of metabolites involved in the PPP of adult patients with NAFLD and AFLD, a protocol was established between the Metabolism and Genetics group of iMed.UL, at Faculty of Pharmacy and the Hepatology Section of Internal Medicine Department at Santa Maria`s University Hospital, both from the University of Lisbon. The protocol was submitted and approved by the hospital ethical council and informed consents were obtained from all the participants in the study.

Since the approval of the study (May 2012) until the present date, 14 patients with hepatic dysfunction (AFLD or NAFLD) were enrolled in the study. A random urine sample was collected when the patient visited the clinician for regular control. Eleven patients had AFLD, and all presented a cirrhotic liver (11/11). Among these,

patient 9 was diagnosed as having HCC, and along the course of this study, patient 12 progressed also to HCC. The remaining three patients had non-alcoholic steatohepatitis (NASH), and none presented a cirrhotic liver. Table 1 summarizes the main features of all fourteen patients enrolled in the study.

3. Results and Discussion

Patients (Table 1) were divided, as already mentioned, into two main groups according to the type of liver dysfunction: *(i)* NASH (Table 2) and *(ii)* AFLD (Table 3). NASH patients' group is a more homogenous group than AFLD patients' group. None of NASH patients developed cirrhosis and/or HCC. In contrast, the AFLD patients' group is a more heterogeneous one, spanning from compensated to decompensated cirrhosis and progressing to HCC in two cases.

The results of sugars and polyols for the NASH and AFLD groups are presented in Table 2 and Table 3, respectively. Table 3 summarizes all patients of the AFLD population, and as shown, patients 2, 4, 9 and 12 presented the highest levels of polyols. These data led us to subdivide the AFLD group into two subgroups: AFLDa (Table 4) and AFLDb (Table 5), with respectively minor and major alterations in polyols' profile.

Patients belonging to the NASH population showed no major abnormalities in their polyols' profile. However, all the patients revealed increased (until 3 fold) ribitol levels, when compared with the reference values. Slight increased excretion of arabitol was detected in patients 3 and 5, and erythritol was slightly elevated in patient 5. In none of these patients sedoheptulose was observed.

The mild alterations observed in glucose, galactose and galactitol excretion levels have no specific significance since these alterations are often observed in situations of liver disease and point out to some deregulation of the PPP non-oxidative branch. However, we must highlight that the number of patients studied so far is too small to allow any conclusion.

Table 1. Fourteen patients were studied and divided into two major groups: AFLD (A) and NASH (B). Individual characteristics like gender, age, NASH or AFLD classification, compensated or decompensated cirrhosis, HCC and alcohol intake situation are summarized.

Patient	Group	Gender		Age (yrs)	NASH	AFLD	Alcoholic Cirrhosis			Abstemious	Non-abstemious
		Male	Female				Compensated	Decompensated	HCC		
1	A		X	60	-	X	X	-	-	-	X
2	A	X		59	-	X	-	X	-	n.a.	n.a.
3	B		X	77	X	-	-	-	-	n.a.	n.a.
4	A	X		61	-	X	X	-	-	-	X
5	B		X	51	X	-	-	-	-	n.a.	n.a.
6	A		X	38	-	X	X	-	-	(Only for 1 mth)	-
7	A	X		61	-	X	X	-	-	X	-
8	A	X		56	-	X	X	-	-	X	-
9	A	X		59	-	X	-	X	X	n.a.	n.a.
10	A	X		49	-	X	X	-	-	X	-
11	B		X	65	X	-	-	-	-	n.a.	n.a.
12	A	X		63	-	X	-	X	X	n.a.	n.a.
13	A		X	64	-	X	X	-	-	X	-
14	A	X		60	-	X	X	-	-	X	-

NASH - nonalcoholic steatohepatitis; AFLD - alcoholic fatty liver disease; HCC – Hepatocellular carcinoma.
n.a. not assessed

Table 2. Urinary carbohydrates results (mmol/mol Creat) of NASH patients. Values presented in red are above the reference values.

Sugar / Polyol	P3	P5	P11	Reference Values [a]
Threitol	15.0	12.9	9.9	5 - 34
Erythritol	48.9	80.9	15.2	19 - 76
Arabinose	17.3	22.5	14.4	8 - 37
Ribose	-	2.9	0.7	-
Fucose	3.7	5.9	6.4	n.d. - 12
Xylitol	16.7	14.2	6.8	n.d. - 20
Arabitol	50.7	65.5	16.4	10 - 44
Ribitol	6.3	15.8	11.0	n.d. - 5
Xylose	3.9	7.2	2.5	4 - 54
Fructose	26.7	3.8	-	5 - 57
Glucose	47.1	109.3	206.4	4 - 28
Galactose	5.0	24.5	40.5	n.d. - 22
Mannitol	49.0	24.7	4.6	3 - 61
Sorbitol	4.2	6.2	2.7	2 - 26
Galactitol	9.7	5.2	6.7	2 - 6
Sedoheptulose	-	-	-	-
***Myo*-inositol**	106.8	54.7	75.7	2 - 23
Sacarose	8.3	12.0	3.5	n.d. -31
Maltose	-	0.7	-	-
Cellobiose	-	0.3	-	-
Lactose	12.5	17.5	5.4	n.d. -7
Melibiose	-	-	-	-

[a] Reference values according to age group

Table 3. Urinary carbohydrates results (mmmol/mol Creat) of AFLD patients. Values presented in red are above the reference values.

Sugar / Polyol	P1	P2	P4	P6	P7	P8	P9	P10	P12	P13	P14	Ref. Val [a]
Threitol	13.8	88.6	6.9	10.2	15.1	15.1	55.0	26.7	47.2	6.3	31.7	5 – 34
Erythritol	24.1	98.5	38.4	13.2	22.2	46.7	124.6	41.6	74.1	46.3	19.6	19 – 76
Arabinose	33.2	32.1	18.1	10.1	12.6	25.1	37.6	16.8	20.3	10.6	11.0	8 – 37
Ribose	5.3	2.0	-	5.7	1.1	-	-	-	-	8.0	-	–
Fucose	14.4	14.0	3.6	2.3	5.0	7.1	9.8	4.6	7.6	4.7	3.7	n.d. – 12
Xylitol	60.2	42.3	549.2	12.7	17.0	22.4	29.5	17.1	26.9	7.5	15.1	n.d. – 20
Arabitol	43.8	108.5	111.0	19.3	27.8	36.2	99.9	34.6	71.2	33.1	29.3	10 – 44
Ribitol	18.1	35.5	90.7	9.3	5.9	12.8	29.1	8.3	25.4	7.4	7.8	n.d. – 5
Xylose	23.1	73.3	9.7	2.7	1.1	17.0	51.7	5.4	8.9	3.2	90.5	4 – 54
Fructose	4.3	114.9	6.0	46.7	42.9	38.8	-	38.2	46.9	20.2	1.0	5 – 57
Glucose	67.5	52.4	305.3	31.3	416.0	69.2	91.1	27.0	59.8	48.7	26.7	4 – 28
Galactose	5.6	6.7	4.6	3.8	3.2	1211.7	9.9	7.2	113.6	41.4	5.9	n.d. – 22
Mannitol	13.7	264.9	63.7	84.1	16.9	1038.4	1387.1	73.1	42.7	957.3	11.2	3 – 61
Sorbitol	8.2	93.3	29.6	2.9	6.6	9.7	25.1	2.4	13.3	1.8	2.9	2 – 26
Galactitol	4.6	17.6	1.9	1.5	1.6	9.6	5.9	7.7	9.3	4.3	3.4	2 – 6
Sedoheptulose	-	-	-	-	-	-	-	-	-	-	-	–
Myo-inositol	16.4	20.2	28.9	3.7	21.8	23.0	11.7	11.1	13.5	9.1	3.9	2 – 23
Sacarose	1.6	110.7	14.6	11.4	22.7	23.3	86.4	27.4	88.0	1.1	23.3	n.d. – 31
Maltose	-	-	-	-	-	-	-	-	-	-	0.4	–
Cellobiose	-	-	-	-	-	-	-	0.4	-	-	0.8	–
Lactose	7.2	22.2	2.4	83.3	3.6	27.9	27.3	8.9	54.6	13.8	19.3	n.d. – 7
Melibiose	-	-	-	0.5	0.4	-	8.1	-	0.4	-	1.3	–

[a] Reference values according to age group

As previously referred, patients of the AFLD group were divided into two subgroups, according to their polyols' pattern. Patients of the AFLDa group (table 4) showed no major abnormalities in these compounds. However, one major finding is that all patients have elevated excretion of ribitol, ranging from slightly above the higher reference value until up to ~ 4 fold. Accordingly, ribitol elevation was a consistent finding throughout all patients enrolled in this study. The extremely high excretion of mannitol in patients 8 and 13 may be explained by the usage of this polyol, as a component of many drugs` excipients, due to its humectant properties and pleasant taste. These patients are under medication not only for their liver dysfunction, but also hypertension (patient 8), gastrointestinal problems and anxiety disorders (patient 13).

Table 4. Urinary polyols results (mmol/mol Creat) of the AFLDa patients. Values presented in red are above the reference values.

Polyol	**P1**	**P6**	**P7**	**P8**	**P10**	**P13**	**P14**	**Ref Val** [a]
Threitol	13.8	10.2	15.1	15.1	26.7	6.3	31.7	5 – 34
Erythritol	24.1	13.2	22.2	46.7	41.6	46.3	19.6	19 – 76
Xylitol	60.2	12.7	17.0	22.4	17.1	7.5	15.1	n.d. – 20
Arabitol	43.8	19.3	27.8	36.2	34.6	33.1	29.3	10 – 44
Ribitol	18.1	9.3	5.9	12.8	8.3	7.4	7.8	n.d. – 5
Mannitol	13.7	84.1	16.9	1038.4	73.1	957.3	11.2	3 – 61
Sorbitol	8.2	2.9	6.6	9.7	2.4	1.8	2.9	2 – 26
Galactitol	4.6	1.5	1.6	9.6	7.7	4.3	3.4	2 – 6
Myo-inositol	16.4	3.7	21.8	23.0	11.1	9.1	3.9	2 – 23

[a] Reference values according to age group

The four patients that were subcategorized as AFLDb (Table 5) present an overall high excretion of the studied polyols. Patient 9, with a diagnosis of HCC, displays high excretion of erythritol, arabitol and ribitol, among other polyols, in the absence of sedoheptulose, pointing to some impairment at the level of the non-oxidative branch of the PPP. Patient 12, after the enrolment in this study, had a liver function deterioration and HCC was established. He displayed an increased excretion of arabitol, ribitol and threitol, and erythritol was near the higher value of the reference values.

Patient 2 presented with decompensated cirrhosis, but no progression to HCC was, until now, observed. His polyols' profile showed high excretion of threitol, erythritol, ribitol and arabitol, also pointing to some impairment in the PPP. Once again mannitol and xylitol were excreted in high amounts, which may be attributed to drug intake. Patient 4 showed no decompensated cirrhosis, but he had not stopped the ingestion of alcohol, therefore the observed polyols' profile might be explained by that finding. This patient was the one that showed the highest excretion of arabitol and ribitol. None of these four patients presented sedoheptulose.

Table 5. Urinary polyols results (mmol/mol Creat) of the AFLDb patients. Values presented in red are above the reference values.

Polyol	P2	P4	P9	P12	Reference Values [a]
Threitol	88.6	6.9	55.0	47.2	5 – 34
Erythritol	98.5	38.4	124.6	74.1	19 – 76
Xylitol	42.3	549.2	29.5	26.9	n.d. – 20
Arabitol	108.5	111.0	99.9	71.2	10 – 44
Ribitol	35.5	90.7	29.1	25.4	n.d. – 5
Mannitol	264.9	63.7	1387.1	42.7	3 – 61
Sorbitol	93.3	29.6	25.1	13.3	2 – 26
Galactitol	17.6	1.9	5.9	9.3	2 – 6
***Myo*-inositol**	20.2	28.9	11.7	13.5	2 – 23

[a] Reference values according to age group

As already referred in chapter 2, the PPP is strictly regulated and different mechanisms may be involved in this complex process. It is known that in many cancers these mechanisms may be disrupted and consequently the PPP will be disturbed. Therefore, we postulate that some mechanisms may also be affected in severe liver dysfunction which may justify the observed altered polyols' profile in the two patients (P2 and P4) with severe liver dysfunction

Transketolase (TKT) is, together with transaldolase, a key enzyme in the non-oxidative branch of the PPP. As previously described, TKT is a thiamine diphosphate and Ca^{2+} ion dependent enzyme. Thiamine deficiency is a well documented effect of long-term alcohol abuse, therefore the abnormal metabolic findings observed in patient

4 may be ascribed to vitamin B1 deficiency. If thiamine levels are low, TKT may be unable of transferring C-1 and C-2 of Xu5P to R5P to form S7P and G3P, or *vice versa*; or to transfer the C-1 and C-2 of Xu5P to E4P to form G3P and F6P, or *vice versa*, leading to an impaired activity in the PPP and an overall accumulation of the intermediate metabolites.

In patient 2, cirrhosis was present but in a decompensated form which can contribute for a more severe impairment of the PPP, leading to the observed accumulation of several polyols (Table 5).

An overall high excretion of urinary polyols was detected in two of the patients (P9 and P12) with HCC. Transaldolase deficiency specific biomarkers, sedoheptulose and/or sedoheptitol, were not presented. Therefore, the hypothesis of a primary defect in the non-oxidative branch of the PPP was excluded. We may postulate that the accumulation of the polyols, in these two cases, is a secondary phenomenon resulting from the disruption of the regulatory mechanisms underlying the PPP. To clarify the possibility of polyol patterns having a diagnostic value in the characterization of liver dysfunction, further studies involving a larger cohort of patients are needed. Moreover, and concerning this clinical phenotype, it will be very interesting to evaluate the effect on specific enzymes of the PPP, such as G6PD, TKT and probably TKTL1, namely not only the respective enzymatic activities but also the protein levels. Due to the direct effect that the PPP deregulation may have in the level of NADPH and its implication on the maintenance of the ratio of reduced (GSH) / oxidated (GSSG) glutathione, cellular redox studies will be relevant to the better understanding of the underlying biochemical processes.

All the studied 14 patients were under personalized therapeutic regimens according to their clinical situation. Therefore, some of the mild alterations, as well as some of the major ones, such as high excretion of xylitol and mannitol, components of drug`s excipients, may be explained by the use of drugs.

In summary, in the light of these preliminary results, and although we have a small number of patients studied so far, we may postulate that an overall altered polyols' profile may be related to liver disease progression and/or severity.

4. Bibliography

[1] G. Bedogni, S. Bellentani, Fatty liver: how frequent is it and why?, Ann. Hepatol. 3 (2004) 63–5.

[2] G. Bedogni, L. Miglioli, F. Masutti, C. Tiribelli, G. Marchesini, S. Bellentani, Prevalence of and Risk Factors for Nonalcoholic Fatty Liver Disease: The Dionysios Nutrition and Liver Study, Hepatology 42 (2005) 44-52.

[3] P. Paschos, K. Paletas, Non alcoholic fatty liver disease and metabolic syndrome, Hippokratia 13 (2009) 9–19.

[4] E.M. Brunt, Nonalcoholic Steatohepatitis, Semin. Liver Dis. 24 (2004) 3–20.

[5] K. Bogdanova, H. Poczatkova, L. Uherkova, D. Riegrova, M. Rypka, J. Feher, G. Marchesini, J. Vesely, Non-alcoholic fatty liver disease (NAFLD)--a novel common aspect of the metabolic syndrome, Biomed. Pap. Med. Fac. Univ. Palacky Olomouc Czech Repub. 150 (2006) 101–4.

[6] G.C. Farrell, C.Z. Larter, Nonalcoholic fatty liver disease: from steatosis to cirrhosis, Hepatology 43 (2006) S99–S112.

[7] L. Pácal, J. Tomandl, J. Svojanovsky, D. Krusová, S. Stepánková, J. Rehorová, J. Olsovsky, J. Belobrádková, V. Tanhäuserová, M. Tomandlová, J. Muzík, K. Kanková, Role of thiamine status and genetic variability in transketolase and other pentose phosphate cycle enzymes in the progression of diabetic nephropathy, Nephrol. Dial. Transplant. 26 (2011) 1229–36

[8] A.K. Samland, G.A. Sprenger, Transaldolase: from biochemistry to human disease, Int. J. Biochem. Cell. Biol. 41 (2009) 1482–94.

[9] N.M. Verhoeven, J.H. Huck, B. Roos, E.A. Struys, G.S. Salomons, A.C. Douwes, M.S. van der Knaap, C. Jakobs, Transaldolase deficiency: liver cirrhosis associated with a new inborn error in the pentose phosphate pathway, Am. J. Hum. Genet. 68 (2001) 1086–92.

[10] N.M. Verhoeven, M. Wallot, J.H. Huck, O. Dirsch, A. Ballauf, U. Neudorf, G.S. Salomons, M.S. van der Knaap, T. Voit, C. Jakobs, A newborn with severe liver failure, cardiomyopathy and transaldolase deficiency, J. Inherit. Metab. Dis. 28 (2005) 169–79.

[11] V. Valayannopoulos, N.M. Verhoeven, M. Karine, G.S. Salomons, S. Daniéle, M. Gonzales, G. Touati, P. Lonlay, C. Jakobs, J.M. Saudubray, Transaldolase deficiency: a new case of hydrops fetalis and neonatal multi-organ disease, J. Pediatr. 149 (2006) 713–717.

[12] C.W. Fung, S. Siu, C. Mak, G. Poon, K.Y. Wong, P.T. Cheung, L. Low, S. Tam, V. Wong, A rare cause of hepatosplenomegaly - Transaldolase deficiency, J. Inherit. Metab. Dis. 30 (Suppl 1) (2007) 62.

[13] M.M. Wamelink, E.A. Struys, G.S. Salomons, D. Fowler, C. Jakobs, P.T. Clayton, Transaldolase deficiency in a two-year-old boy with cirrhosis, Mol. Genet. Metab. 94 (2008) 255–8.

[14] A. Tylki-Szymańska, T.J. Stradomska, M.M. Wamelink, G.S. Salomons, J. Taybert, J. Pawłowska, C. Jakobs, Transaldolase deficiency in two new patients with a relative mild phenotype, Mol. Genet. Metab. 97 (2009) 15–7.

[15] S. Balasubramaniam, M.M. Wamelink, L.H. Ngu, A. Talib, G.S. Salomons, C. Jakobs, W.T. Keng, "Novel heterozygous mutations in TALDO1 gene causing transaldolase deficiency and early infantile liver failure, J. Pediatr. Gastroenterol. Nutr. 52 (2011) 113–6.

[16] W. Eyaid, T. Al Harbi, S. Anazi, M.M. Wamelink, C. Jakobs, M. Al Salammah, M. Al Balwi, M. Alfadhel, F.S. Alkuraya, Transaldolase deficiency: report of 12 new cases and further delineation of the phenotype, J. Inherit. Metab. Dis. [Epub ahead of print] (2013).

[17] R. Hanczko, D.R. Fernandez, E. Doherty, Y. Qian, G. Vas, B. Niland, T. Telarico, A. Garba, S. Banerjee, F.A. Middleton, D. Barrett, M. Barcza, K. Banki, S.K. Landas, A. Perl, Prevention of hepatocarcinogenesis and increased susceptibility to acetaminophen-induced liver failure in transaldolase-deficient mice by N-acetylcysteine, J. Clin. Invest. 119 (2009) 1546–1557.

CHAPTER 5

Pentose phosphate pathway intermediates in liver dysfunction: study in a pediatric group

1. Introduction

The pentose phosphate pathway (PPP) regained the attention of the scientific community after the description by Verhoeven and co-workers [1], in 2001, of the first patient with an inborn error of metabolism (IEM) in the non-oxidative branch of the PPP, a transaldolase (TALDO) deficiency.

After the first reported case of TALDO deficiency, 22 other cases have been reported, until the present date [2-8]. The TALDO deficient patients described in the literature displayed a quite homogenous clinical picture: liver dysfunction (18/23), hepatosplenomegaly (22/23), anemia and thrombocytopenia (21/23), dysmorphic features (17/23) and cardiac problems (20/23). All patients (23/23) had direct or indirect hepatic alterations of unknown cause.

Although the ribose-5-phosphate isomerase (RPI) deficient patient had no liver dysfunction or organomegalies, but rather presented a clinical picture of slowly progressive leukoencephalopathy of unknown origin, accompanied by mild peripheral polyneuropathy [9], it was the study of the PPP, and more specifically sugars' and polyols' pattern, that made the diagnosis possible. Also a benign condition, L-arabinosuria, has been described in 2002, in a patient with dysmorphic features and no liver malfunction [10]. Although this is a benign condition, it was once again the study of the PPP metabolites that led to the diagnosis.

Taking into account the clinical presentation of those new disorders, namely TALDO deficiency, the evaluation of urinary profiles of sugars and polyols in patients presenting liver dysfunction of unknown cause, became a valuable biochemical tool to unveil diagnosis and new defects associated with the PPP. In order to better understand the involvement of this metabolic pathway in liver dysfunction and to shed some light on pathologic significance of altered polyols' profile, we studied a pediatric group with liver dysfunction of unknown cause. For that purpose, a joint protocol was established between our laboratory, Metabolism and Genetics, iMed.UL, at the Faculty of Pharmacy University of Lisbon and the Department of Metabolic Diseases at Pediatrics Hospital, at Coimbra.

As far as we know, this is the first study in a Portuguese group of patients with liver dysfunction regarding the PPP metabolites.

2. Patients

Since the beginning of this collaborative study (June 2012), 11 patients with hepatic dysfunction of unknown cause were enrolled. The first urine of the morning was collected during patients' hospitalization or when they visited the clinician. Samples were immediately frozen, kept at – 20 ºC and sent in dry ice to the laboratory. Samples were kept frozen until time of analysis. Polyols and sugars were analyzed by GC-FID and/or GC-MS as previously described in chapter 3.

Patient 1: *a four-month-old girl. She presented clinically with extrahepatic biliary atresia. She was submitted to Kasai's procedure, but the surgery was not able to restore the biliary atresia and her liver disease was rapidly progressing to hepatic failure.*

Patient 2: *a seven-month-old girl. She was admitted in the Hospital due to a biliary atresia with portal hypertension leading to a cirrhotic liver development. At the date of sample collection, she was awaiting liver transplantation (LT). She also presented a cytomegalovirus (CMV) infection.*

Patient 3: *a two-year-old girl. She presented with a congenital CMV infection with minor alterations of the transaminases levels (normal AST levels; slight elevation of ALT levels: 45-50; Ref. Val.: 10-25). She presented slight facial dysmorphic features. Hepatic biopsy revealed the presence of a slight fibrosis – sequelae of CMV infection. Abdominal echography revealed no morphological alterations of the liver and biliary tract.*

Patient 4: *a five-year-old boy. He presented with hepatic dysfunction of unknown cause, dysmorphic features (low set ears, short neck, enlarged anterior-posterior thorax), failure to thrive and psychomotor retardation, strabismus and ketotic hypoglycemia.*

Patient 5: *a two-year-old boy. He was admitted with hepatic cirrhosis of unknown cause. He is currently awaiting LT. A brain nuclear magnetic resonance (NMR) showed calcification of several vertebral arteries. He had a hepatic biopsy analysis and the results were indicative of an autoimmune hepatitis.*

Patient 6: *a twelve-year-old boy. He presented with hepatitis of unknown cause with high levels of copper, but with no criteria for Wilson's disease. He had normal transaminases levels and a maintained discrete elevation of urea levels. He has complains of dizziness, even when lying down.*

Patient 7: *a ten-year-old girl. She presented a chronic hepatitis of unknown cause. Her liver biopsy revealed a non-alcoholic steatohepatitis (NASH) with mild fibrosis.*

Patient 8: *an eleven-year-old girl. She presented with short stature (136.5 cm; 5-10 percentile) and weight (26.8 Kg; 5 percentile). She presented with elevated transaminases levels, however no organomegalies (liver and spleen within normal reference values) or signs of chronic liver dysfunction were observed. She has no intra- or extra-hepatic biliary atresia. Biochemically she presented normal levels of vitamin B12 and D, with a slight elevation of vitamin E.*

Patient 9: *a seventeen-year-old girl. She was admitted with an autoimmune hepatitis. She has short stature and psychomotor delay with peripheral polyneuropathy and optical neuropathy.*

Patient 10: *a twelve-year-old girl. She presented with hepatomegaly, but with no hepatitis. She has no developmental delay.*

Patient 11: *a twenty-one-month-old boy born after 35 weeks. He was admitted to the Hospital with a neonatal colestasis. He had frequent hypoglycemic episodes and growth retardation, including short stature as well as psychomotor retardation, failure to thrive, genital dysmorphism, large anterior fontanelle and macrocephaly (relative to stature). He also presented with anaemia, secondary hypocortisolism and diarrhea. He has had several childhood infections, but he does not seem to be immunodepressed.*

3. Results

Patients were categorized into four groups according to their ages. Because the excretion of sugars and polyols vary throughout life, the urinary polyols concentrations displayed in Table 1 are correlated with age-matched reference values.

Among the ten of the patients presented in Table 1 nine did not reveal major abnormalities in the polyols' pattern. An interesting finding is that ribitol is elevated in 6 of those patients (60%), being in half of them the only abnormal result.

In patient 4, a slightly elevated excretion of arabitol was also noted. The presence of ribitol plus arabitol may suggest a mild impairment of the non-oxidative branch of the PPP. The urinary organic acids analysis revealed no alterations, but peaks of medication (acetaminophen and phenobarbital) were observed which may affect the normal PPP metabolism. New samples with the patient out of medication intake must be collected and analyzed for clarification of the obtained results.

In patient 5, in addition to the elevated excretion of ribitol, a modest increase in sorbitol and galactitol levels was observed. The presence of these metabolites in moderated levels has been referred as a consequence and not as a primary cause of liver malfunction. Very interestingly, it was found in the urinary organic acids profile of this patient an elevated excretion of ethylmalonic acid, glutaric acid, 3-methyl-glutaric acid, 3-methyl-glutataconic (I and II) acid and 3-hydroxi-3-methyl-glutaric acid, the hypothesis of a mild form of 3-hydroxy-3-methylglutaryl-CoA lyase deficiency was raised. The most common signs and symptoms of this condition are: vomiting; diarrhea;

Table 1. Polyols urinary concentration (mmol/mol creatinine) of patients 1-10.

	3-12 months			2-6 years						6-18 years			
Polyol	P 1	P 2	Ref. Values	P 3	P 4	P 5	P 6	P 7	Ref. Values	P 8	P 9	P 10	Ref. Values
Threitol	1.2	121.9	24 – 79	29.4	31.3	11.7	9.7	13.9	12 – 71	21.7	5.3	10.1	7 – 83
Erythritol	10.4	333.5	89 – 158	61.6	182.6	111.6	40.2	49.3	55 – 405	99.9	27.6	33.6	35 – 179
Xylitol	6.7	104.9	5 – 11	13.7	20.9	37.7	5.4	7.8	5 – 49	16.4	7.2	3.9	3 – 7
Arabitol	7.8	158.2	51 – 99	51.0	138.1	64.2	38.4	41.1	32 – 78	82.2	7.2	27.2	16 – 89
Ribitol	4.0	331.5	10 – 17	13.9	33.3	32.7	10.3	11.6	8 – 11	25.6	7.9	5.1	4 – 11
Mannitol	1.4	351.6	n.d. – 17	12.4	33.5	16.4	21.4	21.6	7 – 48	22.0	11.0	21.2	5 – 74
Sorbitol	3.8	534.1	2 – 13	5.3	12.8	14.2	4.9	5.6	4 – 12	10.3	2.6	3.0	3 – 17
Galactitol	7.4	65.4	–	5.4	9.6	29.3	4.9	5.2	3 – 17	6.0	3.3	6.1	2 – 9
Myo-inositol	4.4	85.8	15 – 113	17.1	25.5	16.3	10.5	7.1	6 – 63	60.3	4.6	3.7	5 – 22

dehydration; lethargy and hypotonia, yet none of these features were present in our patient. A new urine sample is needed to clarify the organic acids' profile and also the carbohydrates' profile.

Patient 8 displays, in addition to the elevated excretion of ribitol, a slight elevation in xylitol and *myo*-inositol excretion. These alterations are only moderate and are not suggestive of a PPP impairment. No alterations were found in the organic acids' profile.

Although patient 9 presented no major alterations in the urinary polyols' profile, we can observe a tendency to low values. The organic acids' profile was assessed and it displayed a mild elevation in methylmalonic acid excretion (24 mmol/mol creatinine; Ref. Value: <5) and also a mild elevation in 3-methylcrotonylglycine. Taken together, these results do not point to an impairment of the PPP, or a specific organic aciduria, but rather a dietary deficiency in vitamins uptake. Further tests are needed to elucidate the organic acids' profile.

The patient with the most severe abnormalities in the polyols' profile was patient 2. She presented an elevation of all, except for *myo*-inositol, the studied polyols as well as in the group of sugars analyzed (data not shown). However, no sedoheptulose was found. Her urinary organic acids profile presented no major abnormalities, although many unidentified peaks were found (maybe due to patients' therapeutic regimen). This polyols' profile is quite similar to the ones of the four patients reported in chapter 4 with the most severe liver dysfunction. As previously referred (chapter 2, section 1.7) the PPP might be enhanced by one, several or a different mechanism, leading to the exacerbation of the PPP activity which may justify the observed pattern. Since the analysis of this sample, the patient was submitted to a LT. It would be of the utmost importance the evaluation of a new urine sample of the patient, in order to evaluate the sugars' and polyols' profile evolution. The collection of new samples has already been discussed with the patient's clinician and in a near future it will be re-evaluated.

The most interesting case was patient 11. Patient's plasmatic acylcarnitines' profile and urinary organic acids' and purine and pyrimidines' profile were assessed, and no alterations were found. The polyols' results are presented in Table 2, and they reveal a strongly elevated excretion of the polyols: erythritol, arabitol and ribitol, plus galactitol and *myo*-inositol.

Table 2. Carbohydrates' urinary concentration (mmol/mol creatinine) of patient 11

Polyol	**P 11a**	**P 11b**	**Ref. Values (1-2 yrs)**
Threitol	70.1	37.3	15 – 122
Erythritol	902.8	936.7	76 – 192
Xylitol	16.7	17.4	7 – 29
Arabitol	161.1	117.4	52 – 88
Ribitol	41.1	23.9	9 – 24
Mannitol	25.0	18.6	n.d. – 81
Sorbitol	8.5	11.8	7 – 56
Galactitol	86.3	70.9	7 – 22
Myo-inositol	103.3	103.4	11 – 76
Sedoheptulose	↑↑	↑↑	–

The most striking result was the presence of an unknown peak with the retention time (*RT*) of the C7-sugar, sedoheptulose.

The carbohydrates' profile of this patient was compared with the one of an already diagnosed TALDO deficient patient (the sample was kindly supplied by Dr. Mirjam Wamelink). In figure 1 the carbohydrates' chromatographic profile of both urine samples: (A) TALDO deficient patient and (B) patient 11, analyzed by GC-FID are showed. In figure 2 the carbohydrates' chromatographic profile of both urine samples: (A) TALDO deficient patient and (B) patient 11, plus the mass spectrum from the unknown peak, analyzed by GC-MS, are displayed. The identity of the peak, as being sedoheptulose was confirmed. The biochemical results, together with the clinical symptoms (in agreement to what has been described in the literature for most TALDO deficient patients), guided us to the suspicion of a TALDO deficiency case.

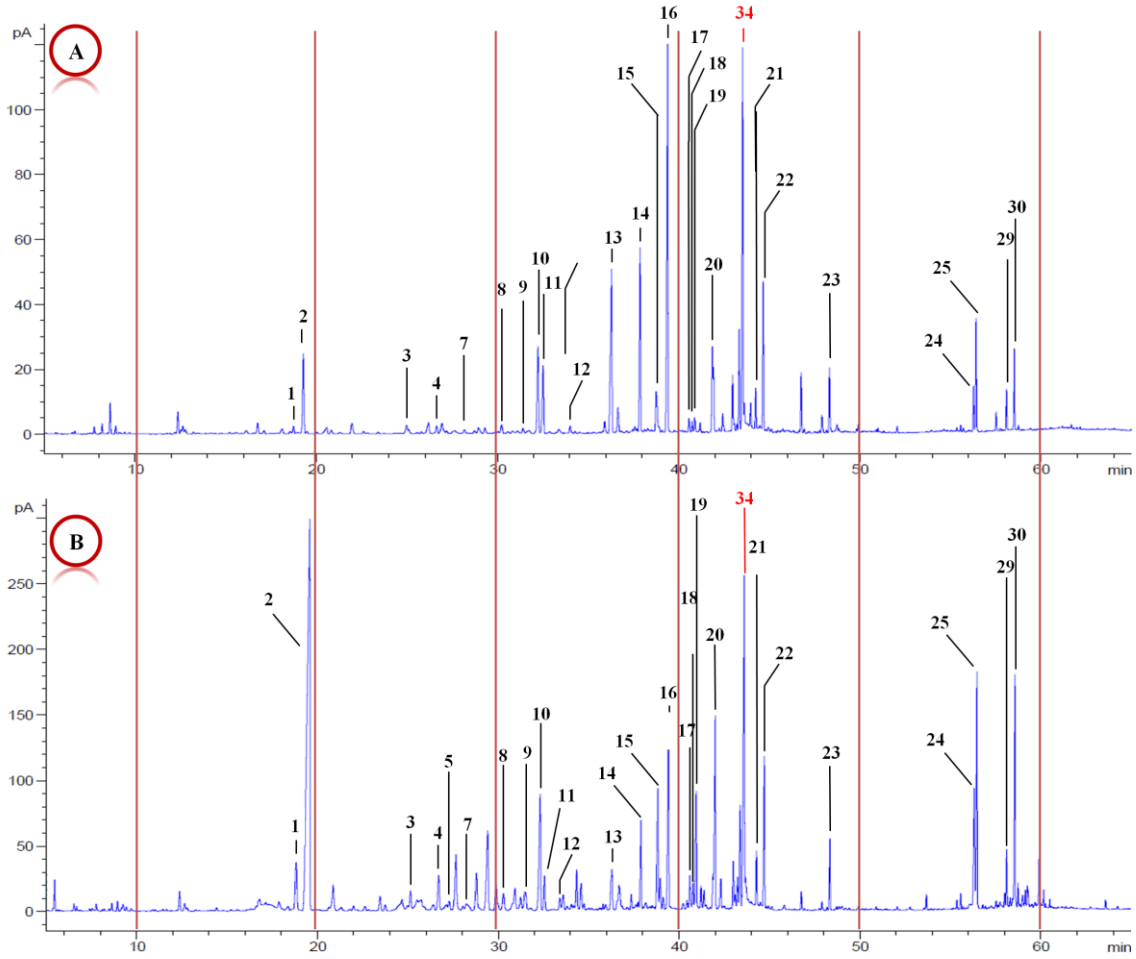

Figure 1. Chromatographic carbohydrates' profile of the TALDO deficient patient (A) and patient 11 (B). The analysis conditions are the same as shown in **Figure 1 in Chapter 3, section 3.3.1**. The peak numbers correspond to the ones displayed in **Figure 2 in Chapter 3, section 4.1.2**. Peak 34 was identified as sedoheptulose.

To support the suspicion of TALDO deficiency further studies were necessary. To our knowledge, all described TALDO deficient patients presented increased excretion of the phosphate form of sedoheptulose, sedoheptulose-7-phosphate (S7P). Therefore, it was recognized as an important biomarker for TALDO deficiency. At the time of the development of this work, in our laboratory, it was not possible to evaluate S7P due to lack of proper methodology. Therefore, the patient's urine samples were evaluated at the Metabolic laboratory, VU University Medical Center, by tandem mass spectrometry (LC-MS/MS), as described by Wamelink and co-workers [11,12]. Interestingly, no S7P was detected.

In light of these new findings, a new hypothesis of diagnosis was raised: sedoheptulokinase deficiency (SHPK). *SHPK* or *CARKL* (carbohydrate kinase-like) gene was first reported by Touchman and co-workers in 2000 [13], when they completely sequenced the genomic region encoding the Nephropathic Cystinosis (*CTNS*) gene. Nephropathic cystinosis is a rare autosomal recessive lysosomal storage disease (MIM# 219800) [14]. The most prevalent mutation is a large deletion of 57,257-bp, accounting not only for the loss of cystinosin, (the integral membrane protein responsible for cystine transport) leading to cystine accumulation within lysosomes; but also the loss of cytoplasmatic CARKL protein (see Figure 3).

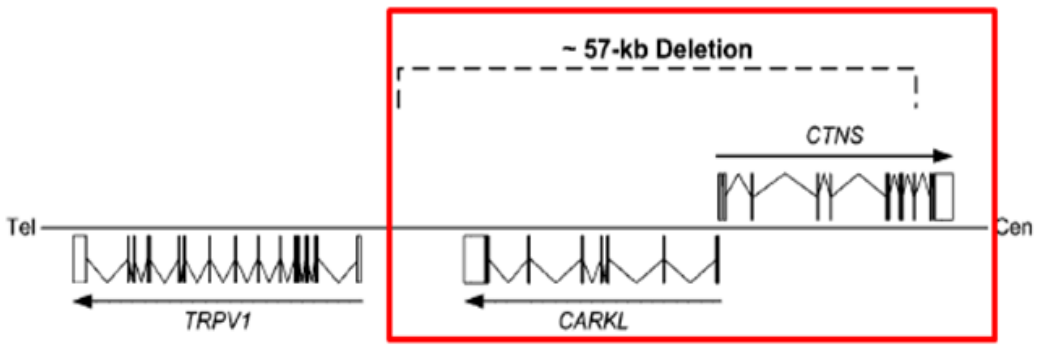

Figure 3. Position and organization of the three genes *TRPV1* (transient receptor potential cation channel subfamily V member 1), *CARKL*, and *CTNS*; and the most common cystinosis mutation (57-kb deletion). Adapted from Wamelink *et al.*, 2008 [78].

The *CARKL* gene is located in chromosome 17 (17p13 region), and is fully contained within the ~57-kb region most commonly deleted in nephropathic cystinosis patients. The CARKL protein was first identified as the SHPK protein, by Wamelink and co-workers in 2008 [15], when they studied the urinary sugars' and polyols' profile of 10 nephropathic cystinosis patients, and found elevated concentrations of sedoheptulose and erythritol in patients homozygous to the 57-kb deletion, when compared to heterozygous patients with other mutations or controls [15].

SHPK catalyses the phosphorylation of sedoheptulose to sedoheptulose-7-phosphate (S7P), being an important regulatory enzyme, responsible for the feeding of S7P molecules to the PPP. Effectively, this allows the reversible function of TALDO and/or TKT, when glyceraldehyde-3-phosphate arising from the glycolytic pathway is

used by the PPP, when increased amounts of NADPH and/or ribose moieties are needed for nucleotides production.

The *CARKL/SHPK* gene was studied in collaboration with the VU University Medical Center. Total RNA was extracted from whole blood samples of the patient and his mother, reverse transcribed into cDNA and then PCR amplified. The open reading frame (ORF) of the *SHPK* gene and the splice sites have also been analyzed by sequence analysis of genomic DNA, and a nonsense mutation, c.355C>T (p.R119X), leading to a truncated non-functional protein, was found in homozygosity. The mother was found to be a carrier for the same mutation. DNA sample from the father was not available for mutational analysis. *TALDO1* gene was also sequenced for differential diagnosis purpose, but no pathogenic mutations were detected. The activity of SHPK was measured in fibroblast homogenates and a strongly reduced formation of S7P was detected (2.9 nmol/hour/mg protein; controls 20-54), indicating SHPK deficiency. To the present date, only two patients, the patient described above and a Dutch baby girl (Wamelink, personal communication), were found. Further tests are needed to fully characterize this patient, once the high frequency of this c.355C>T variant, 8/4292 European control individuals (http://evs.gs.washington.edu/EVS/), does not suggest it might be responsible for an inborn error of PPP metabolism showing a severe phenotype.

4. Final remarks

The study of the urinary profile of sugars and polyols, as Verhoeven and co-workers clearly shown, in 2001, is of the upmost importance not only for diagnostic purposes, but also for a better understanding of the cellular mechanisms. However, at present, the study of sugars' and polyols' profile is not yet done as a routine diagnostic workup in patients with liver disease of unknown cause.

The evaluation of sugars and polyols among the group of selected patients revealed two interesting situations: patient 11 seems to possess a new inborn error of metabolism at the SHPK enzyme level. Until now, as much as we know, an isolated defect in the SHPK enzyme has never been described. Further studies are still in course to fully establish the defect and its link with the patient`s clinical phenotype. Furthermore, patient 2 revealed a very interesting profile associated with a severe form

of liver disease, which is in accordance with our previous observations concerning the adult patients (**chapter 4**). Further studies are necessary for the clarification of these cases.

5. Bibliography

[1] N.M. Verhoeven, J.H. Huck, B. Roos, E.A. Struys, G.S. Salomons, A.C. Douwes, M.S. van der Knaap, C. Jakobs, Transaldolase deficiency: liver cirrhosis associated with a new inborn error in the pentose phosphate pathway, Am. J. Hum. Genet. 68 (2001) 1086–92.

[2] N.M. Verhoeven, M. Wallot, J.H. Huck, O. Dirsch, A. Ballauf, U. Neudorf, G.S. Salomons, M.S. van der Knaap, T. Voit, C. Jakobs, A newborn with severe liver failure, cardiomyopathy and transaldolase deficiency, J. Inherit. Metab. Dis. 28 (2005) 169–79.

[3] V. Valayannopoulos, N.M. Verhoeven, M. Karine, G.S. Salomons, S. Daniéle, M. Gonzales, G. Touati, P. Lonlay, C. Jakobs, J.M. Saudubray, Transaldolase deficiency: a new case of hydrops fetalis and neonatal multi-organ disease, J. Pediatr. 149 (2006) 713–717.

[4] C.W. Fung, S. Siu, C. Mak, G. Poon, K.Y. Wong, P.T. Cheung, L. Low, S. Tam, V. Wong, A rare cause of hepatosplenomegaly - Transaldolase deficiency, J. Inherit. Metab. Dis. 30 (Suppl 1) (2007) 62.

[5] M.M. Wamelink, E.A. Struys, G.S. Salomons, D. Fowler, C. Jakobs, P.T. Clayton, Transaldolase deficiency in a two-year-old boy with cirrhosis, Mol. Genet. Metab. 94 (2008) 255–8.

[6] A. Tylki-Szymańska, T.J. Stradomska, M.M. Wamelink, G.S. Salomons, J. Taybert, J. Pawłowska, C. Jakobs, Transaldolase deficiency in two new patients with a relative mild phenotype, Mol. Genet. Metab. 97 (2009) 15–7.

[7] S. Balasubramaniam, M.M. Wamelink, L.H. Ngu, A. Talib, G.S. Salomons, C. Jakobs, W.T. Keng, "Novel heterozygous mutations in TALDO1 gene causing transaldolase deficiency and early infantile liver failure, J. Pediatr. Gastroenterol. Nutr. 52 (2011) 113–6.

[8] W. Eyaid, T. Al Harbi, S. Anazi, M.M. Wamelink, C. Jakobs, M. Al Salammah, M. Al Balwi, M. Alfadhel, F.S. Alkuraya, Transaldolase deficiency: report of 12 new cases and further delineation of the phenotype, J. Inherit. Metab. Dis. [Epub ahead of print] (2013).

[9] M.S. van der Knaap, R.A. Wevers, E.A. Struys, N.M. Verhoeven, P.J. Pouwels, U.F. Engelke, W. Feikema, J. Valk, and C. Jakobs. Leukoencephalopathy Associated with a Disturbance in the Metabolism of Polyols, Ann. Neurol. 46 (1999) 925–928.

[10] W. Onkenhout, J.E. Groener, N.M. Verhoeven, C. Yin, L.A. Laan, L-Arabinosuria: a new defect in human pentose metabolism, Mol. Genet. Metab. 77 (2002) 80–85.

[11] M.M Wamelink, D.E. Smith, C. Jakobs, N.M. Verhoeven, Analysis of polyols in urine by liquid chromatography-tandem mass spectrometry: a useful tool for recognition of inborn errors affecting polyol metabolism, J. Inherit. Metab. Dis. 28 (2005) 951-63.

[12] M.M Wamelink, D.E. Smith, E.E. Jansen, N.M. Verhoeven, E.A. Struys, C. Jakobs, Detection of transaldolase deficiency by quantification of novel seven-carbon chain carbohydrate biomarkers in urine, J. Inherit. Metab. Dis. 30 (2007) 735-42.

[13] J.W. Touchman, Y. Anikster, N.L. Dietrich, V.V. Maduro, G. McDowell, V. Shotelersuk, G.G. Bouffard, S.M. Beckstrom-Sternberg, W.A. Gahl, E.D. Green ED, The genomic region encompassing the nephropathic cystinosis gene (CTNS): complete sequencing of a 200-kb segment and discovery of a novel gene within the common cystinosis-causing deletion, Genome Res. 10(2000)165-73.

[14] M. Town, G. Jean, S. Cherqui, M. Attard, L. Forestier, S.A. Whitmore, D.F. Callen, O. Gribouval, M. Broyer, G.P. Bates, W. van't Hoff, C. Antignac, A novel gene encoding an integral membrane protein is mutated in nephropathic cystinosis, Nat. Genet. 18 (1998) 319-24.

[15] M.M. Wamelink, E.A. Struys, E.E. Jansen, E.N. Levtchenko, F.S. Zijlstra, U. Engelke, H.J. Blom, C. Jakobs, R.A. Wevers, Sedoheptulokinase deficiency due to a 57-kb deletion in cystinosis patients causes urinary accumulation of sedoheptulose: elucidation of the CARKL gene, Hum. Mutat. 29 (2008) 532-6.

CHAPTER 6

Final remarks and perspectives

Final remarks

In the last 15 years the understanding of the biochemical alterations associated with disruption of the pentose phosphate pathway (PPP), due to primary or secondary causes, regained the attention of the scientific community with the description of two new inborn errors of metabolism in the non-oxidative branch of the PPP: ribose-5-phosphate isomerase deficiency and transaldolase deficiency. Further attention has been paid to sugars' and polyols' profiles. Biomarkers, as well as chromatographic profiles for other specific defects in the PPP, such as L-arabinosuria and essential pentosuria, were established. The evaluation of sugars and polyols also became relevant for the diagnosis and follow up of therapeutic effectiveness of other carbohydrates related diseases (Diabetes Mellitus and Galactosemia), and also for the study of liver and kidney diseases of unknown cause.

The development and validation of the GC-FID method described in **chapter 3,** was achieved with full success since the objectives were accomplished, *i.e.* excellent resolution and reproducibility of the chromatographic parameters and overall precision. Therefore, the optimized method fulfills the requirements to be used in the screening of PPP defects and to the study of metabolic disturbances in sugars and polyols pathways.

The evaluation of the metabolic profiles, within the pediatric group of patients, unraveled a new disorder in the PPP: sedoheptulokinase (SHPK) deficiency. Further studies seem to confirm the genetic defect and, to our knowledge, this is the first reported case of isolated SHPK deficiency. Interestingly, a second patient has now been found (Wamelink, personal communication). Nevertheless, the patients` clinical signs and symptoms are not fully coincident. So, the association of the genotype with the observed clinical phenotype needs to be clarified and additional studies are required.

Moreover, the cross analysis of the results of the two studied groups, adults (**chapter 4**) and children (**chapter 5**) with liver dysfunction, pointed to an important role of sugars and polyols metabolites on the assessment of liver dysfunction progression and/or its severity.

Perspectives

Taking together the work developed along **chapters 3, 4** and **5** aiming to explore the role of the PPP biomarkers in metabolic dysfunction, several questions were raised that need to be answered, either from a strict analytical point of view or in the scope of the cellular mechanisms. This knowlegde will surely lead to a better understanding of the relationship between the altered PPP patterns and liver disease.

The two groups of patients - adults and children - with liver dysfunction revealed interesting findings. The significance of the altered sugar and polyol pattern, observed in association with liver dysfunction progression and severity, needs to be evaluated in a largest cohort of patients. Only then, it will be possible to confirm or refute our preliminary results which allowed us to raise the hypothesis that polyols may be regarded as predictive biomarkers of progression of liver disease to hepatocellular carcinoma.

The discovery of a new defect in the PPP, the isolated form of SHPK deficiency, clearly pointed to the relevance of the evaluation, as a first screening, of the urinary sugar and polyol metabolites in patients with liver dysfunction. Therefore, the analysis of those intermediates will be integrated into the screening panel of metabolic tests in course in the laboratory of Metabolism and Genetics at FFUL, contributing to the expansion of inborn errors of metabolism screening tests offered in Portugal. However, efforts need to be put on the development of analytical methods (HPLC or LC-MS/MS) that will allow the evaluation of sugar phosphate forms, since these compounds are crucial for the differential diagnosis among the PPP defects. Furthermore, the evaluation of some of the carbohydrates metabolites, such as galactitol and sorbitol, gained relevance in the control of galactosemia and diabetes mellitus therapeutic regimens, respectively.

The importance of the PPP towards the redox status of the cell, as the leader pathway in the production of NADPH, clearly suggests that the study of redox status markers will be an area to be explored, aiming the better understanding of the cellular effects caused by PPP disruption. Furthermore, the processes involved in the PPP regulation are far from being fully understood. The PPP turns out to be a target of great interest in liver disease, including cancer, and the possibility of proceeding with this preliminary work is crucial and promising.

Acknowledgements/Agradecimentos

Este mestrado foi uma longa viagem e finalmente o fruto de tanto trabalho, tristezas e alegrias está materializado sobre a forma deste manuscrito que de muito me orgulho. Durante todas as viagens conhecemos locais, pessoas e experienciamos as mais variadas situações e emoções. Nesta "pequena" viagem que foi o meu trabalho e consequente tese de mestrado, e apesar de não terem sido muitos os locais visitados, muitas foram as pessoas que nela entraram e que a tornaram única e importante. A elas dedico esta tese e a elas espero fazer justiça na altura de agradecer.

Antes de mais, o meu primeiro e profundo agradecimento à minha orientadora, a Prof. Doutora Isabel Tavares de Almeida. Muito obrigado por acreditar em mim e no meu trabalho, pelo apoio, conselhos, amizade, orientação crítica e por me ter disponibilizado o espaço e as ferramentas necessárias ao desenvolvimento de todo o trabalho experimental e criativo que levou tanto ao meu crescimento científico como pessoal.

Um agradecimento muito especial à Prof. Doutora Isabel Rivera. Um enorme obrigado por todos os conselhos, ensinamentos, críticas, incansável disponibilidade e acima de tudo pela grande amizade que tem tido ao longo destes anos para comigo.

I would like to express my deep gratitude to Prof. Dr. Cornelis Jakobs, Prof. Dr. Gajja Salomons and Prof. Dr. Henk Blom for all your advices, and for giving me the opportunity to work in your lab and learn the analytical methods that allowed the development of this work. A special thanks to Dr. Mirjam Wamelink, for all the advices and invaluable teachings in the pentose phosphate pathway area.

Gostaria de deixar um agradecimento muito especial à Drª Luisa Diogo e Drª Helena Cortez-Pinto pelo apoio, ensinamentos e constantes trocas de informação sobre os "nossos" doentes. Muito obrigado pela vossa imprescindível ajuda, sem vós esta tese não seria possível.

Gostaria de agradecer aos meus amigos e colegas do grupo Met&Gen com quem passo tantas horas do meu dia de trabalho, e com quem adoro passar tantas outras fora do mesmo. A todos vocês um enorme obrigado.

À Ana Serrão (um enorme obrigado por seres assim: um poço de bondade e amizade. São tantos os dias e horas que passamos juntos que sinto que somos família. Obrigado pelas nossas conversas sérias e malucas (haverá sempre carnitinas!), jantares e almoços, pelos inúmeros conselhos e enorme amizade); Cristina (um enorme obrigado por toda a tua ajuda e conselhos, pela tua sempre boa disposição e alguma maluquice que contagia todos os que estão ao pé de ti e acima de tudo pela tua amizade); Marco (obrigado pelo partilhar do fardo das rotinas em tantas ocasiões, permitindo-me concentrar nos "meus" açucares. É assustador quando do nada começamos a cantarolar (inevitavelmente uma má canção) ao mesmo tempo. Muito obrigado pela tua amizade), Israel (um enorme obrigado pelos conselhos e pela boa disposição que sempre apresentas, nem sempre sendo esse o teu estado de espírito. Obrigado pelos almoços, lanches e jantares e acima de tudo pela tua grande amizade), Joana, Liliana e Luciana muito obrigado pelo vosso apoio e amizade.

Gostaria ainda de agradecer às colegas e amigas do grupo do DNA: Madalena (tu foste a minha primeira colega de bancada e como tal jamais esquecerei as tuas gargalhadas e enorme alegria com que contagias quem te rodeia); Hana Pereira e Sandra Brasil (muito obrigado pela enorme amizade e pelas nossas conversas divertidas ao longo destes anos).

Aos colegas e amigos do grupo das proteínas: Marisa, Henrique, Paulo, João Leandro, Mariana, João Vicente e Ana Isabel pelos bons tempos passados em almoços e jantares, congressos e viagens, e pelas inúmeras conversas divertidas que tivemos um enorme obrigado.

Às professoras do grupo Met&Gen: Prof. Doutora Maria João Silva, Paula Leandro, Margarida Leite, Margarida Silva e Rita Castro o meu profundo agradecimento por todos os ensinamentos que me transmitiram ao longo deste percurso, pelas críticas sempre construtivas e pela amizade.

Às minhas colegas de laboratório: D. Amélia Pereira (muito obrigado por toda a amizade e pelos bons conselhos que me deu e que me permitiram crescer como pessoa), D. Conceição (obrigado pela constante preocupação pelo meu bem estar, pelas conversas bem dispostas e pela amizade) Drª Elisa e D. Lucinda muito obrigado pelo vosso apoio e amizade.

Quero ainda agradecer à Andreia Luz (muito obrigado pelo teu enorme apoio ao longo deste tempo, pelas nossas corridinhas, pelos jantares e conselhos e acima de tudo pela tua amizade); Andreia Carvalho (a menina do "outro" grupo, mas que sempre vinha dar um olá e 3 dedinhos de conversa. Muito obrigado pela sempre boa disposição e enorme amizade) e Ana Pinheiro (muito obrigado pelo teu grande apoio e pelos conselhos).

Um agradecimento muito especial à Sara pelas inúmeras conversas que tivemos, as conversas completamente non-sense e exageradas e as de discussão de trabalho; as piadas tão secas e as gargalhadas de ficar com dores nos maxilares. Muito obrigado pela tua amizade. À Paula um enorme obrigado pelas conversas e conselhos, brincadeiras e piadas non-sense. Muito obrigado ainda pelos almoços e jantares maravilhosos e pela sempre boa companhia. As nossas sessões de cinema e os períodos musicais criativos serão sempre uma alegria. Muito obrigado pela tua grande amizade. Ao Ruben Esse um grande obrigado pelos teus conselhos (que tenho sempre em conta), pelas viagens, pelos almoços, petiscos e jantares, pelas sessões de cinema, pelas sessões de corrida e acima de tudo pela tua amizade. Ao Nicolau um especial agradecimento pelas conversas até altas horas sobre tudo e nada, mas sempre interessantes. Obrigado pelas escolhas cinematográficas que me introduziram no mundo dos clássicos e pelas viagens musicais. Acima de tudo obrigado pela tua amizade.

Por último um agradecimento muito especial à minha família. Ao meu irmão Emilio e Diana um grande obrigado por todo o apoio e conselhos. Obrigado mano por sempre teres uma palavra inteligente e amiga a dar. Aos meus pais, o meu mais especial e profundo agradecimento. Esta tese é tanto minha quanto vossa. Foi graças aos vossos conselhos, incentivos e à confiança que me transmitiram que cheguei aqui. A vocês o meu maior obrigado.

Annexes

Annex 1. Urine Sample Preparation

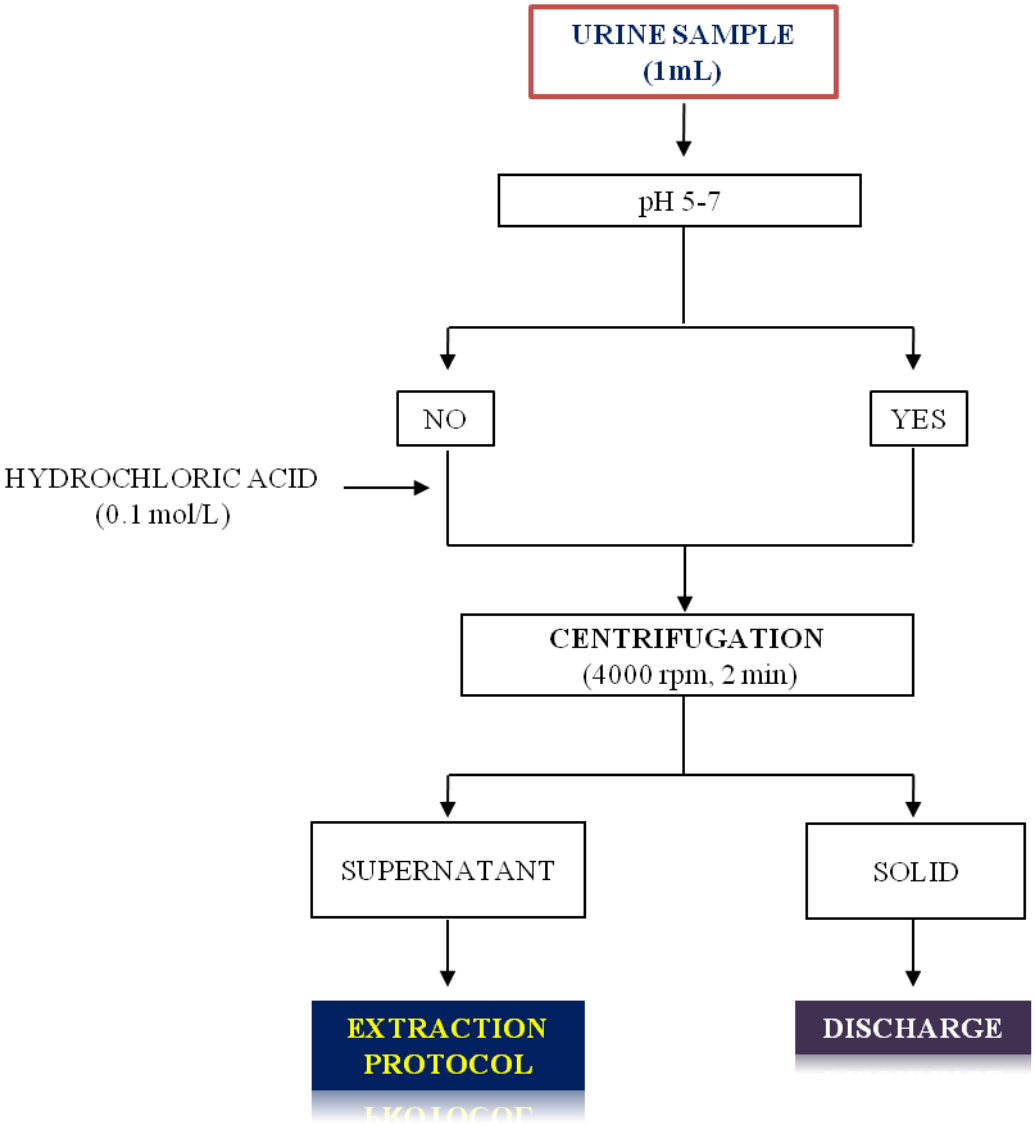

Annex 2. Plasma Sample Preparation

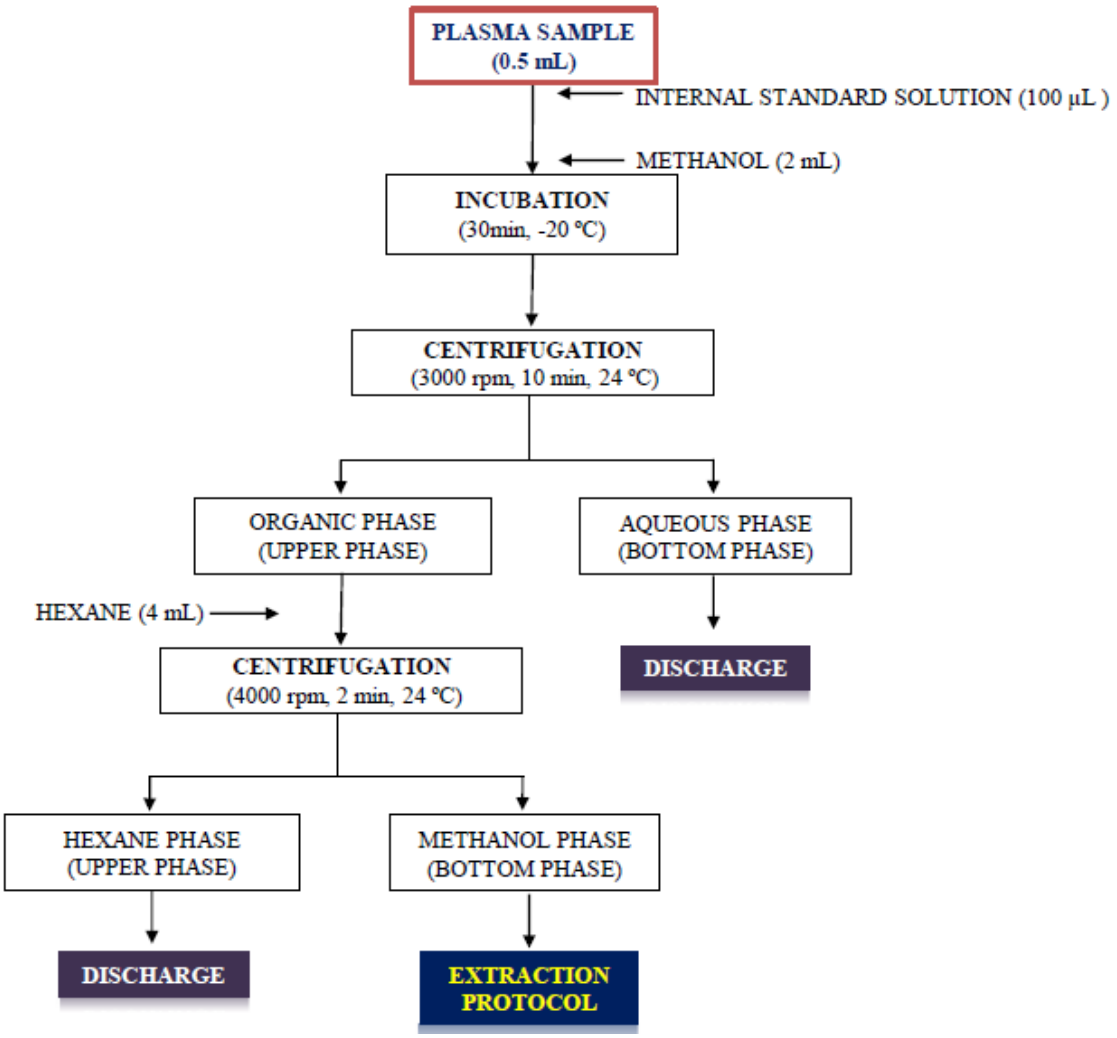

Annex 3. Extraction protocol: Sugars and polyols trimethylsilylether derivatives

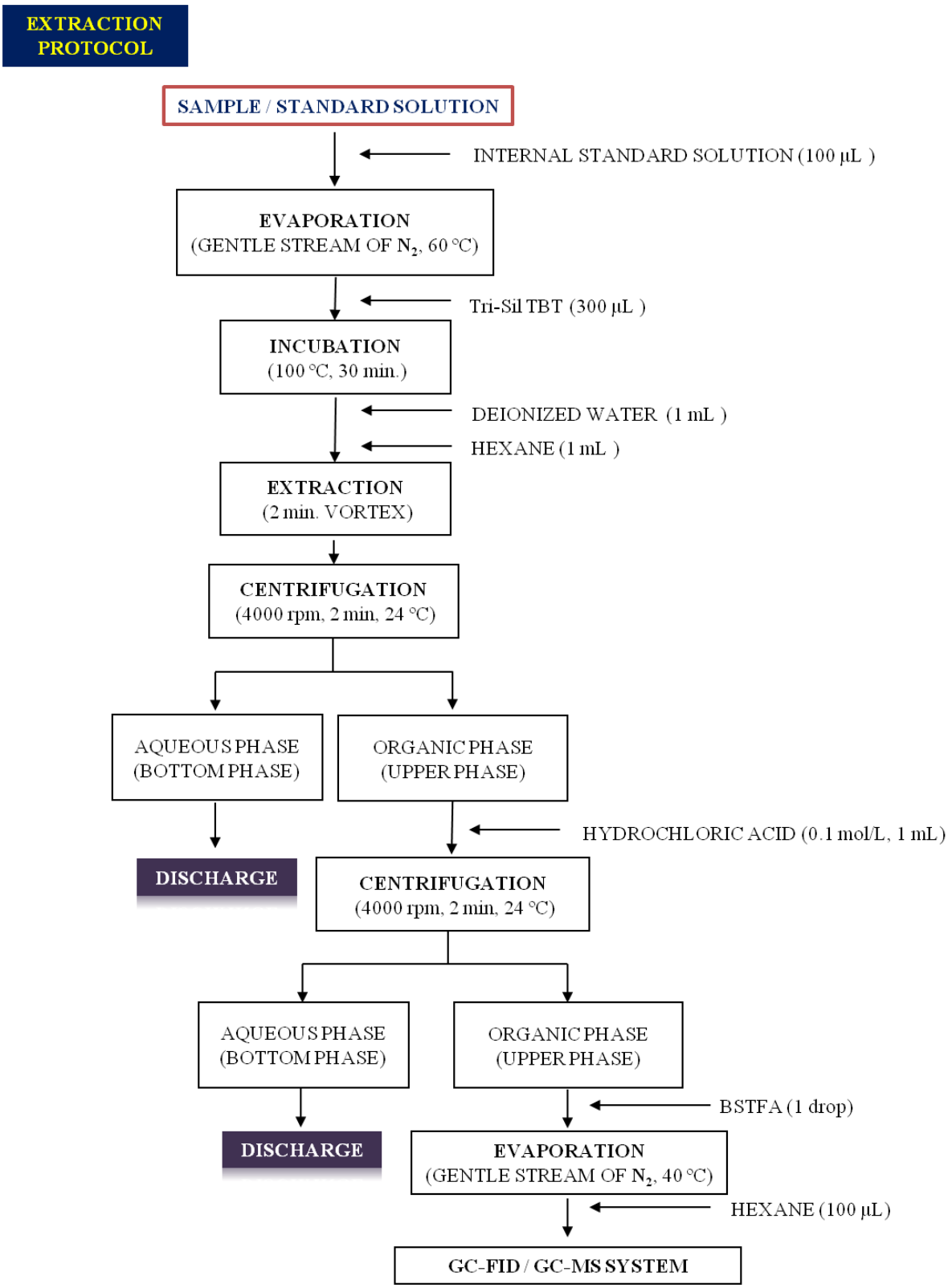

Annex 4. Optimization of the chromatographic resolution conditions

A

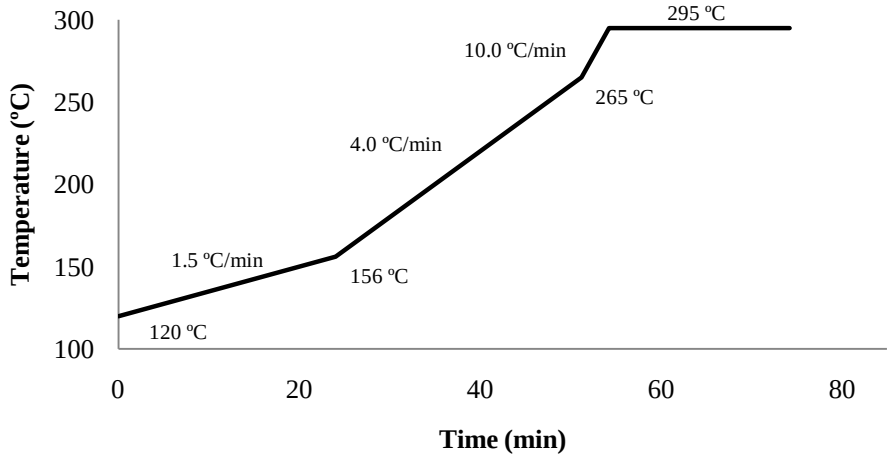

Step	Temperature (ºC)	Rate (ºC/min)	Time (min)
i	120	1.5	0
ii	156	4.0	0
iii	265	10.0	0
iv	295	-	20

A. Oven temperature program: starting at 120 ºC rising to 295 ºC in four steps, with a total run time of approximately 75 min/sample.

B

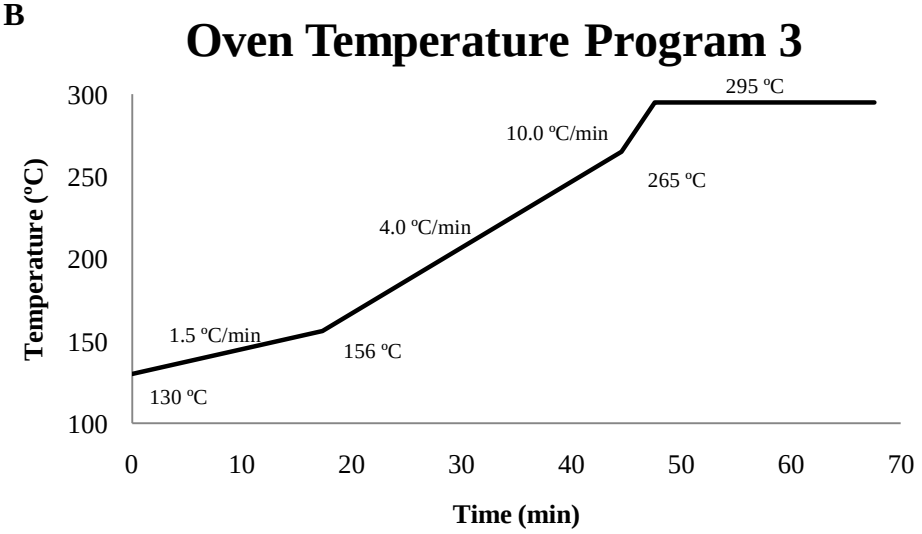

Step	Temperature (ºC)	Rate (ºC/min)	Time (min)
i	130	1.5	0
ii	156	4.0	0
iii	265	10.0	0
iv	295	-	20

B. Oven temperature program: starting at 130 ºC rising to 295 ºC in four steps, with a total run time of approximately 68 min/sample.

C

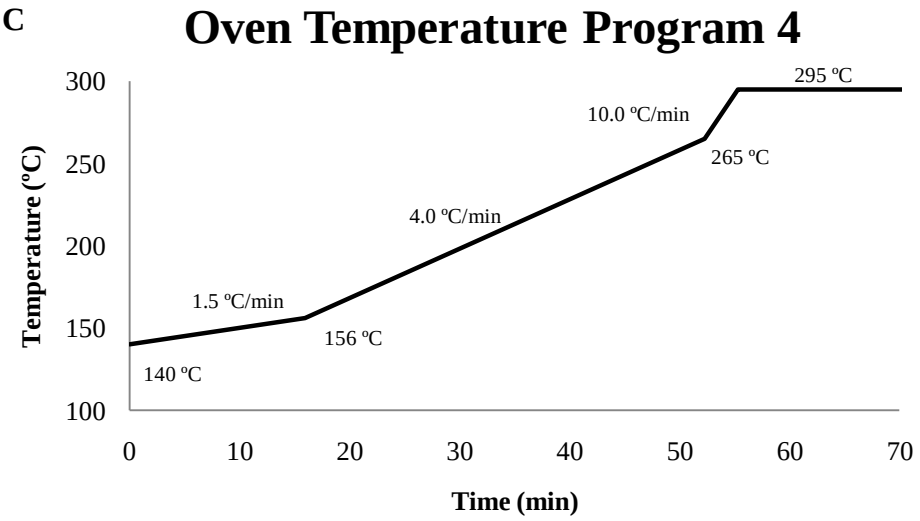

Step	Temperature (ºC)	Rate (ºC/min)	Time (min)
i	140	1.5	0
ii	156	4.0	0
iii	265	10.0	0
iv	295	-	30

C. Oven temperature program: starting at 140 ºC rising to 295 ºC in four steps, with a total run time of approximately 85 min/sample.

Annex 5. Sugars and polyols calibration curves

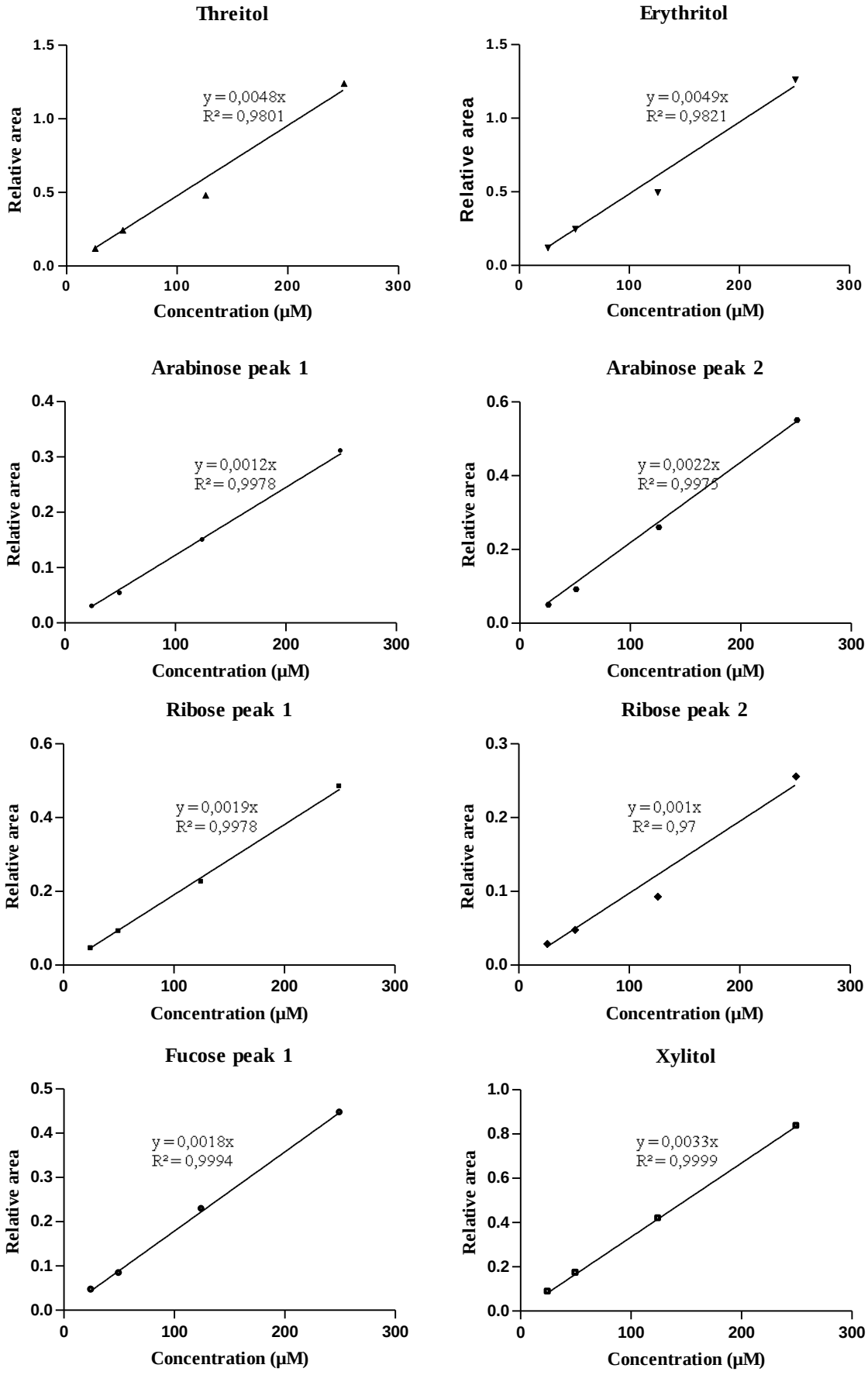

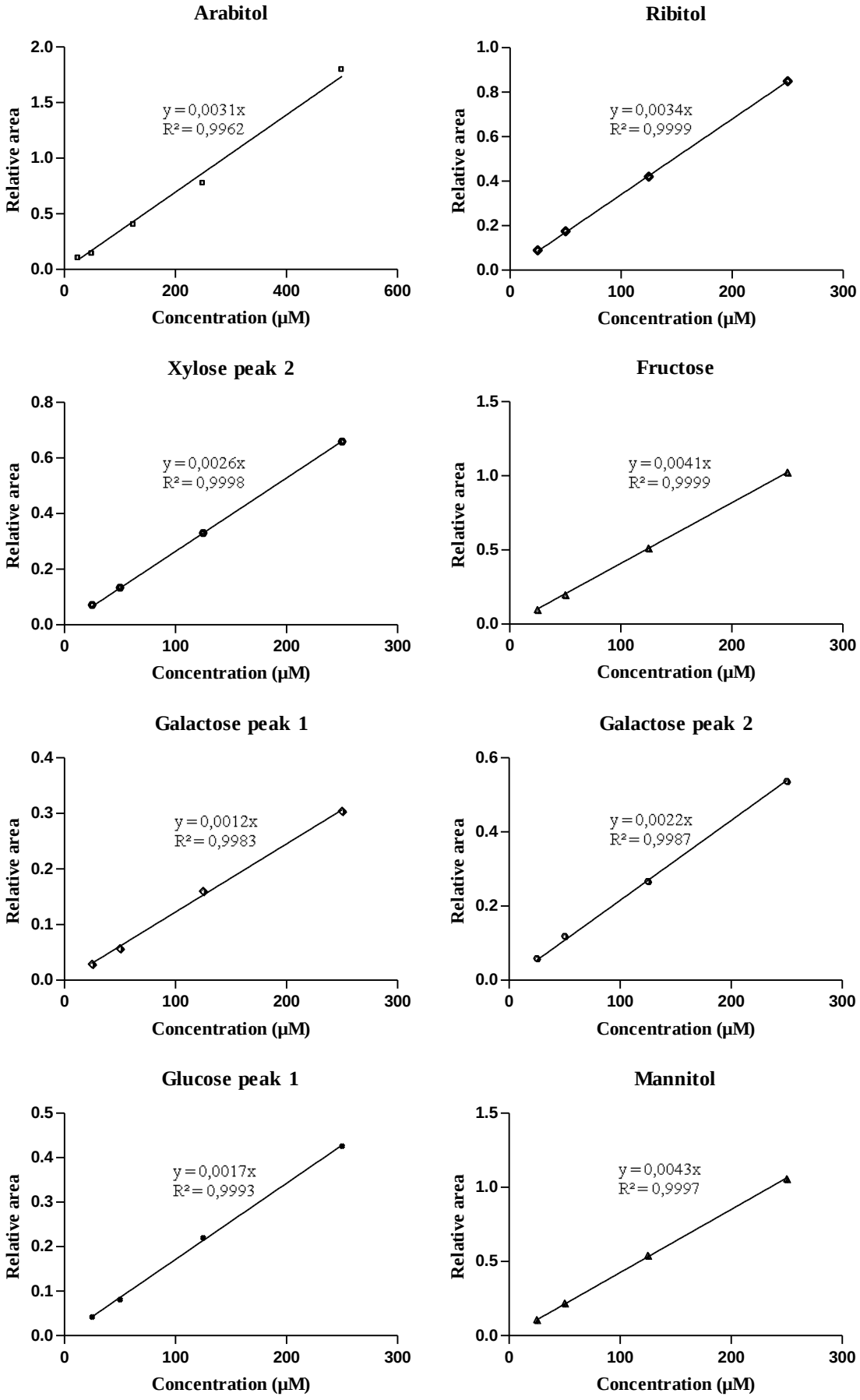
Arabitol
y = 0,0031x
R² = 0,9962
Relative area
Concentration (µM)
Ribitol
y = 0,0034x
R² = 0,9999
Relative area
Concentration (µM)
Xylose peak 2
y = 0,0026x
R² = 0,9998
Relative area
Concentration (µM)
Fructose
y = 0,0041x
R² = 0,9999
Relative area
Concentration (µM)
Galactose peak 1
y = 0,0012x
R² = 0,9983
Relative area
Concentration (µM)
Galactose peak 2
y = 0,0022x
R² = 0,9987
Relative area
Concentration (µM)
Glucose peak 1
y = 0,0017x
R² = 0,9993
Relative area
Concentration (µM)
Mannitol
y = 0,0043x
R² = 0,9997
Relative area
Concentration (µM)

Sorbitol

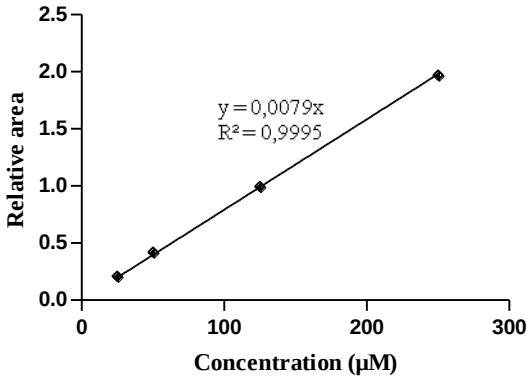

Galactitol

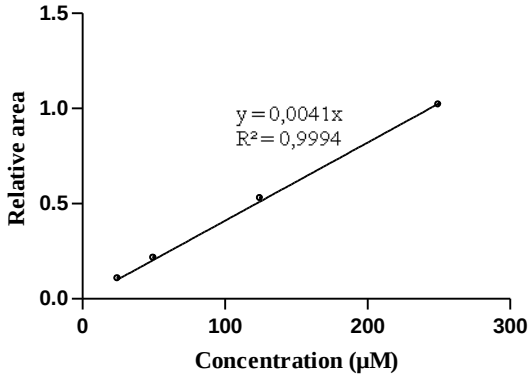

***Myo*-inositol**

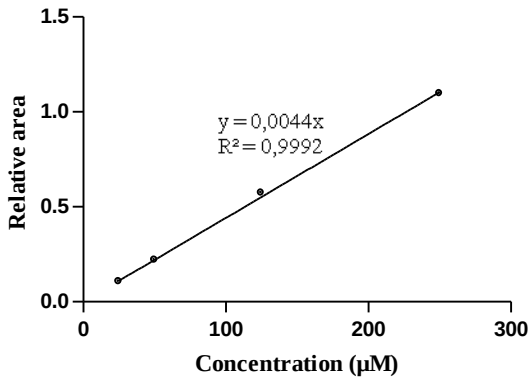

Lactose peak 1

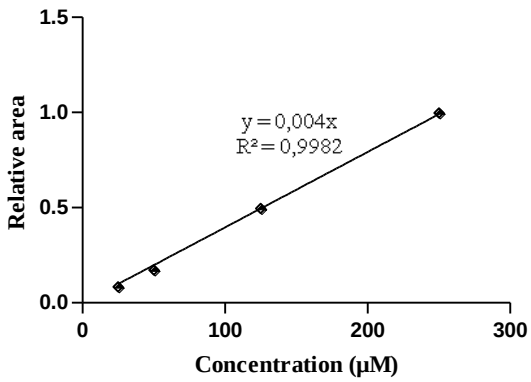

Lactose peak 2

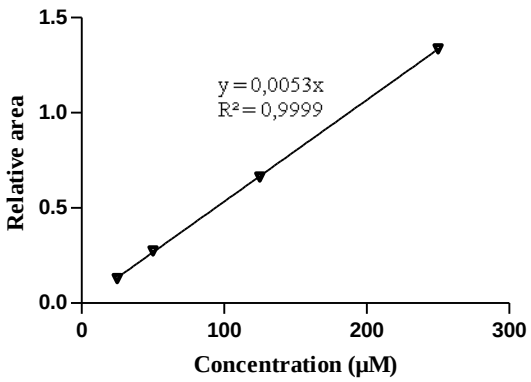

Sacarose

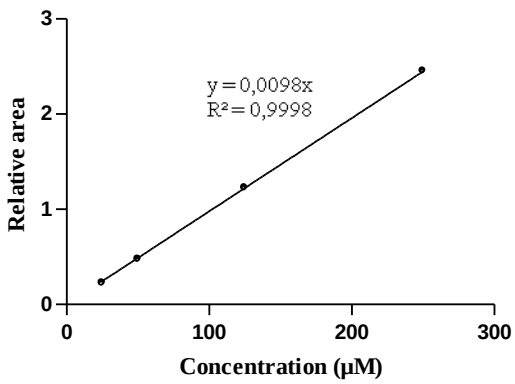

Maltose peak 1

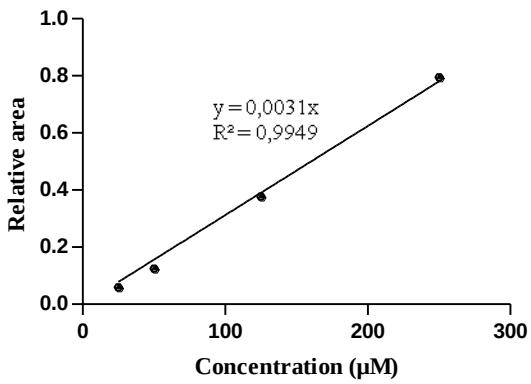

Maltose peak 2

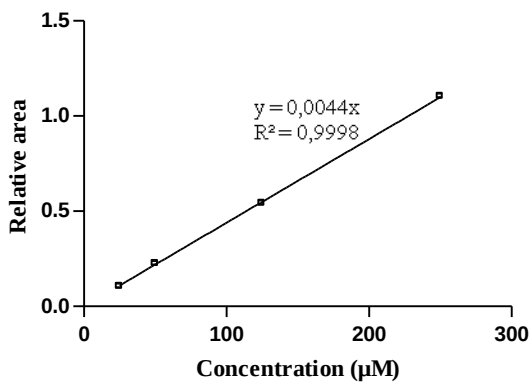

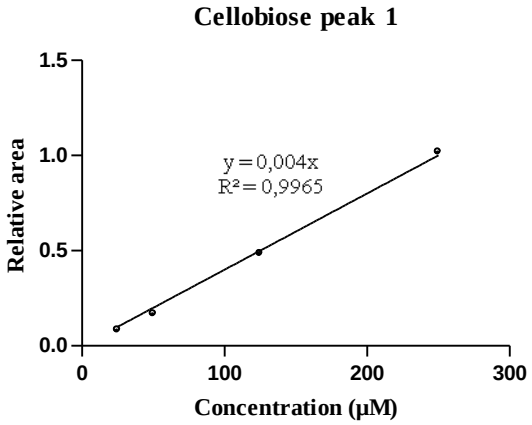
Cellobiose peak 1
Relative area
y = 0,004x
R² = 0,9965
Concentration (µM)
0.0
0.5
1.0
1.5
0
100
200
300

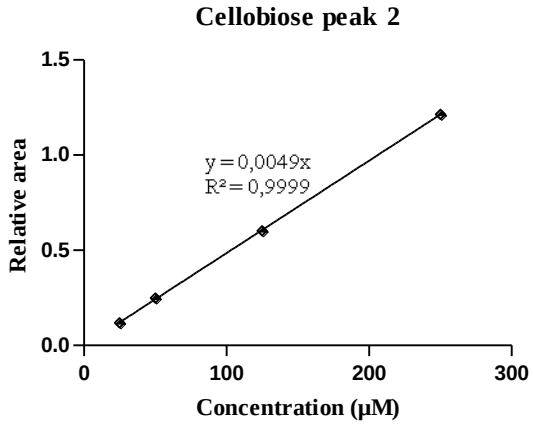
Cellobiose peak 2
Relative area
y = 0,0049x
R² = 0,9999
Concentration (µM)
0.0
0.5
1.0
1.5
0
100
200
300

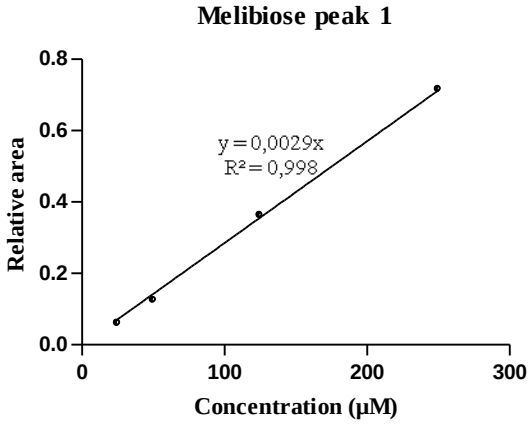
Melibiose peak 1
Relative area
y = 0,0029x
R² = 0,998
Concentration (µM)
0.0
0.2
0.4
0.6
0.8
0
100
200
300

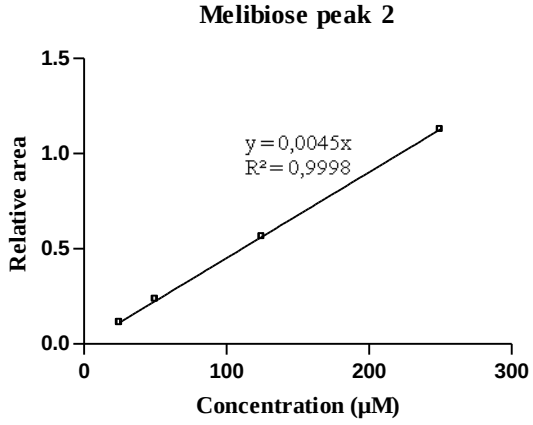
Melibiose peak 2
Relative area
y = 0,0045x
R² = 0,9998
Concentration (µM)
0.0
0.5
1.0
1.5
0
100
200
300